NASA CR-54064
214-S01

FACILITY FORM 602
N64 31453 (ACCESSION NUMBER)
123 (PAGES)
CR54064 (NASA CR OR TMX OR AD NUMBER)
1 (THRU)
(CODE)
27 (CATEGORY)

SUMMARY REPORT

PERFORMANCE STUDY OF A REPETITIVELY PULSED TWO-STAGE PLASMA PROPULSION ENGINE

by

B. Gorowitz, P. Gloersen, A. Ruess, and J. Kenney

prepared for

NATIONAL AERONAUTICS AND SPACE ADMINISTRATION

CONTRACT NAS 3-3570

OTS PRICE
XEROX $ 4.00 ph
MICROFILM $ 1.00

SPACE SCIENCES LABORATORY
GENERAL ELECTRIC
MISSILE AND SPACE DIVISION

NOTICE

This report was prepared as an account of Government sponsored work. Neither the United States, nor the National Aeronautics and Space Administration (NASA), nor any person acting on behalf of NASA:

A.) Makes any warranty or representation, expressed or implied, with respect to the accuracy, completeness, or usefulness of the information contained in this report, or that the use of any information, apparatus, method, or process disclosed in this report may not infringe privately owned rights; or

B.) Assumes any liabilities with respect to the use of, or for damages resulting from the use of any information, apparatus, method or process disclosed in this report.

As used above, "person acting on behalf of NASA" includes any employee or contractor of NASA, or employee of such contractor, to the extent that such employee or contractor of NASA, or employee of such contractor prepares, disseminates, or provides access to, any information pursuant to his employment or contract with NASA, or his employment with such contractor.

Requests for copies of this report should be referred to

National Aeronautics and Space Administration
Office of Scientific and Technical Information
Attention: AFSS-A
Washington, D.C. 20546

CASE FILE COPY

15514

NASA CR-54064
214-S01

SUMMARY REPORT

PERFORMANCE STUDY OF A REPETITIVELY PULSED TWO - STAGE PLASMA PROPULSION ENGINE

by

B. Gorowitz, P. Gloersen, A. Ruess, and J. Kenny

prepared for

NATIONAL AERONAUTICS AND SPACE ADMINISTRATION

August 17, 1964

CONTRACT NAS 3-3570

Technical Management
NASA Lewis Research Center
Cleveland, Ohio
Spacecraft Technology Division
Peter Ramins

GENERAL ELECTRIC COMPANY
Missile and Space Division
Space Sciences Laboratory
P. O. Box 8555
Philadelphia, Penna. 19101

ABSTRACT

31453

A summary is presented of the experimental program conducted during the past contract year for the study of the operating characteristics of a repetitively pulsed two-stage coaxial plasma propulsion engine. The results are presented in graphical form, along with the interpretation of the data and the resultant logic for the successive changes in engine design. The major fraction of the program was devoted to increasing the energy term representing work done on the plasma, $\int_o^t i^2 \dot{L}\, dt$, with respect to the loss term, $\int_o^t i^2 R\, dt$, or, in other words, by increasing $\dot{L}$ with respect to R. Several possible means for increasing $\dot{L}$ were explored, i.e., by altering engine geometry, altering propellant distribution in the engine, and increasing peak currents (since, under certain conditions, $\dot{L}$ was found to be proportional to i) by increasing circuit capacitance and decreasing initial circuit inductance. The energy efficiency trends were monitored by means of exhaust stream calorimetry. Of the above variations explored, propellant distribution and engine geometry proved by far to be the most fruitful. Thrust balance and mass flow measurements were reserved for the more efficient of these configurations towards the end of the contract year. The peak energy efficiency (as defined by the ratio of exhaust stream energy collected in a calorimeter subtending an edge-to-edge half-angle of 15^o to the energy originally stored in the capacitor) obtained at the end of the reporting period was 55% at a 3 KV operating voltage. Peak overall efficiency ($T^2/2\,\dot{m}\,P$) was 42%, at 6 KV, without taking into account possible mass addition from the gun, which was predicted to be small. Terminal current and voltage waveforms were correlated with experimentally obtained magnetic field distributions in the interelectrode region and beyond the muzzle of both the straight cylinder, radially fed gun and the more efficient axially fed form of the gun. Current sheet velocities were current dependent in the former geometry and nearly independent of current in the latter. Specific impulses ($T/\dot{m}\,g$) were in the range of 3000 - 15,000 seconds for the most efficient engine. Particle velocities deduced from current sheet velocities and luminous signals produced upon the arrival of the accelerated plasma at various downstream points were generally higher than the average velocities corresponding to the measured specific impulses. Methods for further improving the performance of the engine system are outlined.

TABLE OF CONTENTS

LIST OF FIGURES

I. INTRODUCTION

The work described here is part of a continuing program for the investigation of the operating characteristics of a two-stage repetitively pulsed coaxial plasma accelerator with the prime objective of improving the overall efficiency of the device. Considerable success has been achieved toward this end as a result of a series of modifications in the electrical, geometric, and propellant loading characteristics of the second stage engine system. A summary of the record of efficiency improvement is shown in Fig. 1. For ease of identification, accelerators incorporating the successive changes to be described here have been placed in model and mod. (modification) number categories. A more or less chronological accounting of the activities sponsored by this contract has been chosen for this report since, in this way, the facts also fall in a reasonably logical sequence.

The general procedure followed during the present contract period can perhaps best be understood in terms of the energy equation obtained from considering the gun circuit equation[1]:

$$\frac{1}{2}\left(\frac{Q_o - Q}{C}\right)^2 = \int_o^t i^2 R\, dt + \frac{1}{2}\int_o^t i^2 \dot{L}\, dt + \frac{1}{2}\left[L(t)\, i^2\right]$$

where $L(t) = L_o + L' x(t)$

Only two terms permanently accumulate energy in this equation, $\frac{1}{2}\int_o^t i^2 \dot{L}\, dt$, representing work done on the plasma, and $\int_o^t i^2 R\, dt$,

representing energy lost in heating the capacitor, leads, and the electrodes. It is apparent that $\dot{L}$ must be increased relative to R in order to improve engine efficiency. Several possible means for accomplishing this were identified (Section 2.4) and the program was geared for studying the changes in engine performance where these alterations were instituted.

Since considerable effort was required during the past contract period to operate the engine system on a thrust balance, it was decided to put this technique temporarily aside in favor of a much easier means for monitoring the engine performance changes during the various alterations that were carried out. Exhaust stream calorimetry was the technique chosen for this purpose. Thusm the engine system left over from the previous contract period was subjected to operation at higher values of capacitance to start off the contract year reported here (Section 2). The next step was the introduction of a much lower inductance energy storage capacitor bank with the promise of better performance of the engine system (Section 3). Since this promise did not become fact, a program of successive engine geometry and propellant distribution changes were carried out until a more efficient configuration was found. These studies were carried out mostly in the second (high power) stage of the engine, with cold gas triggering of the discharge (Sections 4-10). At the same time, the original gun was subjected to B_θ probe and terminal current and voltage waveform studies to learn more about the detailed operation of the two-stage gun (Section 3). When a suitably efficient configuration was obtained, towards the end of the contract period, thrust balance and mass

flow measurements were reinstituted and data were obtained (Sections 10 and 11). B_θ probes and Rogowski loops were used to explore plasma currents both inside and outside of the gun (Section 10) and optical techniques were used to obtain particle velocities outside the gun (Section 11). Finally, the most significant trends obtained during the program are summarized and recommendations for further improvements are given (Section 12).

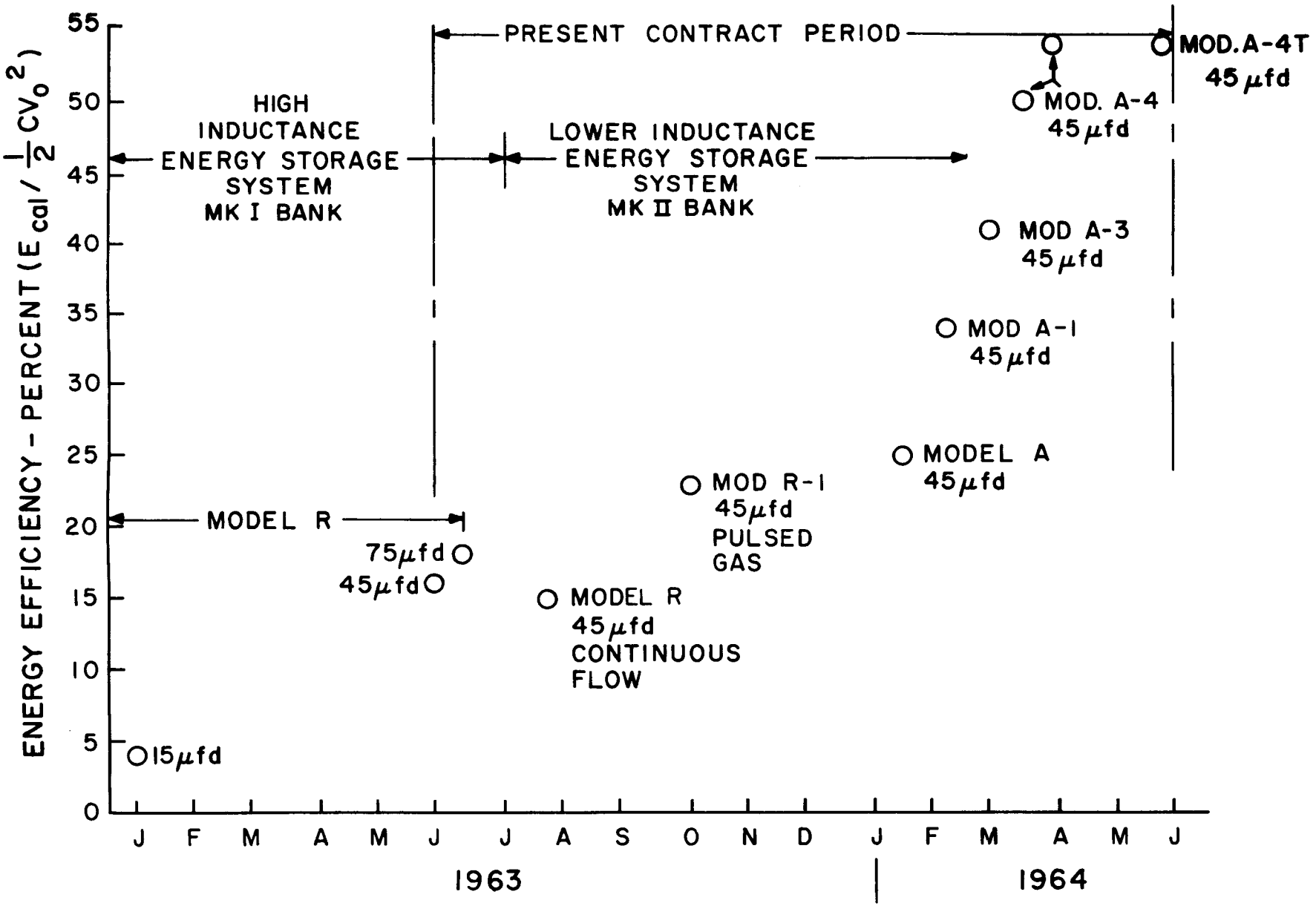

Figure 1. Chronology of Accelerator Efficiency Improvement

2. MODEL R PLASMA ACCELERATOR - Mark 1 Capacitor Bank

2.1 Specifications

a. Model R Accelerator (See also Fig. 2)

Propellant feed:	Radial injection 7.5 cm from the front face of the insulator; continuous flow of about 10^{-6} Kg/sec nitrogen.
Operating mode:	Two stages; both stages coaxial guns.
Outer Electrode:	8.75 cm diameter, 55 cm long.
Inner Electrode:	5.00 cm diameter, end of electrode flush with end of outer electrode.

b. Mark 1 Capacitor Bank

Capacitor:	Cornell Dubelier NRG-204
Capacitance:	Individual units - 15 ufd. Bank - 45 ufd increased to 75 ufd.
Voltage:	20 KV maximum rating.
Unit Inductance:	60 nanohenries
Unit Q:	3.6 @ 100 KC

Initial Circuit Inductance (L_o): 89 nanohenries (for the 45 ufd bank)

Lead Configurations: Three capacitors in parallel.
Parallel copper strips to individual capacitors.

2.2 General Description

The engine studied at the initiation of this contract period was identical to that used during the final stages of the preceding period covered by contract NAS3-2502. In order to determine the effect of increased capacitance on engine efficiency, two 15 ufd capacitors were added to the existing 45 ufd bank to provide a total bank capacitance of 75 ufd.

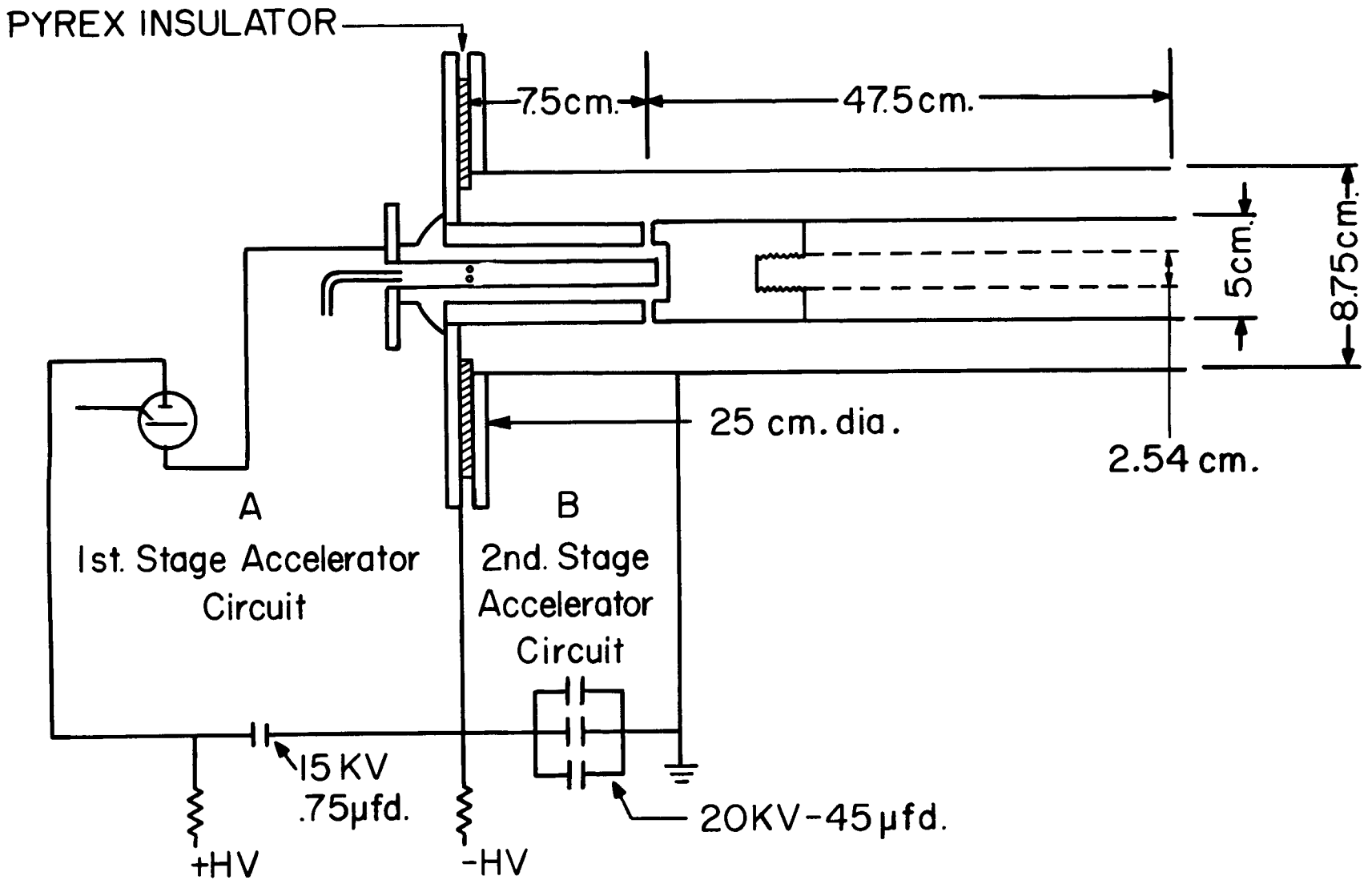

Figure 2. Model R Accelerator and Associated Circuitry

2.3 Exhaust Stream Calorimetry

The 142 gm., 24 cm. diameter conical copper calorimeter used in the previous measurements[1] was again used at a position 15 cm. from the muzzle of the accelerator. Ten to twenty shot samples were taken with the engine fired at a rate of 1 shot per second. The results of these measurements compared with those obtained for 15 ufd and 45 ufd capacitances are shown in Fig. 3 as the ratio of exhaust stream energy per shot to the initially stored energy per shot (energy efficiency). The trend toward increased energy efficiency with increasing voltage and capacitance is clearly demonstrated for this configuration. The maximum energy efficiency obtained from these runs was 16%.

2.4 Discussion

In looking for ways in which to improve the operating efficiency of the engine system, it is useful to contemplate the power terms $1/2\, i^2 \dot{L}$, representing power going into mechanical work done on the plasma, and $i^2 R$ representing power wasted in the system. It is apparent that $\dot{L}$ must be increased relative to R in order to accomplish the improvement. This may be carried out in several ways: (1) increasing the current by decreasing the discharge period, since it is probable (e. g. according to the anisotropic shock model[1]) that $\dot{L}$ is proportional to i; (2) increasing $\dot{L}$ by geometrical changes in the gun; and (3) decreasing R by improving the "Q" of the discharge circuit. The next step chosen for the development of the engine system was along the lines of method (1).

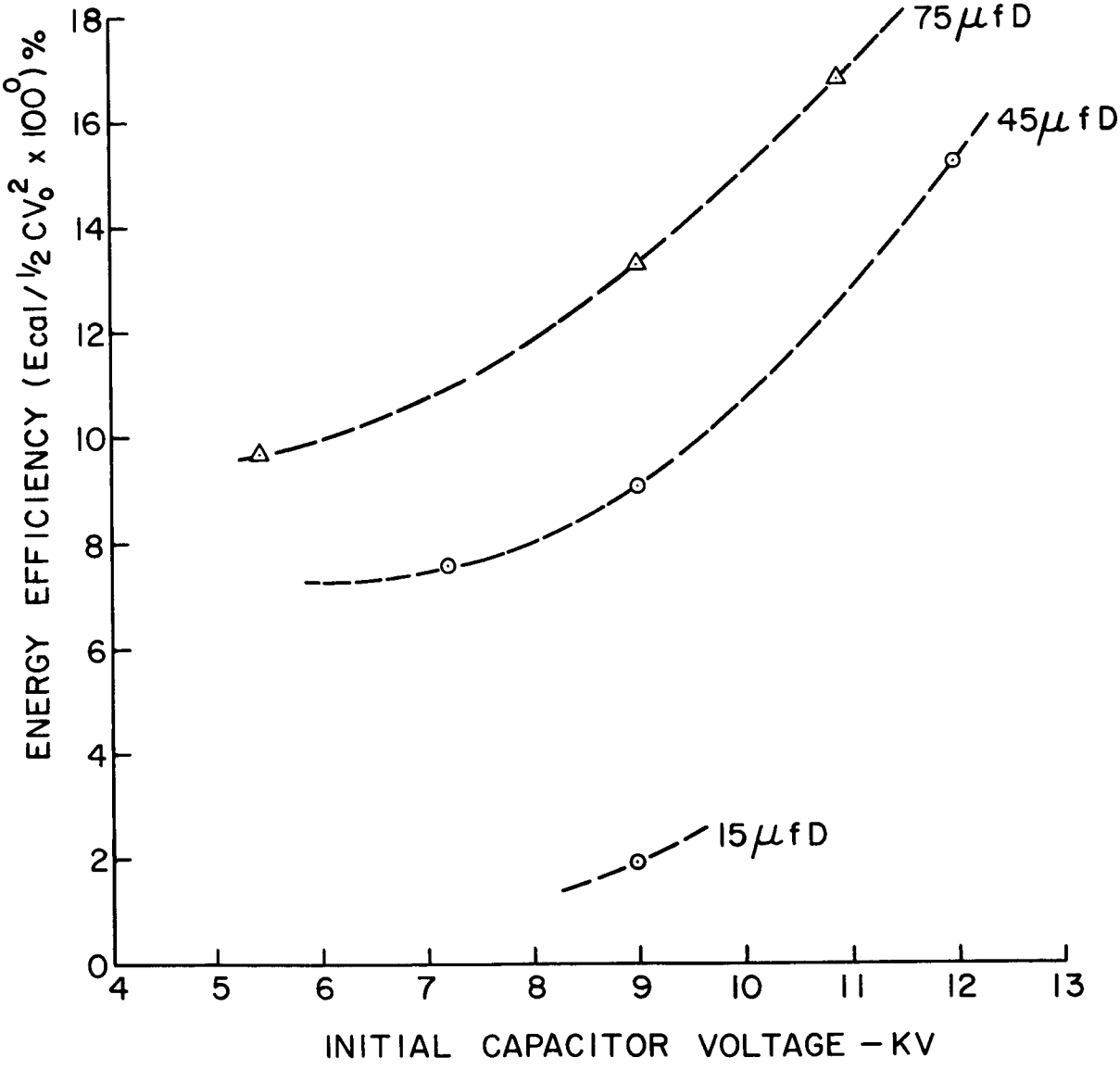

Figure 3. Energy Efficiency vs Initial Capacitor Voltage - Model R Gun, Mark I Bank

The areas most readily accessible for alterations designed to improve the energy efficiencies appeared to be in the capacitor bank. The relatively high equivalent series resistance (low Q), and high inductance of capacitors and leads gave rise to major dissipating factors in the circuit. (The high external inductance results in losses when a crowbar discharge occurs at any time other than at a current zero, since the magnetic field energy stored externally is subsequently dissipated externally.) With this in mind, the Mark II capacitor bank was constructed.

3. MODEL R PLASMA ACCELERATOR - Mark II Capacitor Bank

3.1 Specifications

a. Model R Accelerator (See also Fig. 2)

Propellant feed:	Radial injection 7.5 cm from the front face of the insulator; continuous flow of about 10^{-6} Kg/sec nitrogen.
Operating mode:	Two stages; both stages coaxial guns.
Outer Electrode:	8.75 cm diameter, 55-70 cm long.
Inner Electrode:	a) 5.00 cm diameter, end of the electrode flush with the end of the outer electrode. b) 5.00 cm diameter up to sharp transition to 2.5 cm diameter, 10 cm away from the front face of the insulator. End of the electrode flush with the end of the outer electrode.

b. Mark II Capacitor Bank

Capacitor:	Tobe Deutschmann Laboratories, Inc. Model No. ESC-258.
Capacitance:	5 ufd per unit up to 9 units in parallel for 45 ufd.
Voltage:	12 KV maximum rating.
Unit Inductance:	20 nanohenries.
Initial Circuit Inductance (L_o):	15 nanohenries
Q:	Units 9 @ 100 KC - Bank 5.4 @ 100 KC
Lead Configurations:	Nine units mounted on two, parallel aluminum discs 42" diameter, separated by polyethylene insulator.

3.2 General Description

In line with the decision to increase the peak circuit current, and hence $\dot{L}$, capacitors were chosen with lower internal inductances, more units were placed in parallel to decrease further the stray inductance, and

a lower inductance harness was designed to feed the gun. Since capacitors with superior "Q's" were not readily available, it was not practical to decrease R significantly at the same time as L was increased, but, at least the total internal resistance of a 45 ufd bank of the new units seemed comparable with that of the 45 ufd Mark I bank, based on the figures available from the manufacturers.

Unlike the previous assembly, where the capacitor bank operated in a vacuum environment, the Mark II bank was external to the vacuum tank with only the accelerator barrel projected into the vacuum. A photograph of the assembly is shown in Fig. 4. This arrangement was in use until the final quarter of the present contract, at which time the capacitor bank was transferred to a pressurized housing which was mounted on a thrust balance in the vacuum chamber.

3.3 Accelerator Terminal and B_θ Probe Measurements

Sample oscilloscope traces of the voltage and current transients for this configuration are shown in Fig. 5.

B_θ measurements were made in the interelectrode region of the second stage of this gun. Two B_θ probes (located at the same longitudinal but different azimuthal positions) were used to determine the azimuthal uniformity of the current sheet.

The longitudinal position of the probes was varied from a position ($Z = 0.8$ cm from the front face of the vertical insulator to $Z = 49.8$ cm while the second stage voltage was varied from 4 to 10 KV.

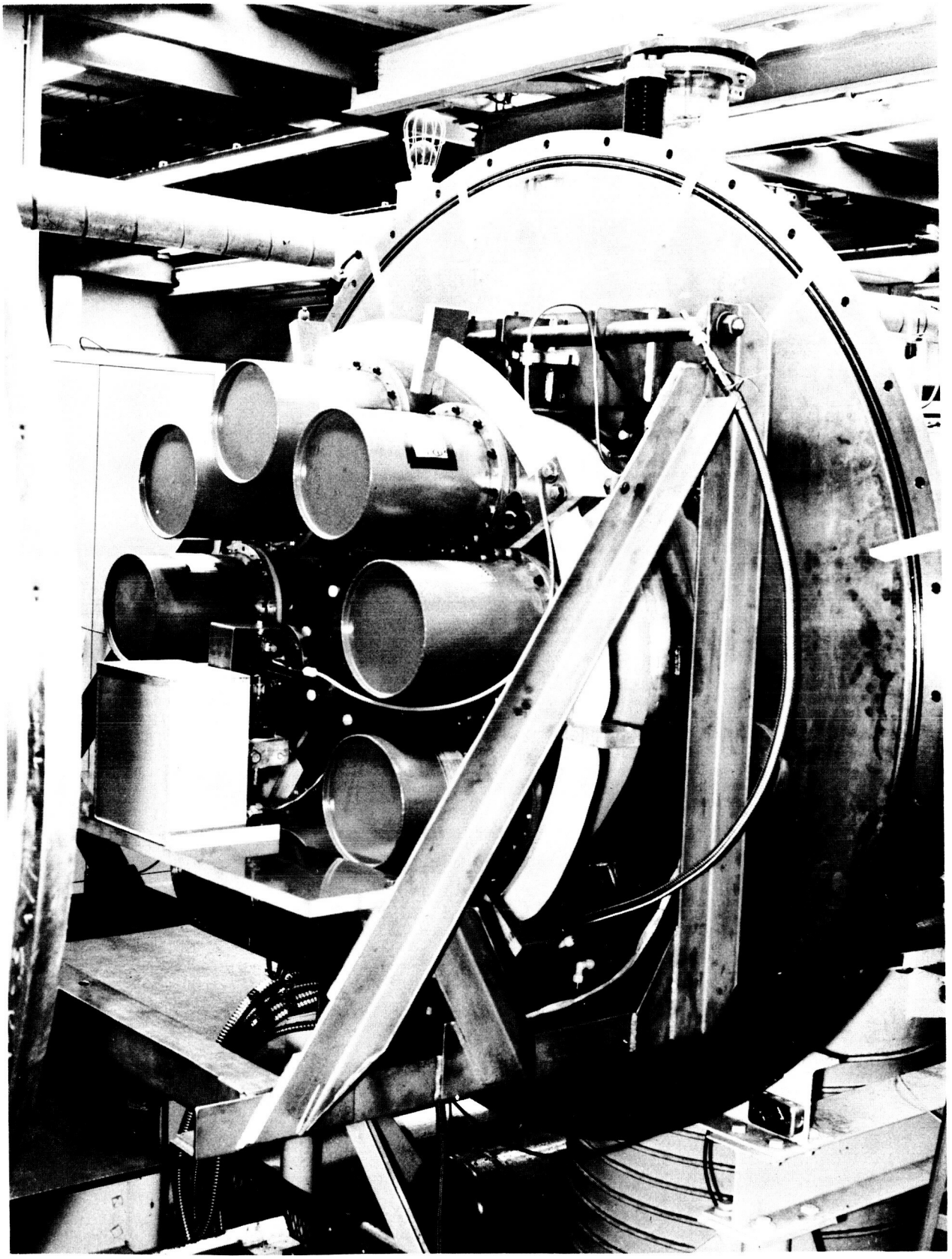

Figure 4. Mark II Capacitor Bank Mounted on Vacuum Chamber Pumping Plate

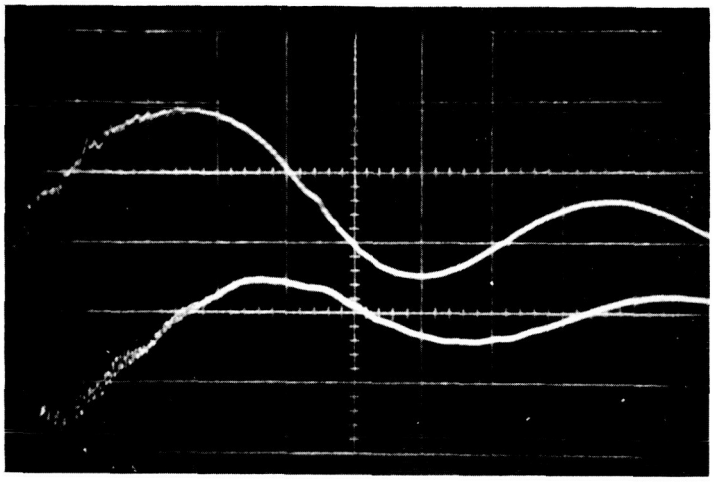

upper-current	110 K amps/cm
lower-voltage	5 KV/cm
capacitance	45 μ fd
time scale	1 μ sec/cm
propellant flow	1 mg/sec, N_2

Figure 5. Voltage and Current Transients - Model R Gun, Mark II Bank.

The results of these measurements show the current sheet velocity to be dependent on both the 2nd. stage initial voltage, and the instantaneous magnitude of the current. At current maximum (t = 1.8 usec.), the velocity was also a maximum and ranged from 9.0 cm/usec at 4 KV to 22.5 cm/usec at 10 KV.

The azimuthal uniformity of the current sheet as determined by the two magnetic field probes was usually within $\pm$ 10%.

A series of B_θ probe signals taken at different axial positions in the gun is shown in Fig. 6. These data are replotted as B_θ vs Z at different times in Fig. 7. The curves serve simply to connect the data points rather than to imply detailed shape of the magnetic field since sufficient data were not available to warrant the use of error bars. Current sheet position as defined by the half-maximum point in the B_θ field, and velocity vs time data for various operating conditions are shown in Fig. 8, along with the integrated Rogowski loop and voltage probe signals taken at the gun terminals. It is of interest to note in Fig. 8 that the current, i_{B_θ}, obtained from the B_θ probe signal at the trailing edge of the current sheet, breaks away from the Rogowski loop signal at about 1 usec, implying either a breech crowbar at this time or establishment of volume current behind the sheet. Also of interest in Fig. 8 is the varying dependence of the current sheet velocity, $\dot{x}$, on the current. This dependence is displayed more clearly in Fig. 9. The current sheet velocity has been corrected to account for an exponentially decreasing density along the axis of the accelerator. For the simple anisotropic shock model[1],

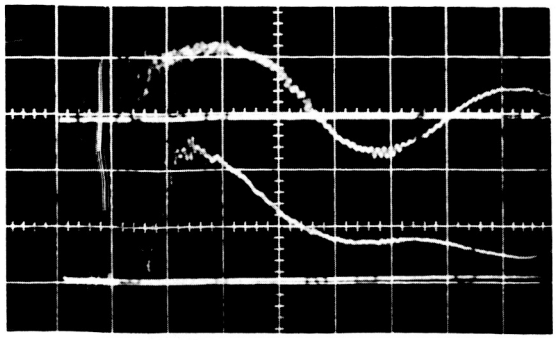

(a) X = 4.8 cm

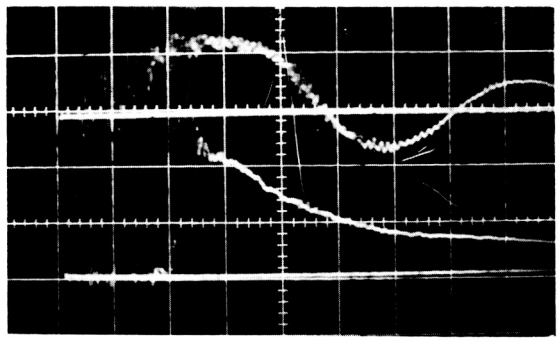

(b) X = 9.8 cm

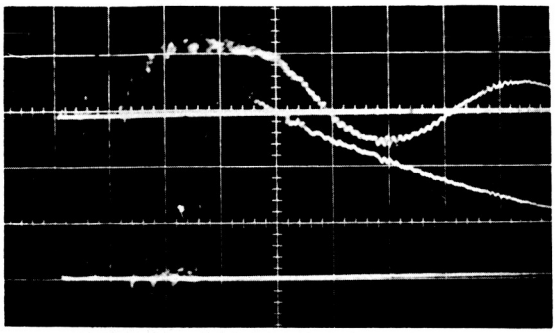

(c) X = 19.8 cm

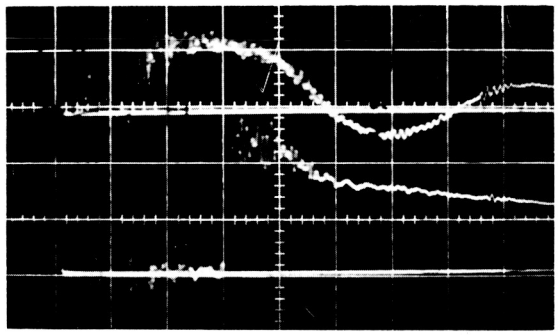

(d) X = 29.8 cm

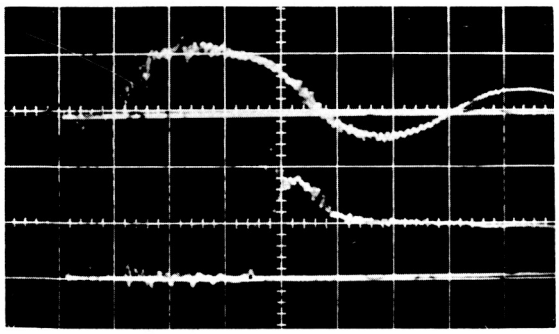

(e) X = 39.8 cm

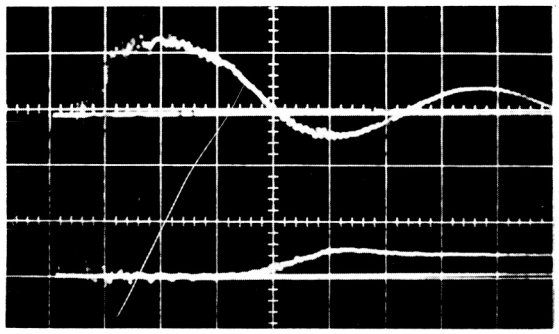

(f) X = 49.8 cm

(a), (b)	B_θ = 7.28 k gauss/cm
(c), (d), (e), (f)	B_θ = 3.64 k gauss/cm
Upper Trace:	Current = 2.07×10^5 amps/cm
	Vo = 10 KV
	t = 1 usec/cm

Figure 6. B_θ Probe Signals at Several Axial Positions in the Model R Accelerator.

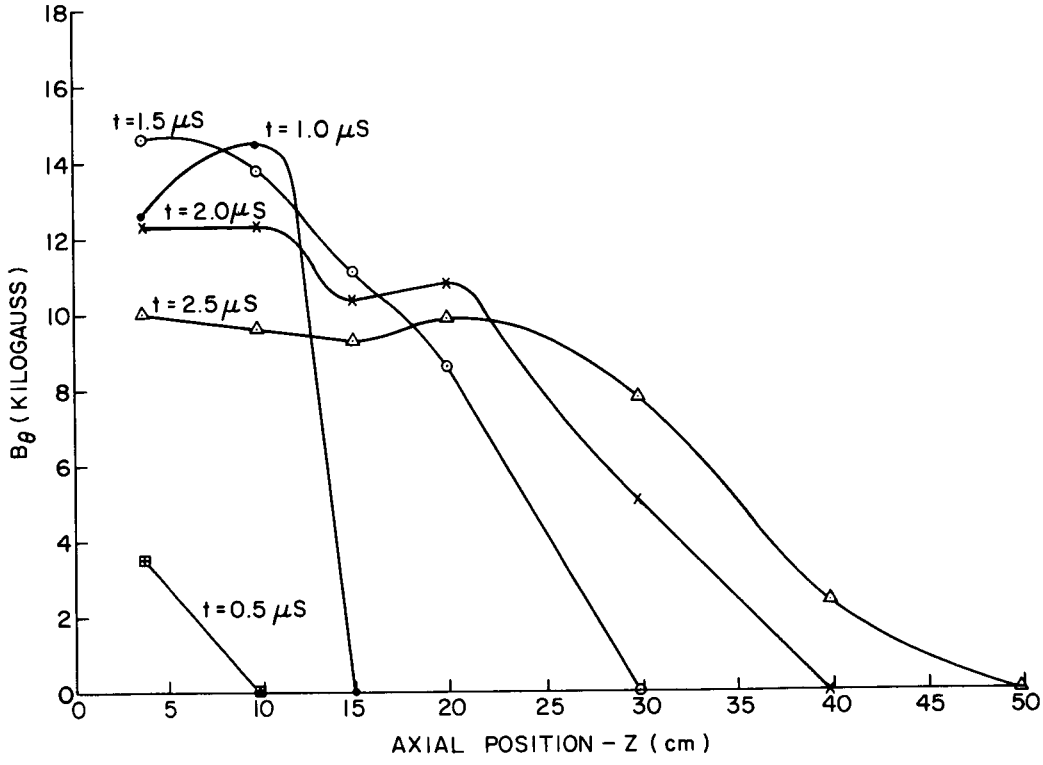

Figure 7a. B_θ vs Position - Model R Gun.

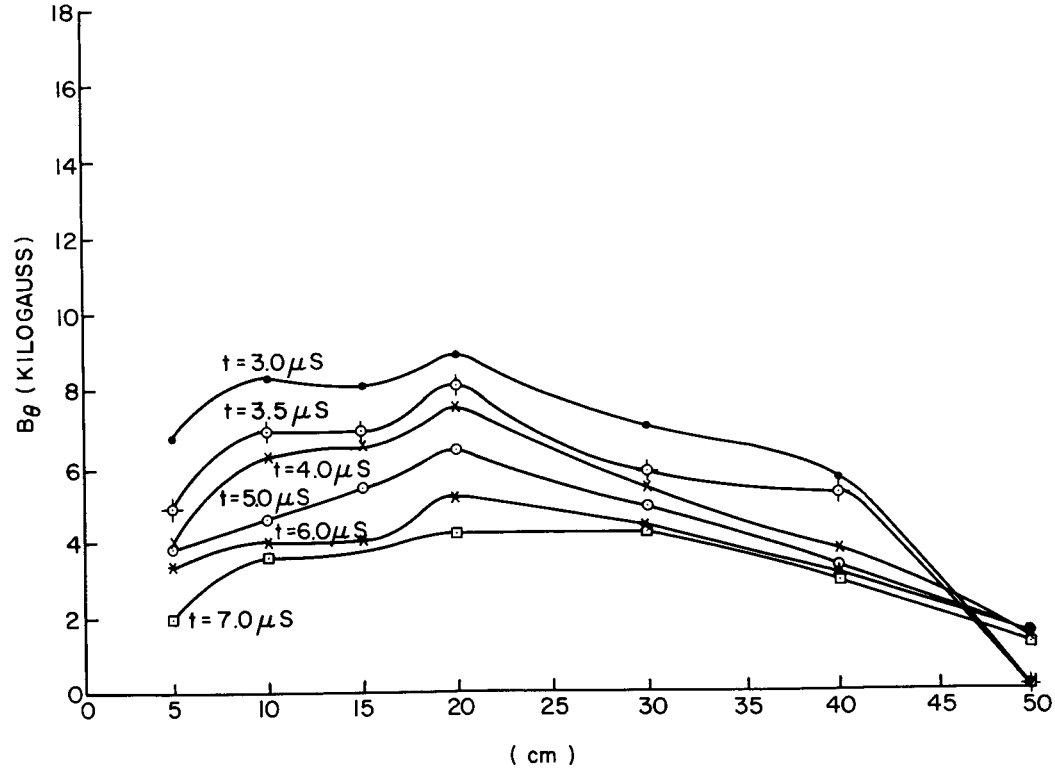

Figure 7b. B_θ vs Position - Model R Gun.

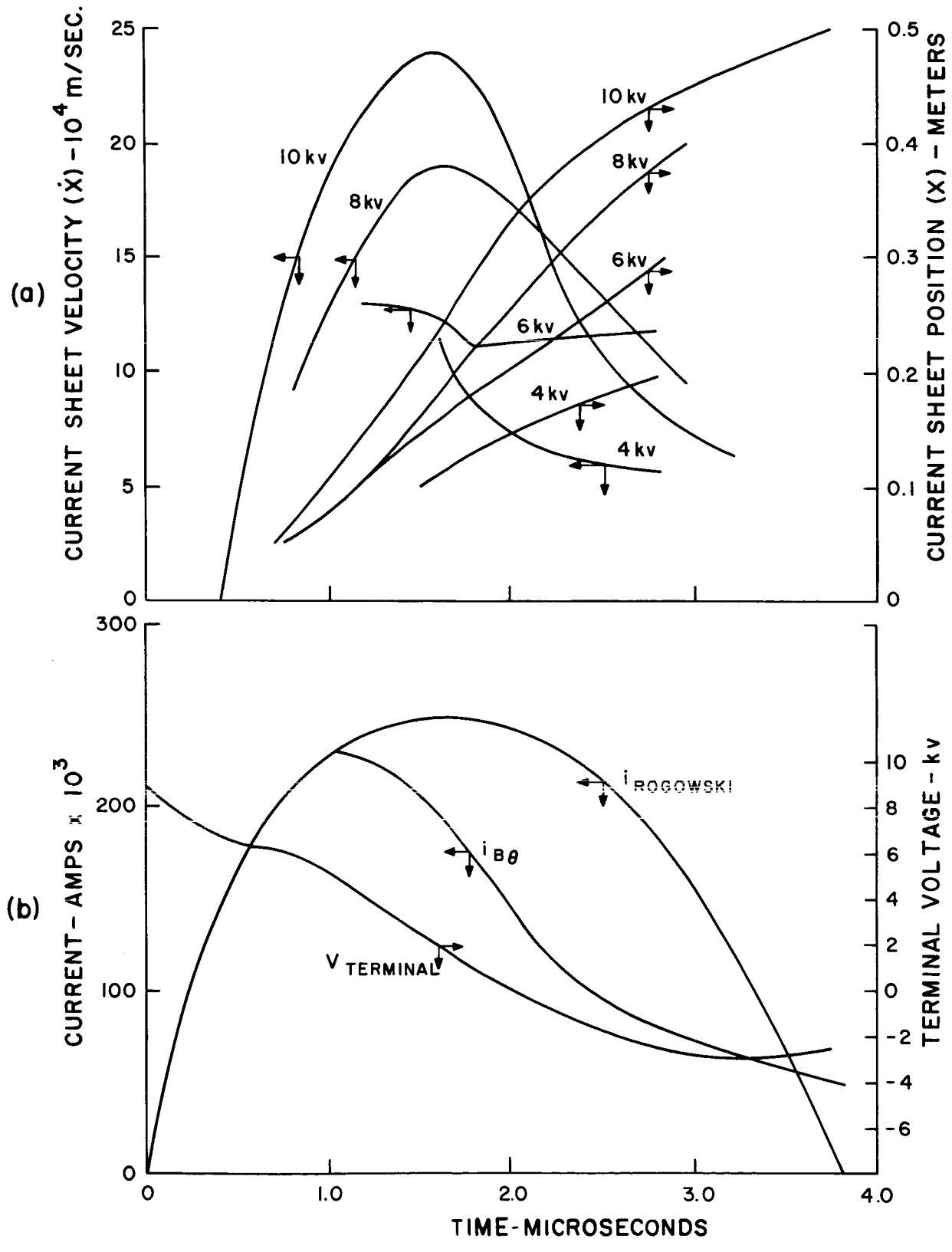

Figure 8a. Current Sheet Position and Velocity vs Time-Model R Gun.
8b. Terminal Current and Voltage Waveforms - Model R Accelerator.

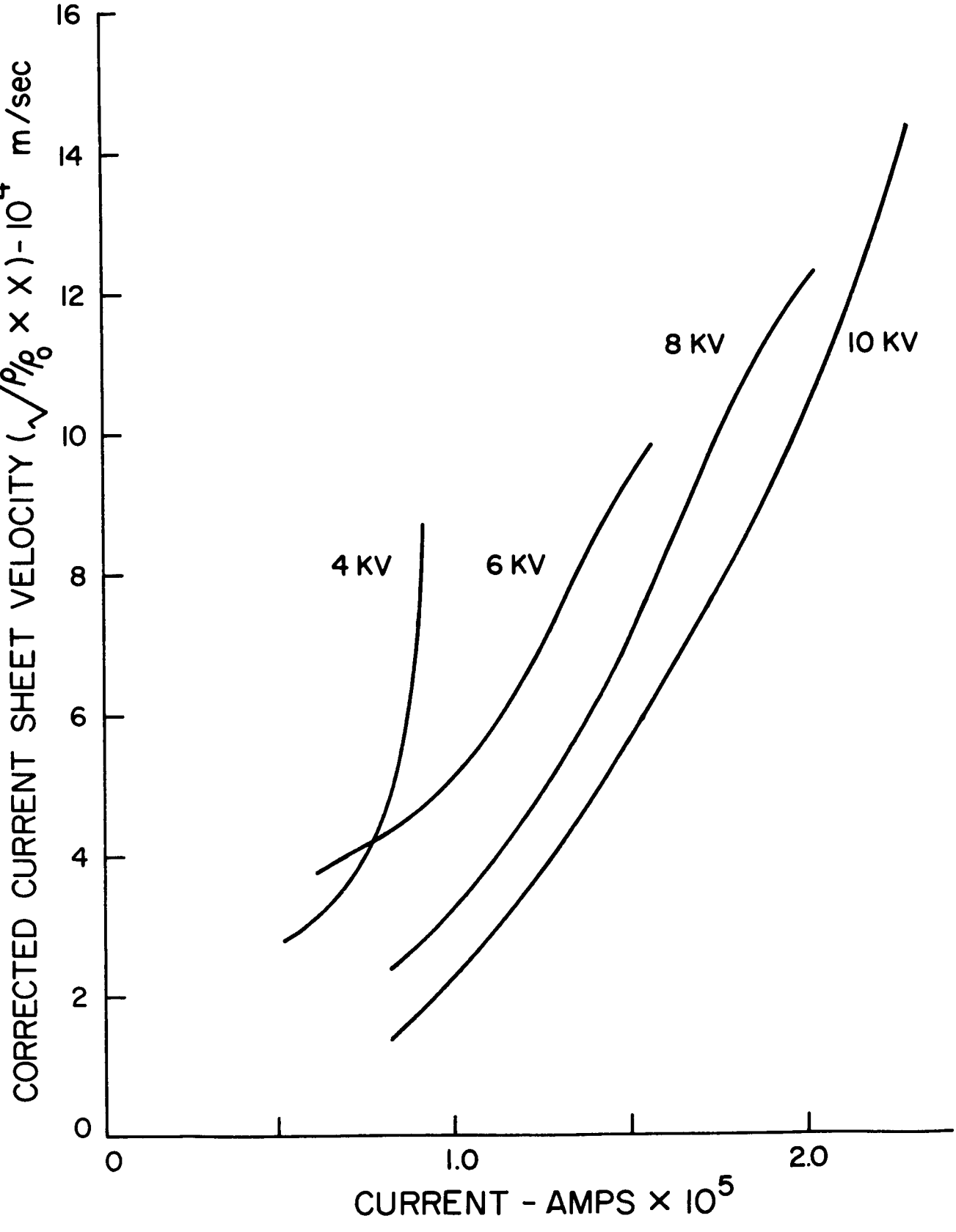

Figure 9. Corrected Sheet Velocity vs Current - Model R Gun.

this correction factor is $(\rho/\rho_o)^{1/2}$ where ρ_o has arbitrarily been chosen to be at the gas ports. For the Model R accelerator, there is approximately a two-orders-of magnitude change in density along the axis. The current is that obtained from the B_θ probes and thus is only the current in the sheet.

When the density correction is not taken into account, or when a $(\rho/\rho_o)^{1/2}$ correction (snowplow model) is applied instead, the relationship shown in Fig. 9 becomes a double-valued function of the current. That is, the ordinates obtained during current rise do not correspond to those obtained during current fall.

An accounting of electrical energy as a function of time for 10 KV operating conditions is shown in Fig. 10. In Fig. 10, L and $\dot{L}$ were obtained directly from the data of Fig. 8, and R was obtained from the Q measurements described later in section 10.6.

In adding up the energies from various components in Fig. 10, it should be realized that at least 10% errors in each factor could add up to explain that after 1 microsecond, the sum is greater than the initial energy. It can be seen that about 35% of the total initial energy is dissipated in the external resistance for the circuit at the point of complete discharge of the capacitor (t = 2.0 μ sec) and about 58% is ultimately dissipated there.

3.4 Exhaust Stream Calorimetry

For purposes of comparison with the measurements performed previously, the same calorimeter and calorimeter calibration techniques

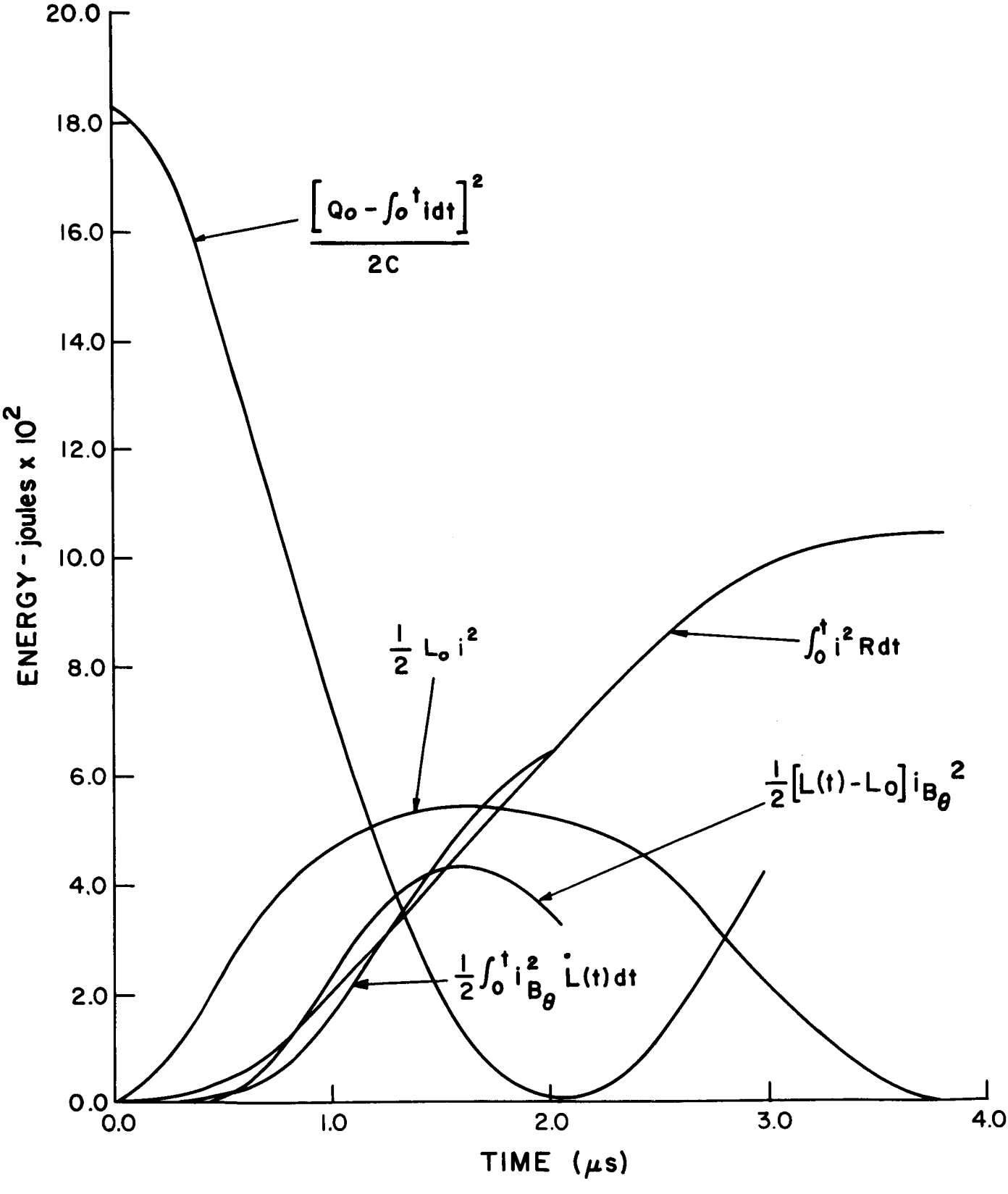

Figure 10. Electrical Energy Inventory as a Function of Time - Model R Gun.

were employed throughout the major portion of the contract period. To show the trend of energy efficiency vs voltage, some of the results are plotted in the graph shown in Fig. 11.

A comparison of these results with those obtained with the Mark I capacitor bank indicate no significant increase in energy efficiency.

Attempts to improve this efficiency by variation of accelerator length between 50 and 70 cms were unsuccessful. A definite improvement was achieved by decreasing the diameter of the central electrode from 5 to 2.5 cm. This resulted in an increase of the inductance per unit length of the accelerator and hence $\dot{L}$ relative to R, since the sheet velocity did not become significantly smaller. The results for the 2.5 cm diameter electrode are plotted in Fig. 11. With the 2.5 cm diameter electrode, energy efficiency was over twice that observed with the 5 cm unit at voltages below 10 KV. At voltages above 10 KV, no significant increase in efficiency was obtained with 2.5 cm unit. In no case, however, did the calorimeter measured efficiency exceed 16% with Model R accelerator.

3.5 Discussion

The above data gave insight into the methods for further improving the operation of the engine system.

Terminal measurements indicated three main differences between the electrical characteristics of the Mark II and the Mark I banks: 1) the current waveforms were in general shorter in duration for the Mark II bank (25% shorter in the first half cycle; 230% shorter in the succeeding half cycles); 2) the first half cycle of current was 180% longer in duration than

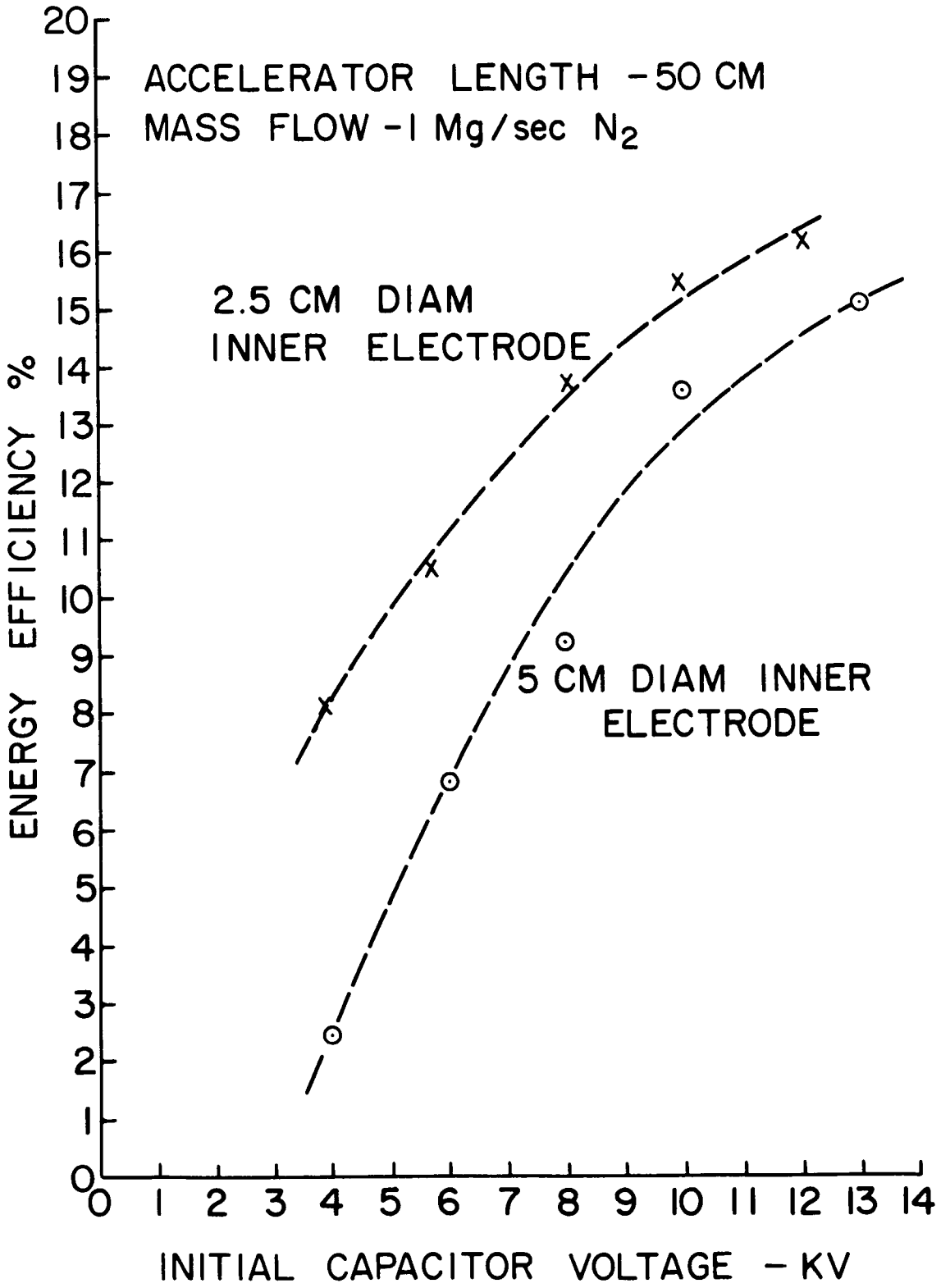

Figure 11. Energy Efficiency vs Initial Capacitor Voltage - Model R Gun, Mark II Bank.

the succeeding ones for the Mark II bank; all half cycles were approximately equal in duration for the Mark I bank; 3) the first half cycle current peak for the Mark II bank was 15% higher than that for the Mark I bank. These facts, together with the assumption that $\dot{L}$ is proportional to the current, imply that $\dot{L}$ was greater for the Mark II bank than for the Mark I, since R was essentially the same for both. In spite of this increase in $\dot{L}$ and decrease in external i^2R losses (as indicated by approximately equal first half cycle currents and much lower reversal currents), the energy efficiency was unchanged. This implies a greater energy loss in the gun itself for the Mark II bank.

Increasing $\dot{L}$ by changing the gun geometry proved to be a more fruitful approach to improving the efficiency of the engine system, at least at the lower operating voltages. This approach was continued in the remainder of the program.

It was felt at this point that most of the useful data had been obtained with the present experimental arrangement using the relatively simple continuous propellant mode of operation, and that another logical step in increasing the energy efficiency of the thrustor would be to investigate the effects of significant alterations in the propellant density distribution in the gun barrel just prior to breakdown. To this end, a gas propellant injection valve[2] utilized earlier[3] for single shot studies was modified for use on a repetitive basis and incorporated in subsequent gun configurations.

A number of advantages were anticipated in adopting the pulsed gas injection mode of operation for the repetitively fired gun: 1) higher mass loading per shot without overloading the vacuum system with the gas flow between shots; 2) the opportunity for more accurately determining the degree of mass utilization of the discharge itself, since the mass of interest would no longer be a small fraction of the total mass flow as it was for continuous flow; 3) the ability to operate in the laboratory at moderately low power levels an engine with high mass utilization, (Efficient mass utilization with continuous propellant would require a pulsing rate between 500 - 1000 sec^{-1} and 1.1 megawatts or more of input power to operate the 45 ufd storage bank at 10 KV); and 4) a wider range of propellant flow rates, (under continuous operation, the flow rates were limited to values between 0.5×10^{-6} and 4.5×10^{-6} Kg sec^{-1}. Below the lower limit, the discharge could not be triggered; above the upper limit, the second stage could not support the energy storage bank potentials); and 5) more flexibility in shaping the prefire density distribution of the propellant.

4. MOD. R-1 PLASMA ACCELERATOR

4.1 Specifications

*Propellant feed:	Radial injection 7.5 cm from the front face of the insulator; continuous flow of about 10^{-6} Kg/sec nitrogen with a gas pulse from a fast acting valve superimposed, or gas pulse only.
Operating mode:	Single stage, gas pulse triggered.
Outer Electrode:	8.75 cm diameter, 55 cm long.
Inner Electrode:	5.00 cm diameter, end of the electrode flush with the end of the outer electrode.
Capacitor Bank:	Mark II

4.2 General Description

The first stage of the Model R accelerator was removed and a fast acting valve identical to that used in earlier experiments was substituted for it. For purposes of examining the effect of pulsed injected gas superimposed upon a continuous flow of propellant through the accelerator, a controlled leak was introduced into the valve. The flow was adjusted to a rate of 10^{-6} Kg sec^{-1}, the usual flow rate for the previous Model R accelerators. For the sake of comparison, the gun was operated also with the gas pulse alone.

4.3 Exhaust Stream Calorimetry

With the calorimeter 20 cm downstream from the accelerator muzzle, the measured efficiencies ranged from 16 to 22% in the voltage range from 4 to 12 KV. The results are plotted in Fig. 12. It should be noted that the efficiency at the lower voltage was about 5 times that measured previously with continuous propellant flow alone, while that the upper range was about

---

*-Change from Mod. R Accelerator

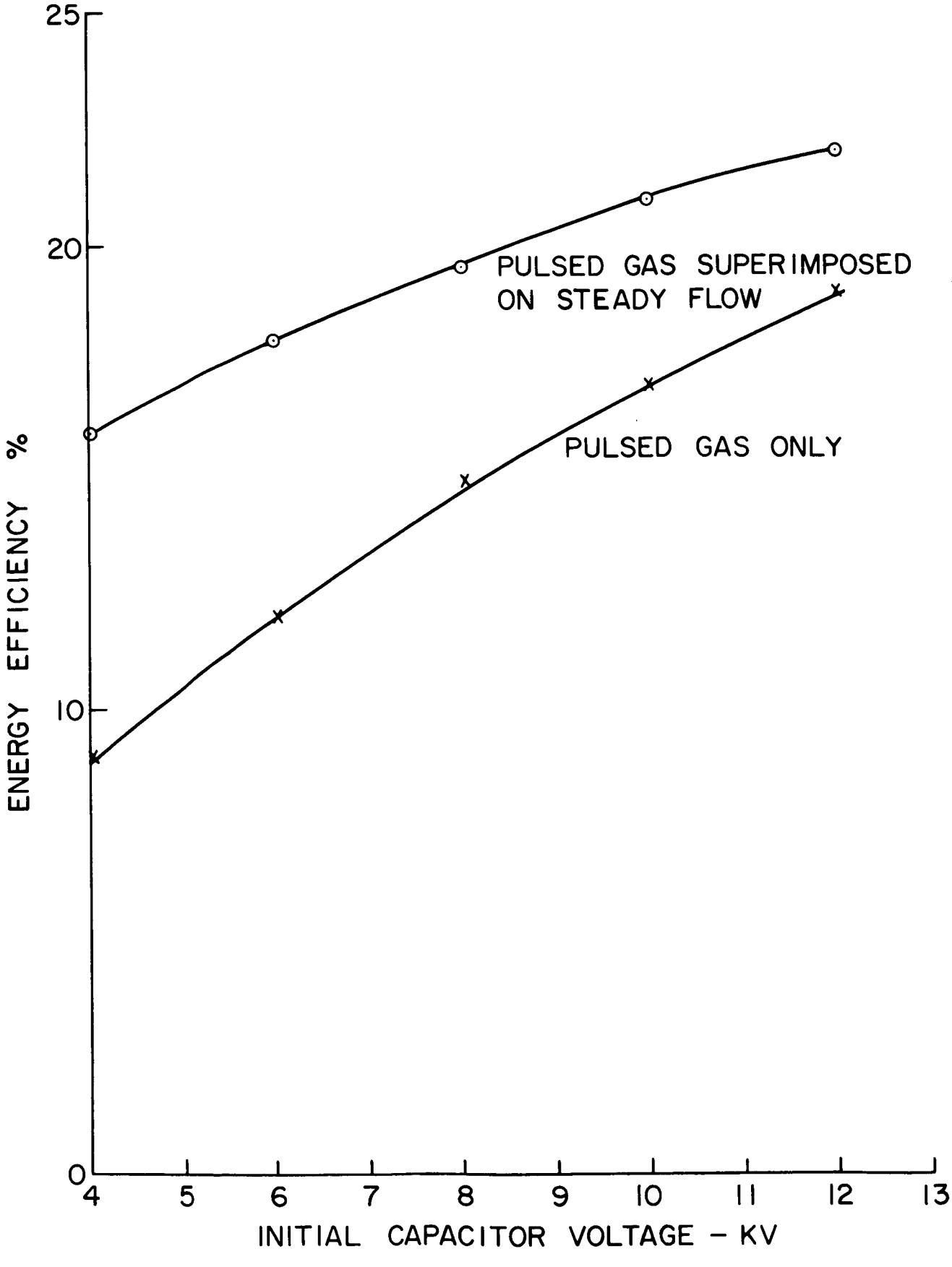

Figure 12. Energy Efficiency vs Initial Capacitor Voltage - Model R-1 Gun.

40% higher than the best values obtained earlier.

Efficiencies measured with pulsed gas injection alone into an accelerator with continuous flow eliminated, were approximately 25% lower than the above values.

4.4 Discussion

The pronounced effect on efficiency due to changes in the propellant loading of an otherwise similar accelerator appeared to present another significant means to improve further engine performance. The fact that the best efficiencies were obtained with accelerators having propellant distribution along the entire length of the barrel prior to gas triggered breakdown, suggested that such gas loading must be accomplished, but without resort to continuous flow and its inherent deficiencies discussed earlier. The succeeding Mod. R-2 accelerator was an attempt to fulfill the predicted propellant distribution requirements. It utilized internal switching arrangements intended to permit more complete filling of the accelerator barrel and closure of the valve prior to initiation of the discharge.

5. MOD. R-2 PLASMA ACCELERATOR

5.1 Specifications

*Propellant feed:	Radial injection 19.25 cm from the front face of the insulator; pulsed nitrogen into 10^{-5} - 10^{-6} mm background.
*Operating mode:	Two-stage; first stage is an internal series switch triggered by the arrival of the gas pulse near the breech.
*Outer Electrode:	8.75 cm diameter 37.5 cm long.
*Inner Electrode:	5.00 cm diameter; end of the electrode flush with the end of the outer electrode.

5.2 General Description

Two variations of what was essentially an internal series switch were examined. One configuration shown in Fig. 13, consisted of a tri-axial arrangement of electrodes with the intermediate electrode initially electrically "floating" and inner and outer electrodes connected to the high potential and ground side, respectively, of the capacitor bank. Propellant was pulsed from a point almost midway along the length of the inner electrode into the space separating it from the intermediate electrode, thus allowing it to diffuse toward both the breech and the muzzle of the accelerator. At the breech, it was permitted to flow radially toward the outer electrode through holes placed around the periphery of the intermediate electrode. With sufficiently high density achieved between the electrodes in the region of the holes, breakdown of the discharge was initiated. Measurements indicated delay times between opening of the valve and ignition of the discharge ranging

---

*-Changes from Mod. R-1 Accelerator

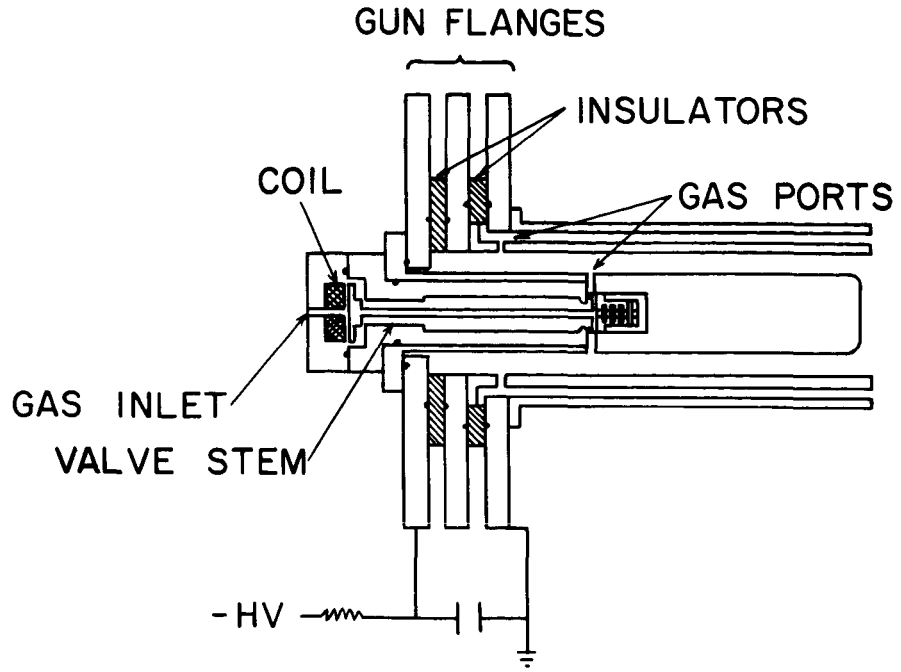

TRIAXIAL CONFIGURATION

Figure 13a. Internal Series Switch, Mod. R-2 Accelerator Configurations.

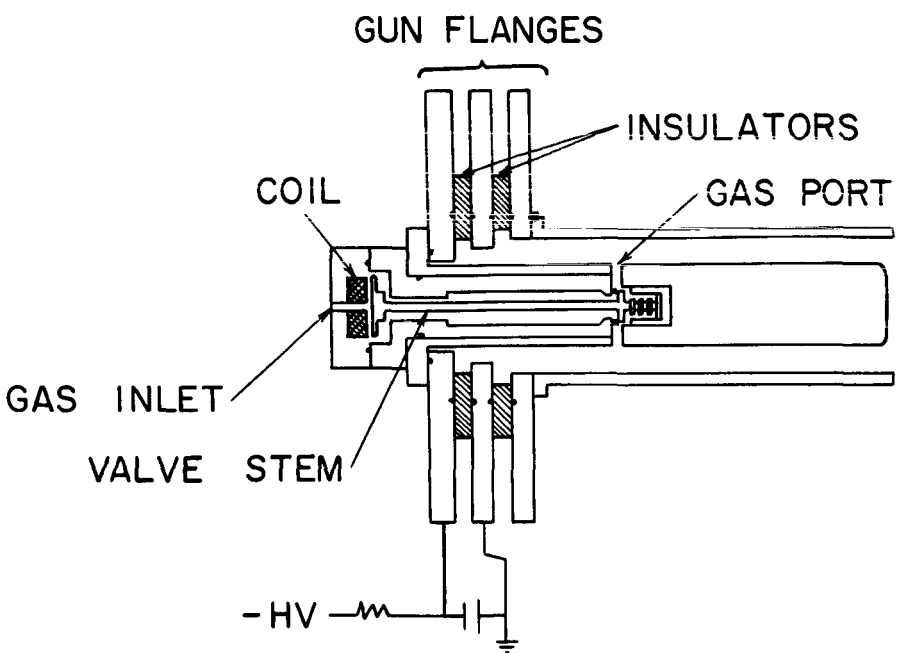

FLOATING OUTER ELECTRODE CONFIGURATION

Figure 13b. Internal Series Switch, Mod. R-2 Accelerator Configurations.

from .4 - .9 milliseconds, depending on valve operating voltage. Calorimeter measurements of efficiency proved disappointing, however. (See below)

Another configuration not requiring the third cylindrical electrode was tested. In this design, the outer electrode was initially electrically isolated from both the intermediate ground potential capacitor flange and the high potential inner electrode. Here too, propellant was admitted approximately midway along the inner electrode axis and allowed to diffuse toward both the breech and the muzzle of the accelerator. Triggering took place automatically when the gas density at the breech was sufficiently high for breakdown between the high potential inner electrode and the ground flange. It was postulated that the field at the flanges might be of sufficient magnitude and orientation to "blow" the discharge into the region between the cylindrical electrodes so that the outer electrode became a current carrier and the sheet could be accelerated along its length in the same manner as if it had been directly connected to ground. Experimental results indicated the predicted delays between valve actuation and discharge initiation (up to 1 millisecond), and proper operation of the accelerator.

5.3 Exhaust Stream Calorimetry

The highest energy efficiency achieved with the triaxial configuration was 6%, while that for the succeeding configuration increased to only 12%.

5.4 Discussion

The poor performance of these accelerators can most likely be attributed to the undesirably high resistance introduced by the series gaps and

intermediate electrodes. In view of the disappointing performance of the configurations incorporating internal series switches, this approach was set aside in favor of more fruitful modifications aimed at improving propellant distribution.

6. MODEL A PLASMA ACCELERATOR

6.1 Specifications (See also Fig. 14)

*Propellant feed:	Axial injection 5 cm from the front face of the insulator; pulsed nitrogen into 10^{-5} - 10^{-6}mm background.
*Port size:	Six holes, each 0.4 mm diameter.
*Operating mode:	Single stage; gas triggered discharge.
*Outer Electrode:	8.75 cm diameter 35 cm long.
*Inner Electrode:	5.0 cm diameter to a distance 3.5 cm from the front face of the insulator, followed by a 27^{o} transition to 2.5 cm diameter, a straight section 1 cm long, and a second 27^{o} transition to 1.27 cm diameter. End of the electrode flush with the end of the outer electrode.
Capacitor Bank:	Mark II

6.2 General Description

A center electrode was constructed in which it was anticipated that the combination of the fast acting valve and appropriate nozzle design would permit injection of jets of propellant which extend a substantial distance along the length of the accelerator prior to buildup of sufficient gas density in the interelectrode space to initiate breakdown of the discharge. The means for producing these streams was centered in a set of hypodermic needles arranged around the periphery of the electrode at the valve seat.

6.3 Calorimetric Measurements in the Exhaust Stream

The highest energy efficiency obtained with this configuration

---

*-Changes from Mod R Series Accelerators

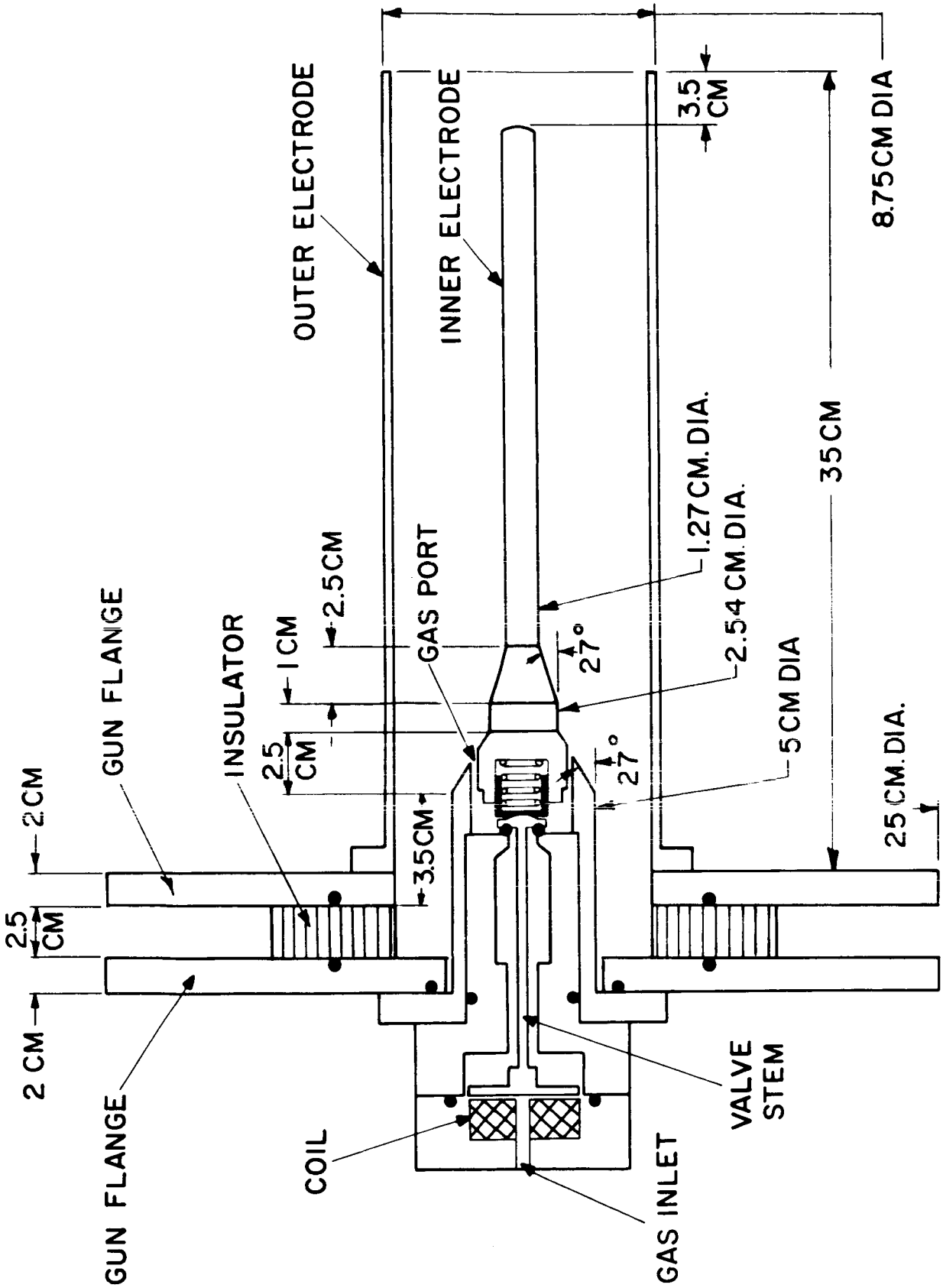

Figure 14. Model A Accelerator

was 25% with 6 KV initially on the energy storage bank. At 8 KV, a value of 22% was determined. Operation of the accelerator was erratic at this voltage, however, with considerable premature breakdown of the discharge.

6.4 Cold Gas Travel Prior to Breakdown

An attempt at obtaining the axial distance traversed by the cold gas prior to breakdown was made by inserting a barrier near the gas ports to cause early breakdown by diverting the gas radially towards the outer electrode. The breakdown appeared to occur about 100 ± 20 microseconds sooner with the barrier in place, implying that the gas travelled for about 100 microseconds (or only about 4 cm, assuming the front to move at sonic velocity in nitrogen) before breakdown.

6.5 Discussion

The jet action predicted for this particular configuration did not appear to be born out to the extent desired in practice. Enlargement of the injector holes was the next logical stop in this empirical approach, since this would at least result in a greater portion of injected propellant in the interelectrode space and less in the nozzles at the time of discharge.

7. MOD. A-1 PLASMA ACCELERATOR

7.1 Specifications (See also Fig. 14)

Propellant feed:	Axial injection 5 cm from the front face of the insulator; pulsed nitrogen into 10^{-5} - 10^{-6} mm background.
*Port Size:	Six holes, each 1.35 mm diameter.
Operating mode:	Single-stage; gas triggered discharge.
Outer Electrode:	8.75 cm diameter 20, 25 and 35 cm long.
Inner Electrode:	5 cm diameter to a distance 3.5 cm from the front face of the insulator, followed by a 27^{o} transition to 2.54 cm diameter, a straight section 1 cm long, and a second 27^{o} transition to 1.27 cm diameter. End of the electrode 3.5 cm from end of outer electrode. Another configuration eliminated the second transition and utilized a straight section 2.54 cm diameter.
Capacitor Bank:	Mark II

7.2 General Description

This accelerator was identical to the Model A configuration with the exception that the hypodermic needle injectors were removed and the remaining holes used as injector nozzles.

7.3 Parametric Studies with Exhaust Stream Calorimetry

An immediate consequence of enlarging the port size of the Model A accelerator was the achievement of increased calorimetrically measured energy efficiencies throughout the range of voltages examined. Variation of efficiency with voltage, capacitance, and gun length was studied

---

*-Changes from Model A Accelerator.

systematically with this configuration, and the following trends were revealed: An optimum initial voltage existed for each gun length. An optimum gun length also existed for the specifications given for the Mod. A-1 accelerator. The efficiency trends with voltage are shown in Fig. 15. Figure 16 shows the maxima of the curves of Fig. 15 to more clearly indicate the approximate optimum gun length for these particular operating conditions.

Some of the 5 microfarad units were removed from the bank to examine the efficiency trend with capacitance for the 20 cm gun length. These data are shown in Fig. 17. It is of interest to note that the continual increase of efficiency with capacity noticed previously with a 55 cm gun (Model R: 15-75 mfd) is not indicated here. In fact, the 30 mfd bank seems to perform slightly better than the 45 ufd bank for the 20 cm long gun. Repetition of these trend measurements for the 25 cm gun did not seem worthwhile, and they were not carried out.

All of the above data were obtained with an accelerator electrode radius ratio of 7 to 1. For a radius ratio of 3.5 to 1, obtained by using a 2.5 cm diameter inner electrode, and a 25 cm long outer electrode the best efficiency obtained was 24%, but no well-defined peak was observed in the range of variables studied. The results for 7:1 and 3.5:1 radius ratios are compared in Fig. 18.

7.4 Discussion

The use of axial injection of propellant coupled with a more appropriate accelerator configuration resulted in the attainment of a peak energy efficiency

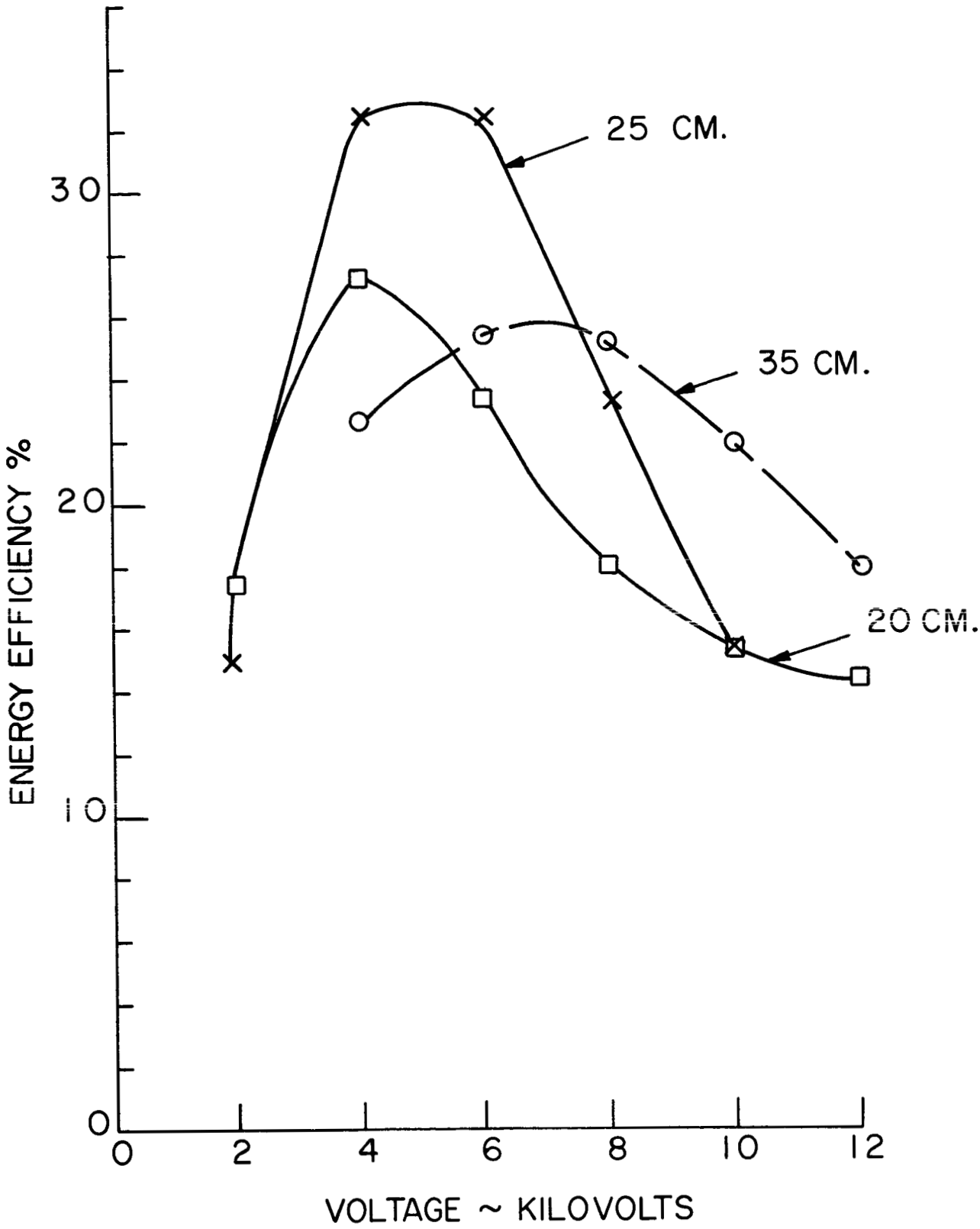

Figure 15. Energy Efficiency vs Initial Capacitor Voltage - Mod. A-1 Gun.

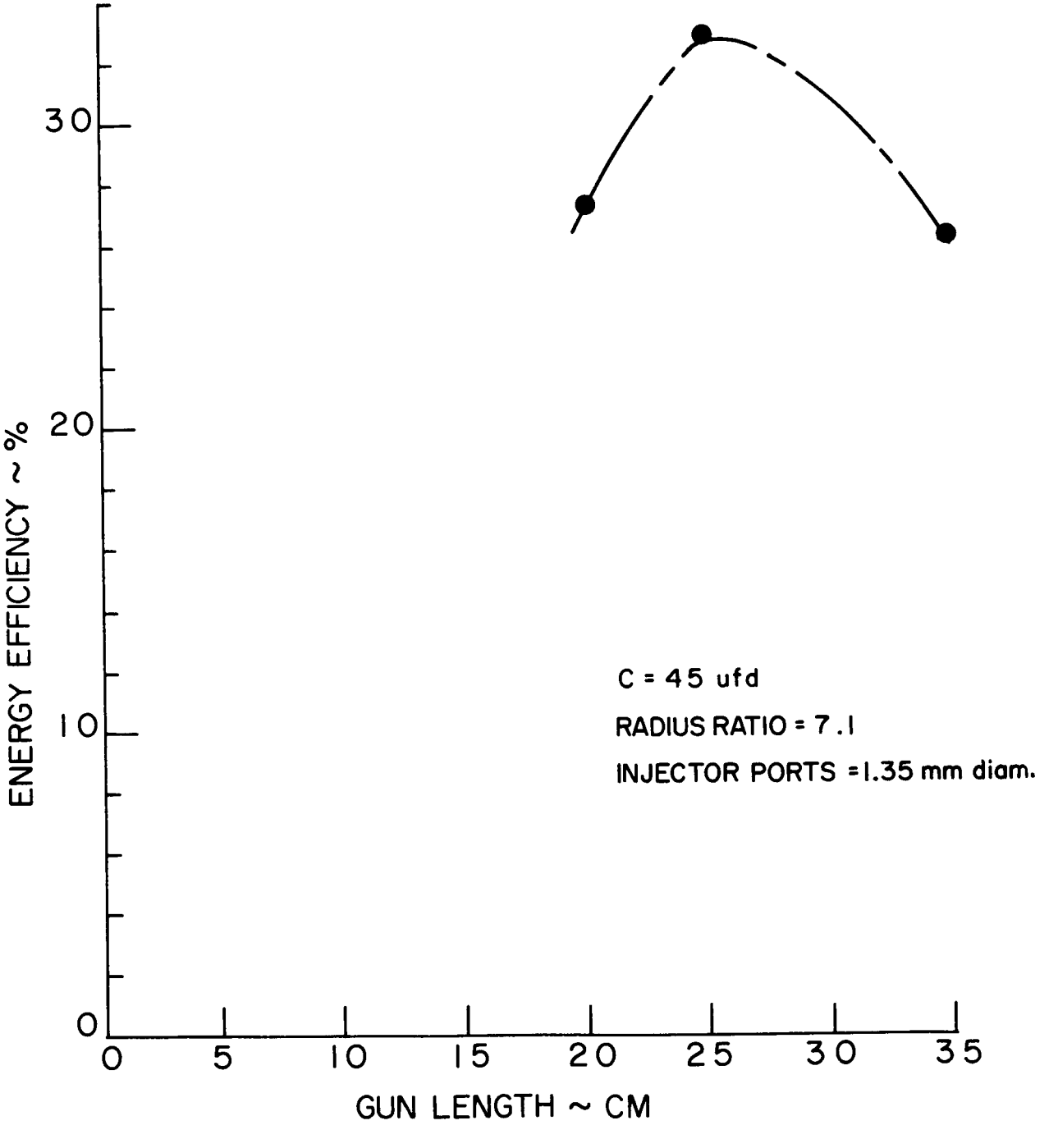

Figure 16. Energy Efficiency vs Length - Mod. A-1 Gun.

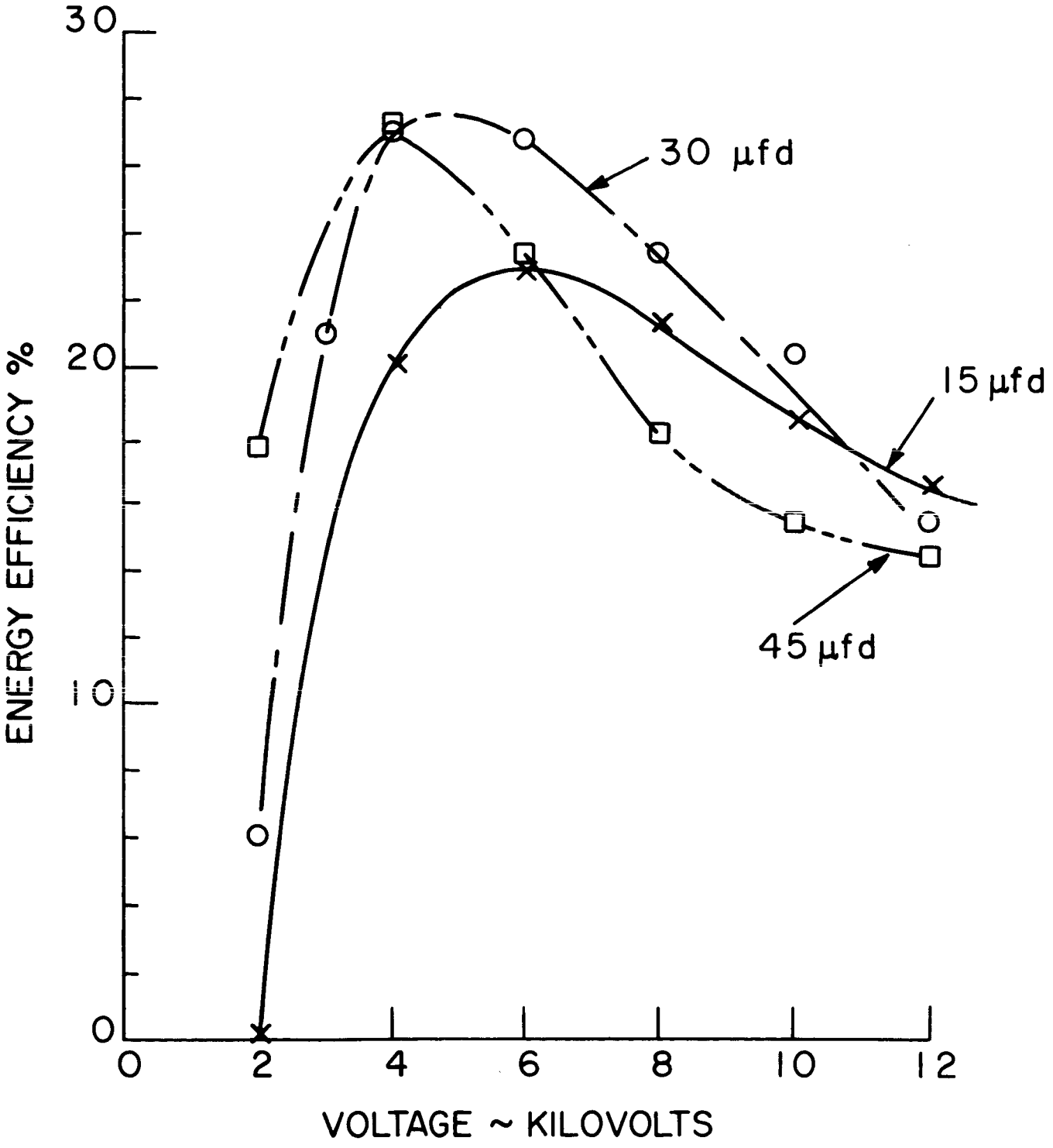

Figure 17. Energy Efficiency vs Initial Capacitor Voltage for Different Bank Capacitiances - Mod. A-1 Gun.

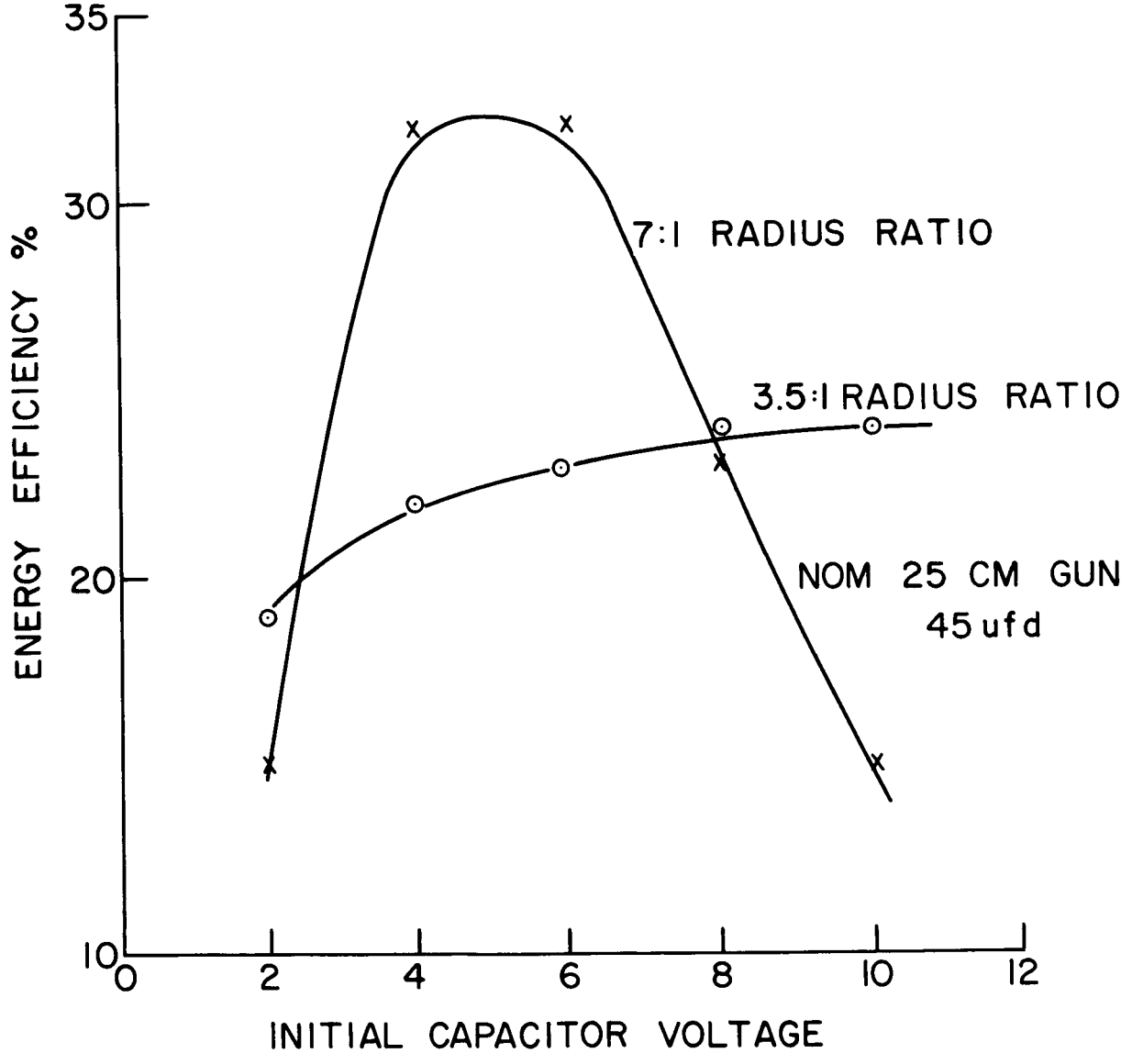

Figure 18. Energy Efficiency vs Initial Capacitor Voltage for Different Radius Ratios - Mod. A-1 Gun.

of 33%. In order to derive the maximum benefit from axial propellant injection, however, it is desirable to have better control of both the location and the time of initial discharge. The return to a two-stage approach, with a first stage for ignition of the discharge, presented a possible means of accomplishing these ends in addition to lowering the density at which the accelerator could be triggered, and lowering the initial inductance of the circuit at the onset of the discharge.

8. MOD. A-2 PLASMA ACCELERATOR

8.1 Specifications (See also Fig. 19)

*Propellant feed:	Axial injection 1 cm behind the front face of the insulator; pulsed nitrogen into 10^{-5} - 10^{-6} mm background.
Port size:	Six holes, each 1.35 mm diameter.
*Operating modes:	Two-stage, with breech trigger electrodes, and single stage, with gas-triggered discharge.
Outer Electrode:	8.75 cm diameter, 20 cm long.
*Inner Electrode:	27^{o} transition from 5 cm diameter to 2.54 cm diameter at the insulator, straight section 1 cm long followed by 27^{o} transition to 1.27 cm diameter. End of the electrode 3.5 cm from the end of the outer electrode.
Capacitor Bank:	Mark II

8.2 General Description

The configuration of the Mod. A-1 accelerator was modified as specified to accommodate the first stage which was a set of six trigger electrodes protruding through the flange of the high potential inner electrode and through the interflange pyrex insulator. A drawing of the arrangement is shown in Fig. 19. The first stage discharge consisted of ignition transformer discharges of about 15 KV between the trigger electrodes and the grounded electrode.

8.3 Exhaust Stream Calorimetry

In single stage operation, the former peak efficiency of 33% dropped

---

*-Changes from Mod. A-1 Accelerator.

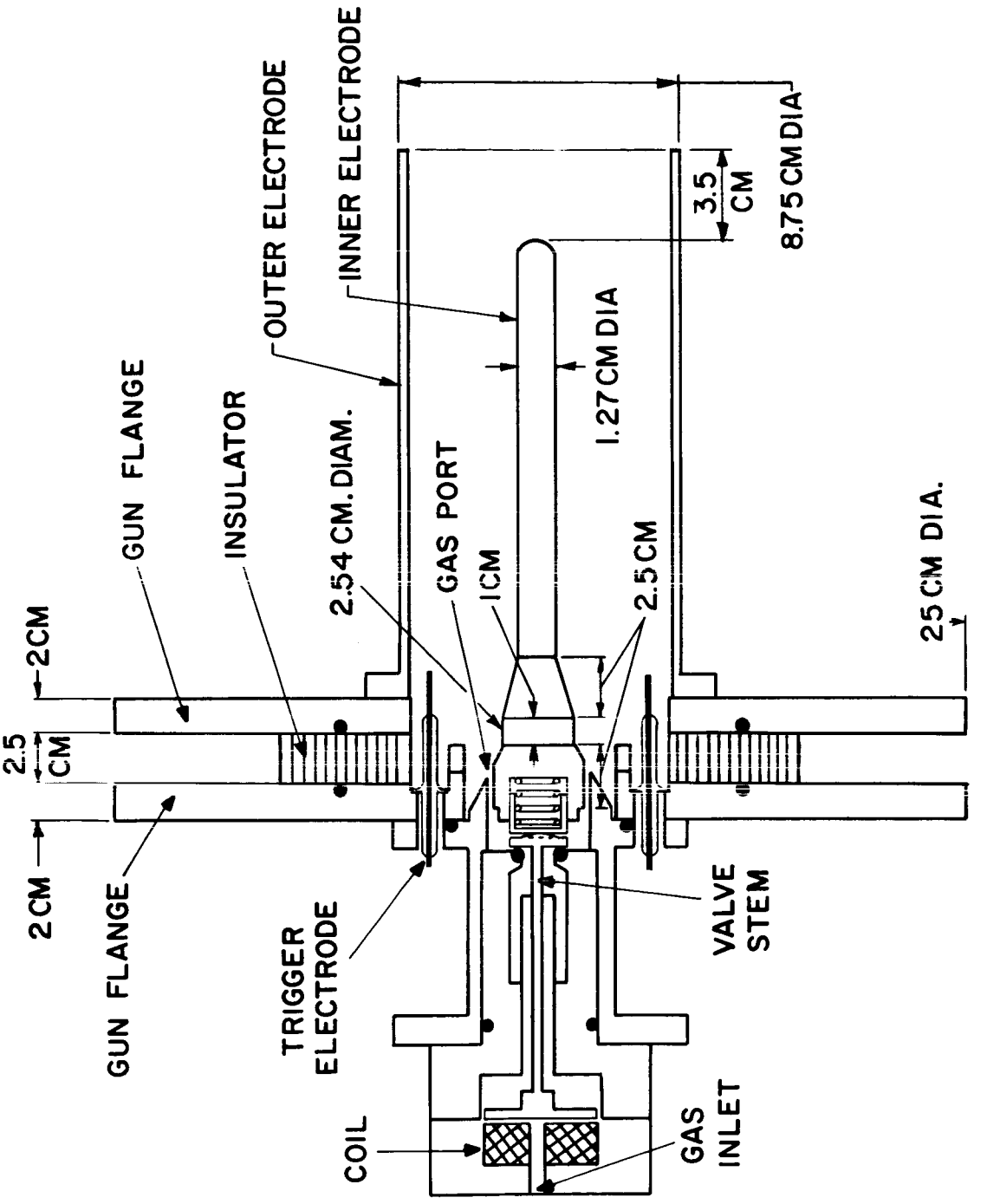

Figure 19. Mod. A-2 Accelerator.

to about 20%, presumably as a result of moving the gas ports closer to the breech, placing the inner electrode transition at the breech, and/or installing a different glass insulator required for the trigger electrodes. When the trigger electrodes themselves were removed from this configuration, no change in performance resulted. When the unit was operated in the two-stage mode, the peak efficiency rose to 30%, indicating that the two-stage breech-triggered operation might be applied successfully to more efficient single stage configurations, as well.

8.4 Pre-fire Gas Distribution

In operating the trigger electrodes to fire the second stage at times prior to 1200 microseconds after the valve discharge (at which time cold gas triggering normally took place), it was found that the second stage discharge could be initiated reliably and instantaneously anywhere in the period from 700 to 1200 microseconds after the valve discharge. Operation of the trigger electrodes earlier than at 700 microseconds failed to ignite the second stage instantaneously; in fact, earlier triggering usually resulted in delayed second stage breakdown, at about 700 microseconds. The implication is that gas just begins to fill the barrel at 700 microseconds, then flows for 500 microseconds (or about 20 cm in the gun barrel) before cold gas breakdown occurs. This appeared to represent a factor of five improvement over the extent to which the gun barrel was filled prior to cold gas breakdown in the Model A gun.

8.5 Discussion

The use of the discharge triggering first stage brought a net increase in efficiency for this particular configuration, demonstrated that significant propellant flow times were obtainable, and indicated that the time and location of discharge initiation might be controllable. Rather than determining the source of the dilatory effect on efficiency at this time, the original Mod. A-1 inner electrode configuration was reinstituted, the trigger electrodes temporarily removed, and the examination of additional effects of geometric changes continued.

9. MOD. A-3 PLASMA ACCELERATOR

9.1 Specifications

Propellant feed:	Axial injection 5 cm from the front face of the insulator; pulsed nitrogen into 10^{-5} - 10^{-6} mm background.
Port size:	Six holes, each 1.35 mm diameter.
Operating mode:	Single-stage; gas triggered discharge.
*Outer Electrode:	12.5 cm diameter 20 cm long.
*Inner Electrode:	5 cm diameter to a distance 3.5 cm from the front face of the insulator, followed by a 27^{o} transition to 2.54 cm diameter, a straight section 1 cm long, and a second 27^{o} transition to 1.27 cm diameter; end of the electrode 3.5 cm from the end of the outer electrode. Another configuration eliminated the second transition and utilized a straight section 2.54 cm diameter.
Capacitor Bank:	Mark II

9.2 General Description

An increase was made in the diameter of the outer electrode from 8.75 cm diameter to 12.5 cm diameter. The change to a larger electrode radius ratio was made not only to increase the inductance per unit length of the accelerator, but to decrease the losses due to particle-wall collisions and to provide more extensive gas filling of the barrel prior to breakdown.

9.3 Exhaust Stream Calorimetry

The next significant improvement in energy engine efficiency was brought about by this increase in electrode radius ratio from 7:1 to 10:1.

---

*-Change from Mod. A-2 Accelerator.

With other initial conditions unchanged, peak energy efficiency increased from 33% to 40.8%. The results of a series of measurements with a 20 cm gun length are included in Fig. 20.

9.4 Exhaust Stream Spreading

A carriage was designed and placed into operation to permit exhaust stream calorimetry at various points along the axis of the gun. At the time the design was fixed, the dimensions were such as to permit capturing the entire exhaust stream from the 8.75 cm diameter gun at the point of closest approach of the carriage, taking into account the half-angle spreading of about 23^{o} observed in the previous contract period[1]. Space limitations and the demands for flexibility of arrangements within the tank precluded making generous allowance for any larger spreading, or for the larger diameter barrels which were later studied. Calorimeter derived efficiencies plotted as a function of intercepted half angle are shown in Fig. 21. If calorimetric data at higher interception angles had been available, as for the A-4 gun, higher energy efficiencies probably would have been observed.

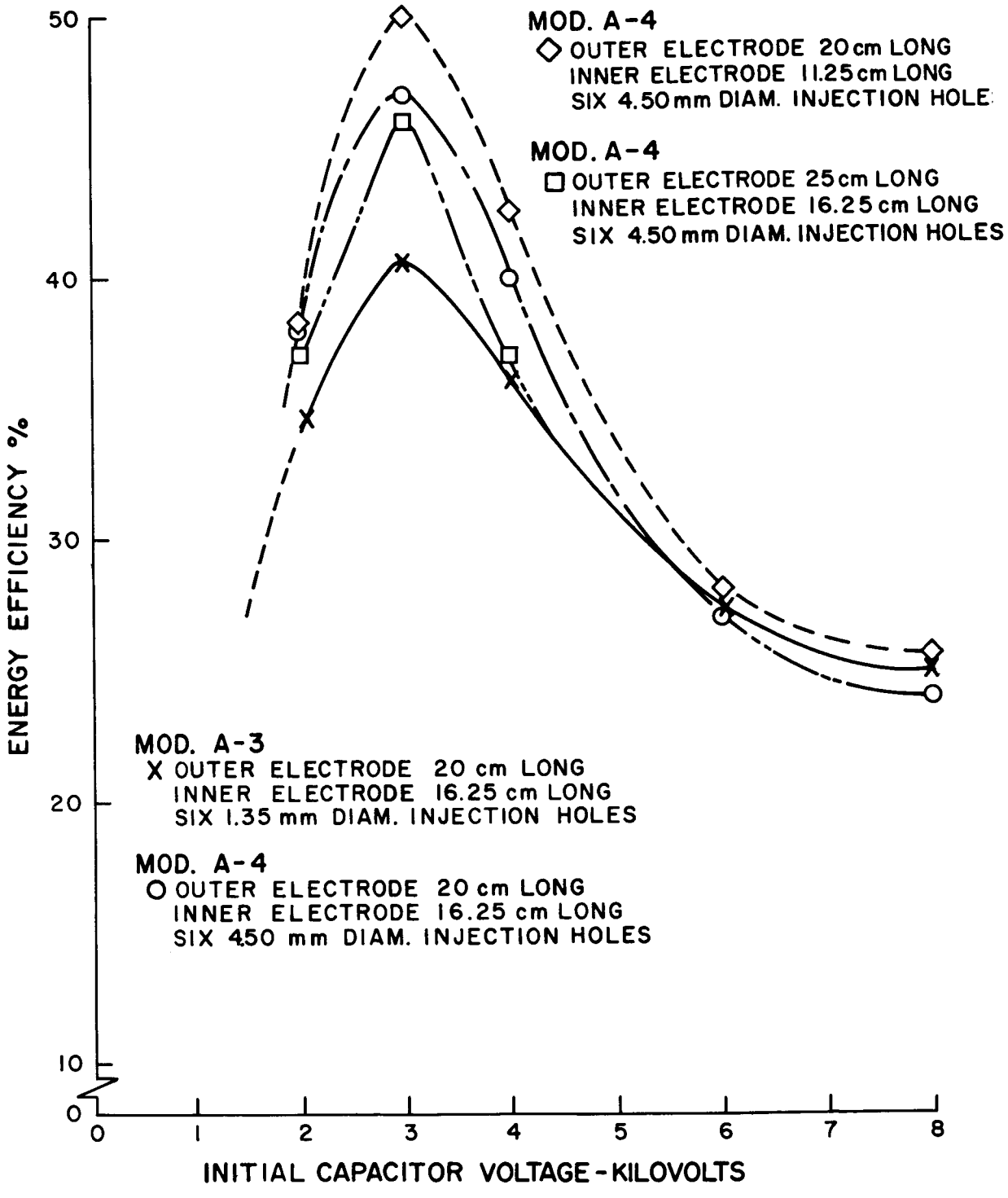

Figure 20. Energy Efficiency vs Initial Capacitor Voltage - Mod A-3 and Mod A-4 Guns.

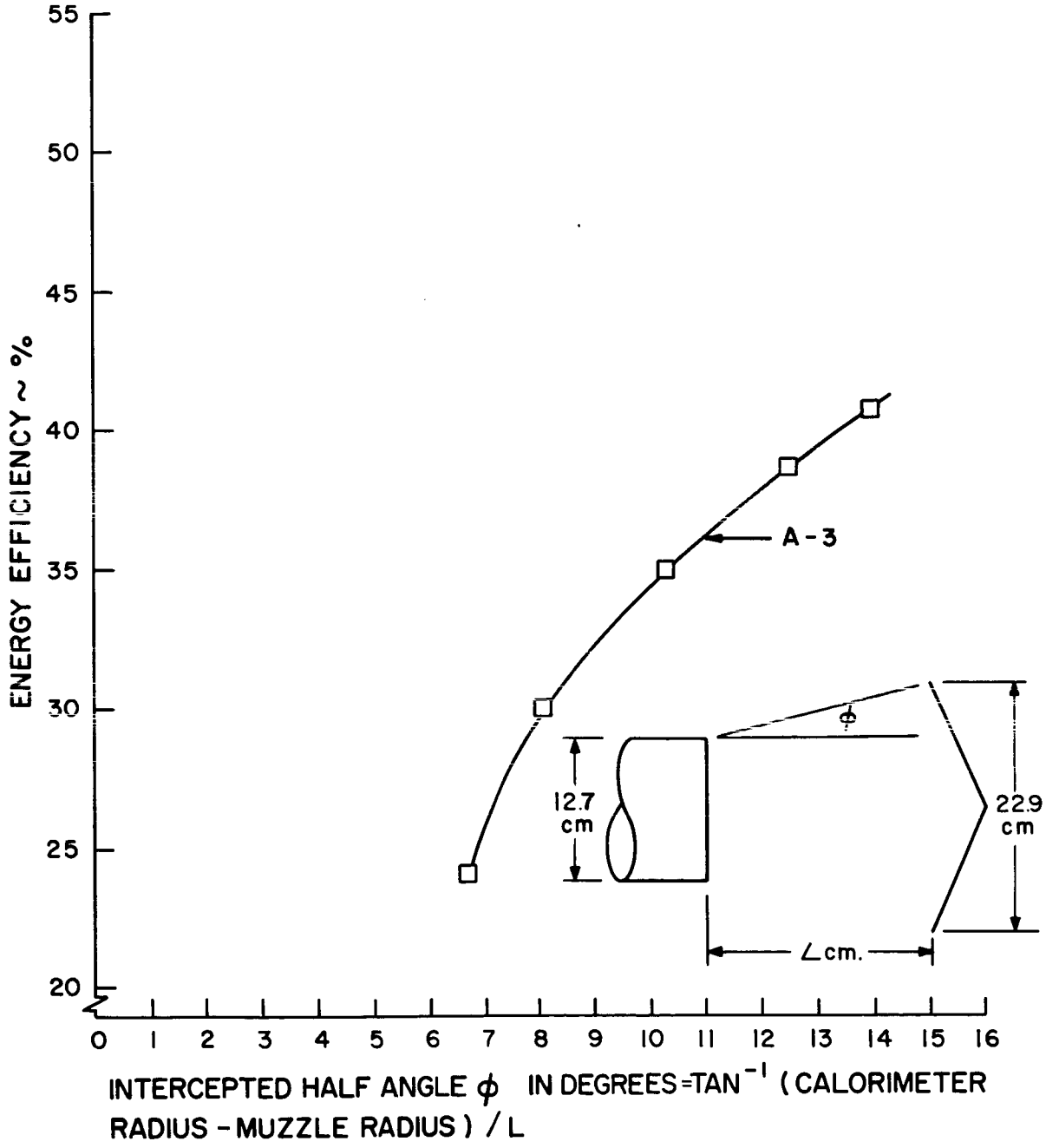

Figure 21. Energy Efficiency vs Half Angle of Spreading - Mod. A-3 Gun.

9.5 Terminal Waveforms (See Fig. 22)

It is significant that the first half cycle period for the current was increased by almost 50% over that observed with the Model R gun with the Mark II bank (see Fig. 5b). This indicates that $\dot{L}$ for the Mod. A-3 gun is considerably higher than that for the Model R gun. The less than 10% reversal compared to over 30% for the Model R gun implies, also, that a greater fraction of the initially stored energy was utilized during the first half cycle of current. In fact, only 13% of the initially stored energy was dissipated in the resistance of the Mark II bank as compared with 58% for the same bank (with the same resistance) using the Model R accelerator. It should be noted that the almost equal ringdown period for the two guns was in accord with the fact that the external circuit inductances were not significantly different.

9.6 Discussion

The trend to increased efficiency with increased radius ratio suggested that a next step might have been a further increase in the diameter of the outer electrode or a decrease in the diameter of the inner electrode. The diameter of the central hole in the existing capacitor bank flange through which the barrel protruded was too small to permit ready installation of a larger outer electrode, however. At the same time, it was felt that the 1.27 cm diameter of the inner electrode was at a minimum to preserve structural integrity in an accelerator operating at a reasonable power level. The emphasis was shifted temporarily to possibly further improvement of gas loading as well as study of the effects of changes in inner electrode lengths with stationary outer electrode lengths.

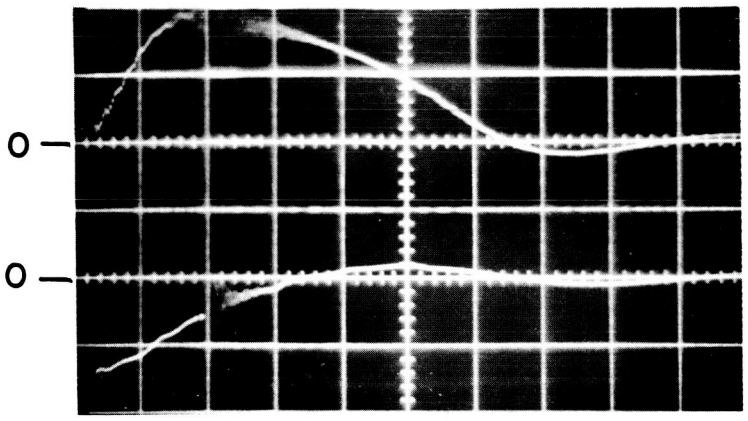

Figure 22a. Voltage and Current Transients - Mod. A-3 Gun.

Upper Trace Current - 22.4 K amps/cm.
Lower Trace Voltage - 2 KV/cm.
t = 1 usec/cm.

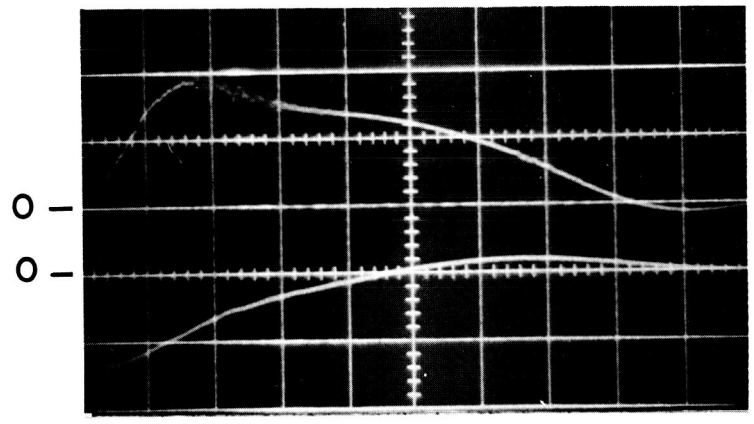

Upper Trace Current - 22.4 K amps/cm.
Lower Trace Voltage - 2 KV/cm.
t = 1 usec/cm.

Figure 22b. Voltage and Current Transients - Mod. A-4 Gun.

10. MOD. A-4 PLASMA ACCELERATOR

10.1 Specifications (See also Fig. 23 and 24)

Propellant feed:	Axial injection 5 cm from the front face of the insulator; pulsed nitrogen into 10^{-5} - 10^{-6} mm background.
*Port size:	Six holes, each 4.50 mm diameter.
Operating mode:	Single stage; gas triggered discharge.
Outer Electrode:	12.5 cm diameter, 20 and 25 cm long.
*Inner Electrode:	5 cm diameter to a distance 3.5 cm from the front face of the insulator, followed by a 27^{o} transition to 2.54 cm diameter, a straight section 1 cm long, and a second 27^{o} transition to 1.27 cm diameter; end of the electrode 3.5 cm from the end of the outer electrode, then varied from 0 to 12 cm from the end of the outer electrode.
Capacitor Bank:	Mark II

10.2 General Description

With electrode radius ratio limited to a maximum of 10:1, the only additional configuration changes studied during this contract period involved the effects of shortening of the inner electrodes to the lengths specified and enlarging the injection port diameters to 4.5 mm.

In order to once more study the effects of the presence and operation of a triggering first stage, the accelerator flanges were modified to accommodate the trigger electrodes described earlier. This time, however, the interior geometry of the electrodes was not significantly altered.

---

*-Changes from Mod. A-3 Accelerator.

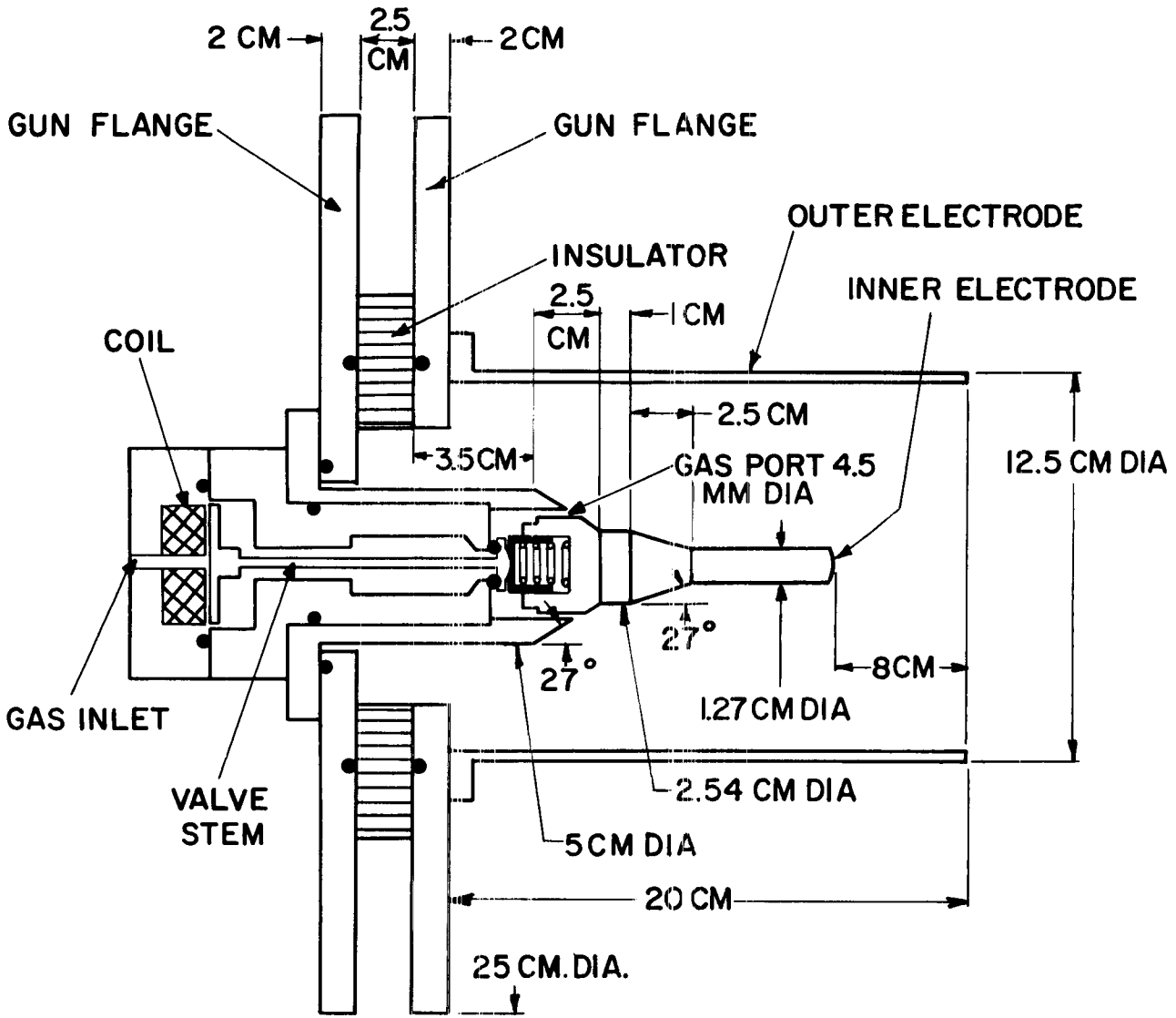

Figure 23. Mod. A-4 Accelerator.

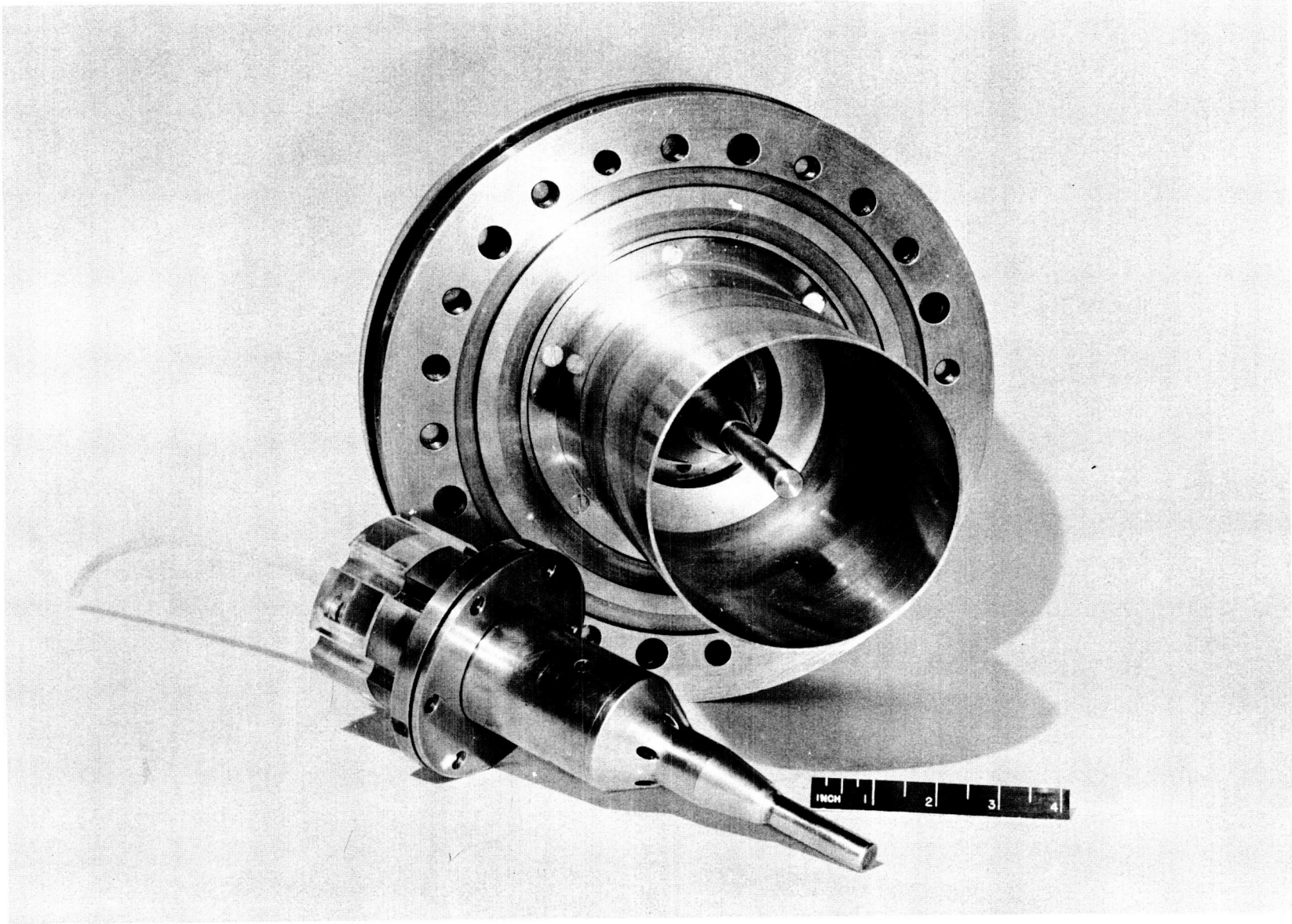

Figure 24. Mod. A-4 Accelerator.

10.3 Exhaust Stream Calorimetry

For reasons which will be discussed later, a new calorimeter was used in a portion of the measurements to be described in this section. This new calorimeter was also used in most of the succeeding measurements. The results for the original unit are described first, while those for the new unit with the same accelerator are described in the next section.

10.3.1 Measurements with the Original Calorimeter

Several trends were studied for the Mod. A-4 Accelerator, each leading either to optimum or increased efficiency.

The enlargement of the propellant injection holes to 4.5 mm diameter resulted in boosting the peak energy efficiency to 47.5% (see Fig. 20), presumably as a result of further improvement of the prefire distribution of the propellant in the gun barrel.

As shown also in Fig. 20 the 20 cm length outer barrel seemed slightly more efficient in operation than the previous optimum length of 25 cm realized for the Mod. A-1 gun.

Another important factor in improving the gun efficiency is the discovery that optimum results are obtained when the inner electrode is shorter than the outer. This is illustrated by the data summarized in Fig. 25.

The highest energy efficiency achieved as a result of these parametric studies was 50%.

10.3.2 Measurements with New Calorimeter

The calorimeter measurements of energy efficiency have been carried out using calibration procedures and measuring techniques deemed conservative. For example, the radiative losses incurred between shots (nine shots are accumulated for one calorimetric reading) have been neglected. Measurements indicated that in the course of a run of nine shots fired about a second apart, as much as 10% of the total energy collected by the calorimeter may be lost in radiation. In order to minimize this loss and permit better sampling of accelerator performance, a calorimeter of considerably greater mass (980 gms vs 142 gms) but only slightly larger diameter (25 cms vs 23 cm) than the unit used previously was installed. In order to minimize possible losses due to sputtering ablation, the calorimeter incorporated a somewhat reentrant design. Drawings of the old and new units are shown in Fig. 26.

With the distance between the calorimeter and the muzzle end of the gun the same as with the previous calorimeter, the new energy efficiencies measured were approximately 10% higher than those obtained previously. Peak efficiency was 54% at 3 KV. Additional data showing the trend in efficiency vs voltage for the particular gun used are shown in Fig. 27.

Also shown in Fig.27 are the results of measurements on a Mod. A-4 gun accelerator in which the interflange space, and hence the stray inductance of the flange assembly, was decreased by over 50% through use of a thinner interflange insulator. The peak efficiency measured was unchanged from

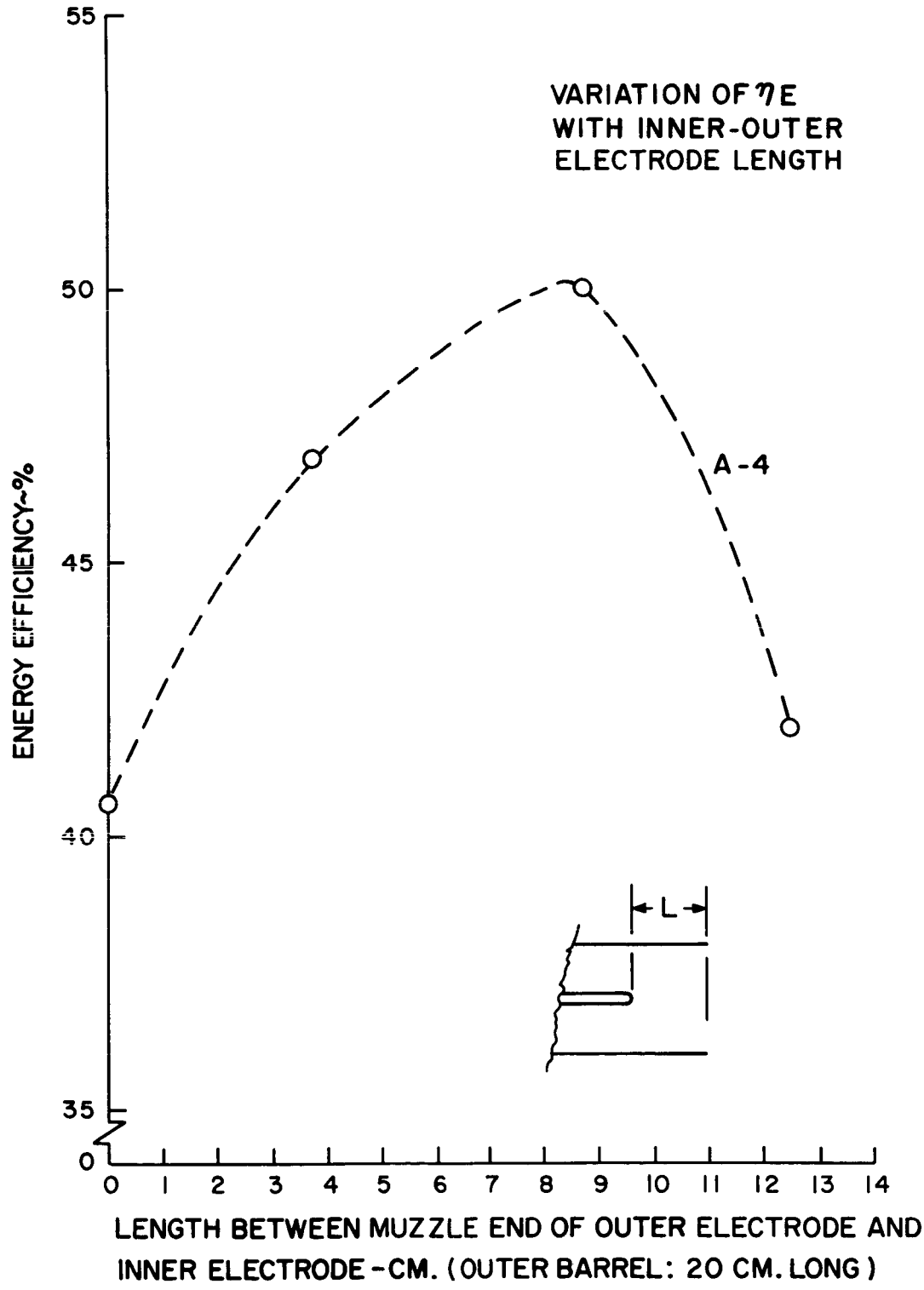

Figure 25. Energy Efficiency vs Difference in Inner - Outer Electrode Lenth - Mod. A-4 Gun.

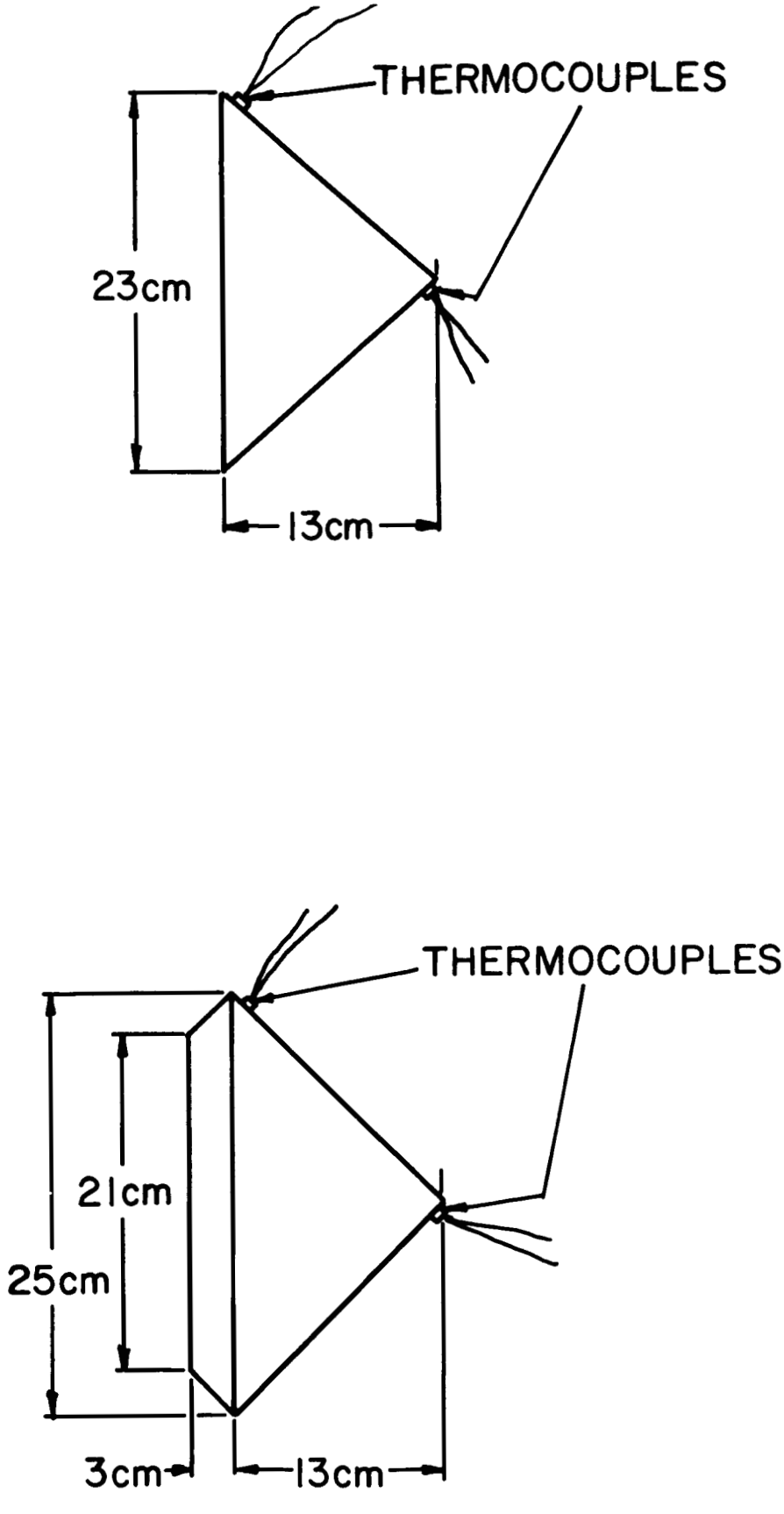

Figure 26. Calorimeters for the Determination of Energy Efficiency.

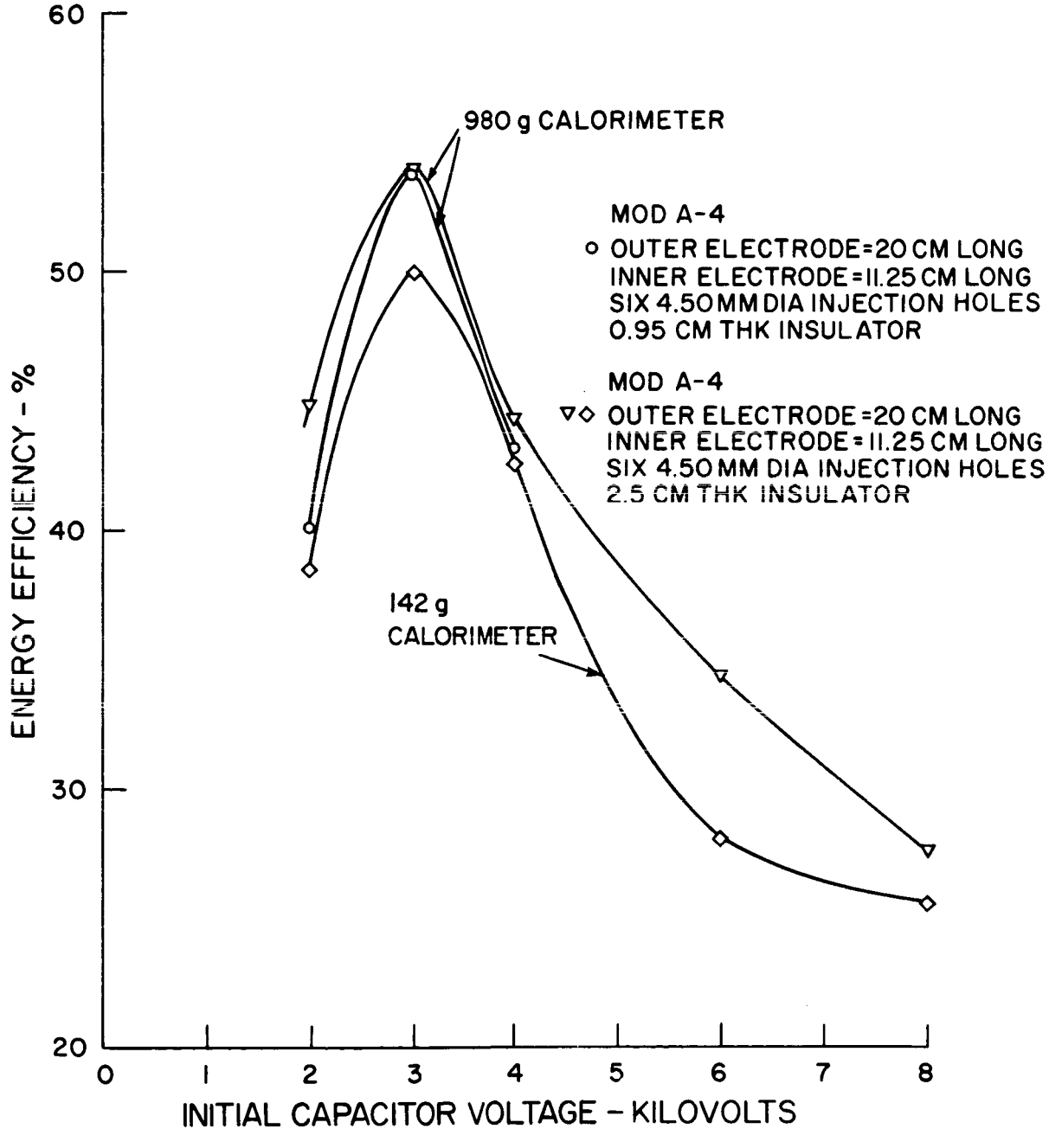

Figure 27. Energy Efficiency vs Initial Capacitor Voltage - Mod. A-4 Gun Improved Calorimeter.

previous values at 3 KV, and was slightly lower at other voltages.

10.3.3 Some Comments on the Interpretation of Calorimeter Data

Some questions have been raised as to the extent to which recombination and radiation from the accelerator contribute to the energy collected by the calorimeter. A few order-of-magnitude estimates are made here to establish an upper limit for such contributions.

The most straightforward computation involves the ionization and dissociation energies carried by the plasma exhaust stream. This involves knowing the number of particles ejected per pulse. Assuming that only propellant species are accelerated (as evidenced by some earlier spectrometric measurements), then an upper limit to this number is given by the number of particles inserted into the accelerator per shot. The largest amount of nitrogen injected per shot in all of the experiments to date has been about 150 micrograms. Using 15 eV for the energy of ionization of nitrogen atoms and 7.5 eV for the energy of dissociation of the molecule, the stream could carry as much as 19 joules per shot of ionization and dissociation energy, assuming complete dissociation and ionization. Under the most efficient operating conditions, 203 joules are discharged through the system, so that less than 10% of the total energy is so utilized.

Determination of the thermal (random) energy content of the stream will have to wait until cross-sectional exhaust stream measurements have been made with a calorimeter for the Mod. A-4 gun.

Radiation from the gun has also been suggested as a possible source of energy collected by the calorimeter. Part of the possible sources of radiation have already been accounted for in the dissociated and ionized species. In fact, if these species radiate prior to entry into the calorimeter, then most of their energy will escape the calorimeter, so that we have already overcompensated for this possibility. The only other reasonable source of radiation is from the collisions of electrons either in the volume of the discharge or at the electrodes, the acceleration of ions in the cathode fall potential region, and the collisions with the walls by heavy particles having transverse motion. An estimate of the first two contributions may be obtained by the following argument: Using as typical the less than 100 volt drop across the current sheet as reported by Burkhardt and Lovberg[4], let us choose 100 volts as an upper limit of potential drop experienced with 3 KV (54% efficiency) operation. The maximum current under the best operating condition is about 40,000 amperes and the time interval is about 7 microseconds, so an upper limit of energy invested in resistive losses in the current sheet is 28 joules, of which, if all radiated, only 7 joules at most can be intercepted by the calorimeter, representing an upper limit of 4% of the total energy from this source. As for the conversion of transverse energy into radiation at the electrodes, the determination will have to await the acquisition of exhaust stream cross-sectional characteristics data, but, of the total amount of energy so converted, only one quarter can be collected.

B_θ probe measurements in the vicinity of the calorimeter position 20 cm from the gun show that the field is less than 150 gauss (the limit of detectability in the probe signal) at that location at all times so that inductive and i^2R heating of the calorimeter may be neglected.

It should be re-emphasized that all of these estimates are obtained by making the least favorable assumptions. An experiment was performed to obtain empirical knowledge of the contribution to the calorimeter due to radiation from the heated electrodes: The gun was fired 200 shots with the calorimeter extracted. The calorimeter was immediately moved in front of the gun (within 30 seconds) at the end of the discharge period. No energy at all was radiated to the calorimeter, so the temperature of the gun had not significantly risen.

10.3.4 Measurements of Extended Loop Currents

In order to further substantiate the validity of using exhaust stream calorimetry to indicate directed energy in the exhaust, a few additional experiments were performed. One of these involved determination of the magnitude of any current loops exterior to the interelectrode volume. A calibrated, glass-enclosed Ragowski loop with a 7.5 cm diameter was placed at varying distances downstream from the muzzle. With the center of the loop on the axis of the accelerator and 15 cm from the muzzle, currents as high as 1000 amperes were measured when an initial capacitor voltage of 3 KV was used. At 2 KV, 500 ampere currents were measured. At a distance 75 cm from the muzzle, less than 30 amperes were measured at 3 KV, with less than 10 amperes at 2 KV.

Using the worst possible assumptions, i.e., that all of the terminal voltage at peak current appears across the current plume (1.6 KV), the maximum possible peak power dissipated there can be no more than 1.6 MW. On the other hand, the peak power in the gun due to the time - dependent inductance ($\dot{L}$ = .046 ohms, I = 4×10^4 amps) was 74 MW. Thus, even under the worst assumption, only 2.2% of the total peak power can be dissipated in the plume.

10.3.5 Auxiliary Calorimeter Measurements

As a final verification of the contention that the magnitude of I^2R heating was small compared to the heating of the calorimeter from conversion of directed kinetic energy, calorimeters of larger size and improved design were constructed and placed at a distance from the muzzle which the Ragowski loop measurements indicated to be free of gun currents.

The first calorimeter employed was a single cylindrical unit weighing 2535 gms, 45 cm in diameter and 45 cm long, with cone 12 cm long with its apex towards the gun. The distance from the leading edge of the calorimeter to the muzzle of the gun was varied from 12 cm to 70 cm by mounting the calorimeter on a carriage assembly which was positionable from the exterior of the vacuum tank. At 3 KV, with 25-50 shot samples, efficiencies ranged between 55% - 64% at the 12 cm position and 45% - 55% at the 70 cm position. The relatively wide spread of efficiency readings at any single position was due not to the performance of the accelerator but to the reliability of the

measurements which were hampered by a combination of poor heat distribution in the large surface of light gauge metal, radiation cooling, particularly of the section of calorimeter positioned above the diffusion pump cold cap, and the small temperature rise measured by the limited number of thermocouples in the single unit.

In an attempt at obtaining better data, a two-section calorimeter of heavier metal, radiation shielded, and with more thermocouples, was installed. It consisted of a forward cylindrical section with a 45 cm diameter, a 25 cm length, and a weight of 2366 gms and a downstream combination cylinder and inverted cone, with a 45 cm diameter, a 12 cm length, and a weight of 3680 gms. The units were 1 cm apart and enclosed by a separate aluminum foil housing which served as a radiation shield. A photo of the calorimeter, without shield, is shown in Fig. 28. Seventy-five shot samples were used for each measurement. With the leading edge of the cylinder 75 cm from the gun muzzle, an efficiency of 55% was measured at 3 KV. Of the 55% total, 18.5% was accounted for in the forward cylinder, with 36.5% in the downstream cone-cylinder combination.

The readings appear to verify the earlier measurements with the smaller calorimeter at closer proximity to the gun. It is possible that any decrease in heating due to minimization of effects other than those due to plasma kinetic energy may have been compensated for by improved calorimeter design. This could result in enhanced trapping of the incident plasma and any possible sputtered calorimeter wall material.

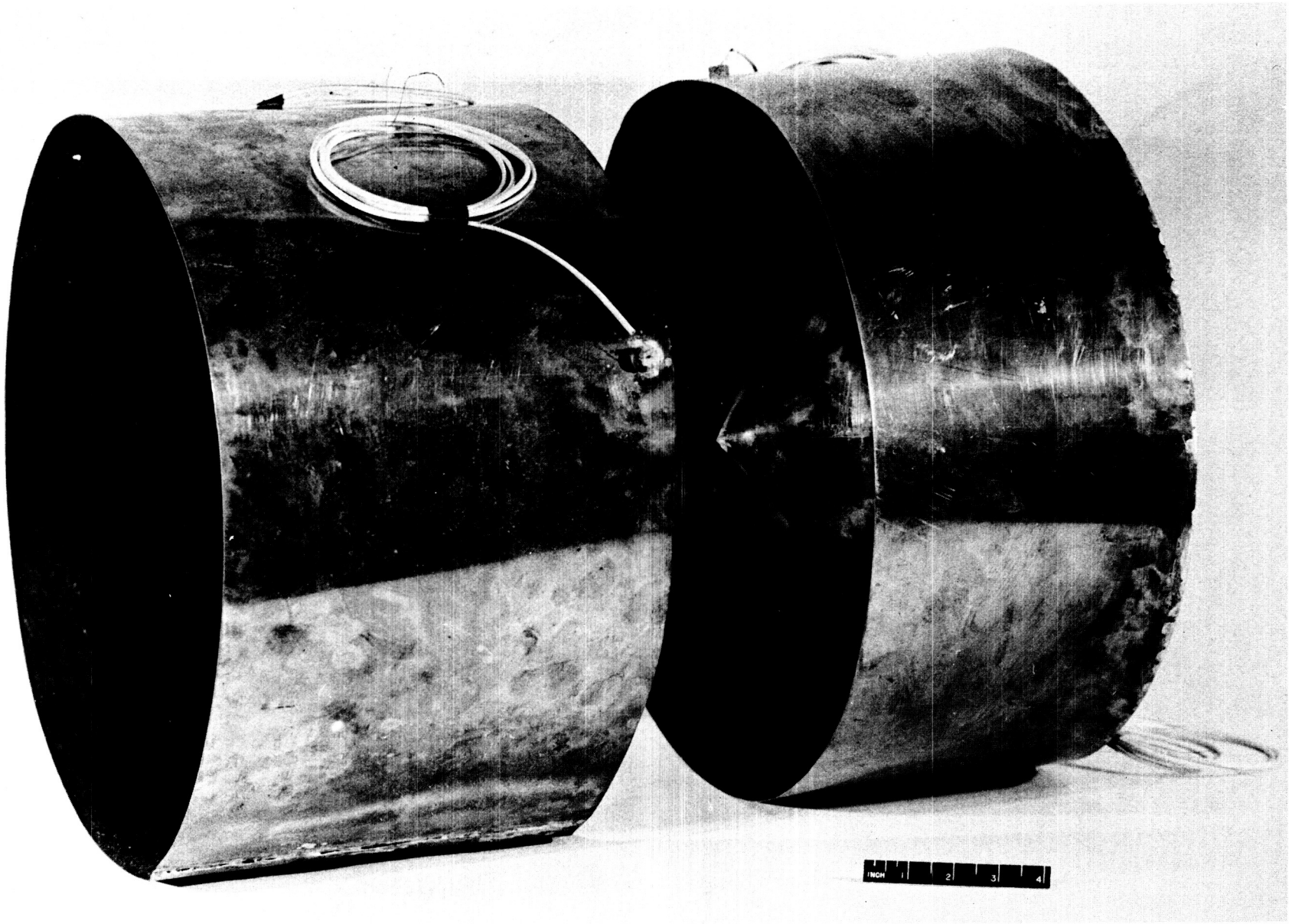

Figure 28. Large, Two Section Calorimeter.

10.4 Exhaust Stream Spreading

Calorimeter derived efficiencies as a function of axial position were obtained again as for the Mod. A-3 gun, with the smaller calorimeter described in section 10.3. The efficiencies plotted as a function of intercepted half angle are shown in Fig. 29, along with the data from the larger calorimeter.

When the smaller diameter calorimeter was suspended so that its leading edge was 2 cm from the muzzle of the accelerator, 63% of the energy initially stored in the capacitor was collected in the calorimeter. Taking into account the fact that 13% of the energy was dissipated in the resistance of the energy storage system (section 10.5), then only about 87% of the initially stored energy is available for the accelerator. It appears that about 72% of this energy leaves the accelerator in one form or another, and that 28% or less may be lost to the electrodes.

10.5 Terminal Measurements

An oscilloscope trace of representative voltage and current waveforms is shown in Fig. 22b. The same comments apply here as were made for the Mod. A-3 accelerator in section 9.5. In addition, the first half cycle period has been extended by about 35% indicating a further increase in $\dot{L}$. Using the energy storage bank resistance as determined in section 10.6, the I^2R losses up to voltage-zero were 27 joules or 13% of the total energy.

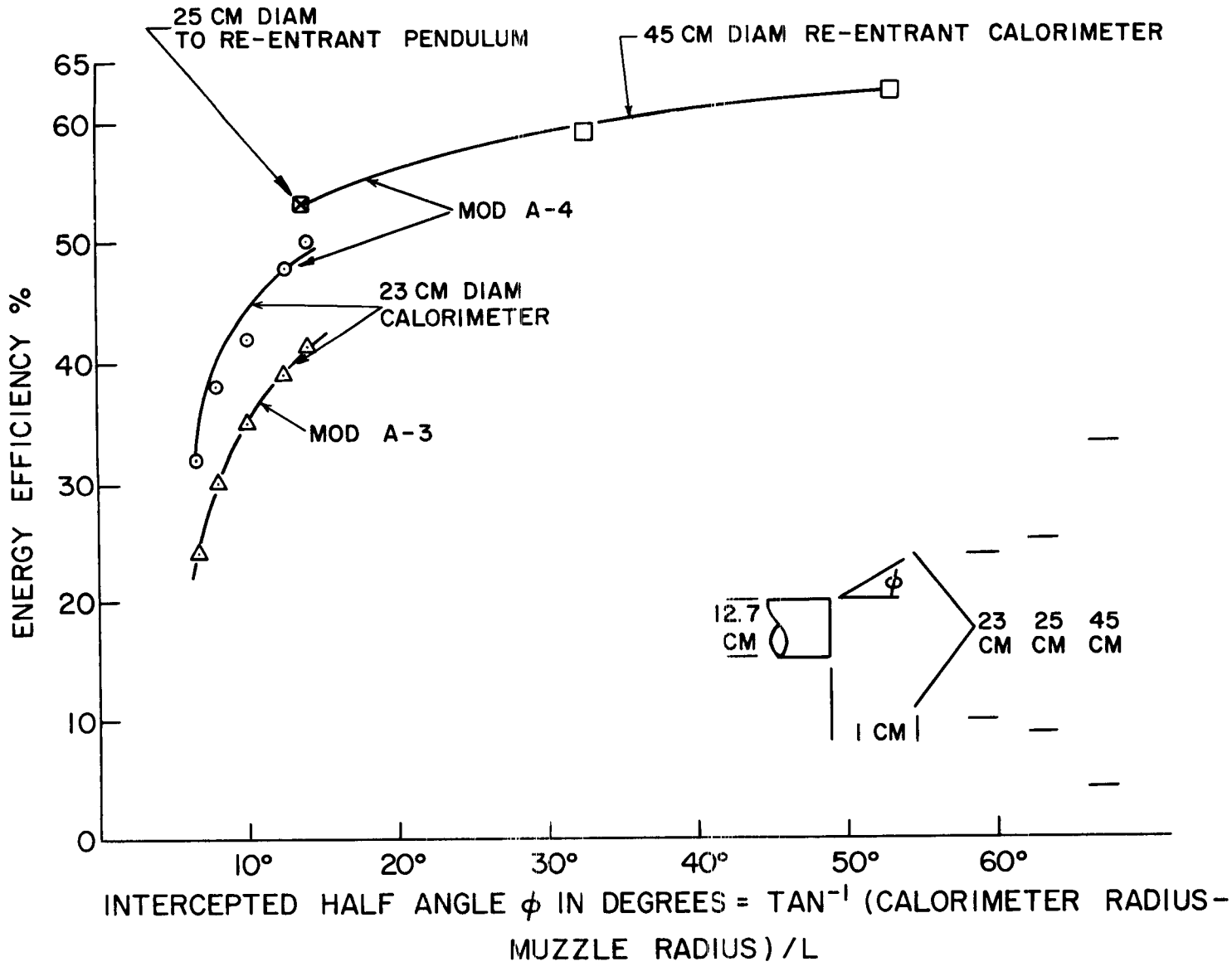

Figure 29. Energy Efficiency vs Half Angle of Spreading - Mod. A-4 Gun.

10.6 Q Measurements on the Energy Storage System

For the purposes of energy bookkeeping, the energy storage system was defined as including the coaxial gun flanges; the gun was defined as only the coaxial cylinders up to the glass insulator.

The discharge method was one of those used to obtain the Q of the system. An ignitron was connected between points on the two gun flanges to which the coaxial cylinders were connected. The L, R, and C of the entire circuit was then determined by the conventional frequency and decrement measurements. The resistance of the energy storage system was determined assuming a knowledge of the characteristics of the ignitron. The latter information is not common knowledge, however, and had to be determined by experiment in the following way: It was assumed that the ignitron resistance is inversely proportional to the current over the range of currents used. The data are tabulated as follows:

f	V	R_{tot}
70 KC	4 KV	.0070 ohms
70 KC	2 KV	.0085 ohms

(10.1)

Where $R_{tot} = R_{\text{storage system}} + R_{\text{ignitron}}$

$$= R_o \sqrt{\frac{\omega}{\omega_o}} + R_{o_{i_g}} \cdot \frac{V_o}{V}, \quad \text{where } V_o = 4 \text{ KV}$$

$$\omega_o = 140\pi \times 10^3 \text{ radians sec}^{-1}$$

(10.2)

The data (10.1) give two equations in two unknowns from (10.2).

The solutions are:

$$R_o = .0055 \text{ ohm}$$

$$R_{o_{i_g}} = .0015 \text{ ohm} \qquad (10.3)$$

Thus the energy storage resistance was found to be

$$R = .0055 \sqrt{\frac{\omega}{\omega_o}} \quad \text{ohms} \qquad (10.4)$$

taking into account the skin effect. (It should be noted that d.c. measurements of the energy storage resistance up to the capacitor terminals indicated values of about .0006 ohms.)

The Q of the storage system is

$$Q = \frac{\omega_o^{1/2}}{\omega^{3/2} C R_o} \qquad (10.5)$$

so that the Q of the system at 100 KC was found to be 5.37 as compared with 9.05 for the individual capacitor units measured at the same frequency.

10.7 B_θ Probe Measurements on the Mod. A-4 Accelerator

A series of B_θ probe measurements were made at various axial positions in and out of the gun, with 2, 3, and 4 KV initially on the energy storage capacitor bank. Some examples of the 2 and 3 KV series are shown in Fig. 30 and 31, along with the Rogowski loop signals taken at the gun terminals. Relatively clean traces were obtained at 2 KV, but both signals became progressively worse as the initial voltage was increased to 3 and 4 KV, as had been experienced with the Mod. A-1 accelerator. The hash

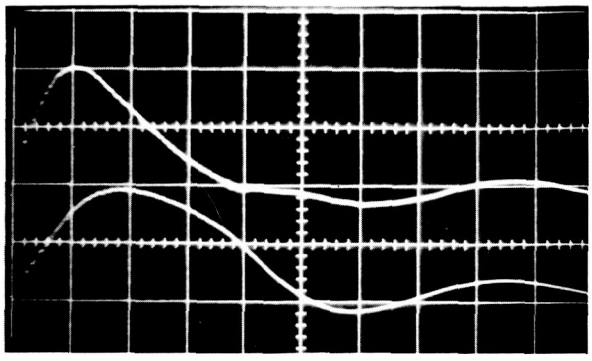

(a) Z = 1 cm

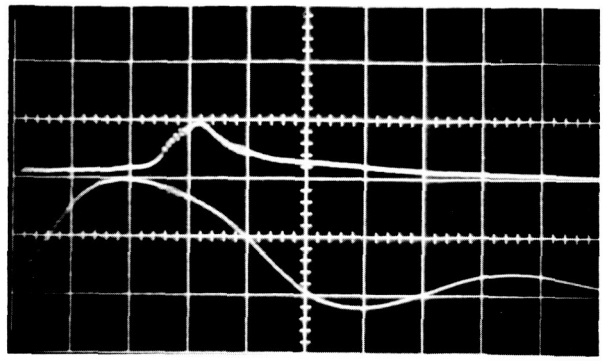

(d) Z = 17.8 cm

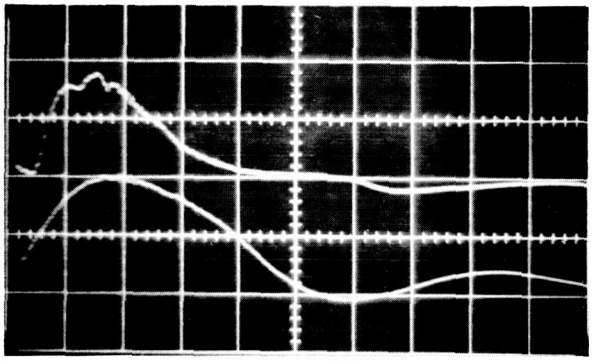

(b) Z = 6.6 cm

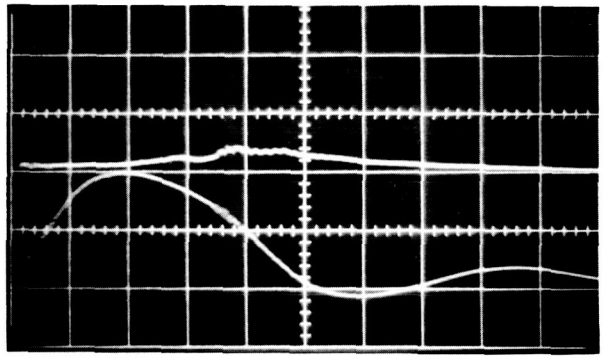

(e) Z = 23.4 cm

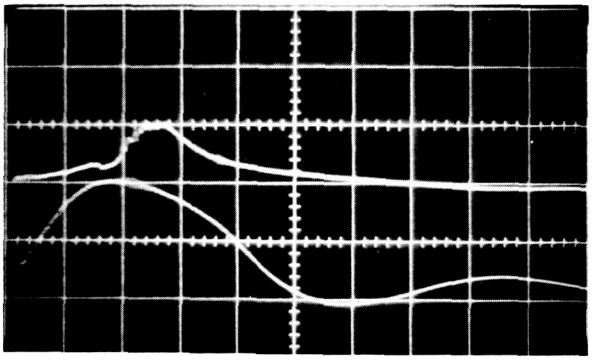

(c) Z = 12.2 cm

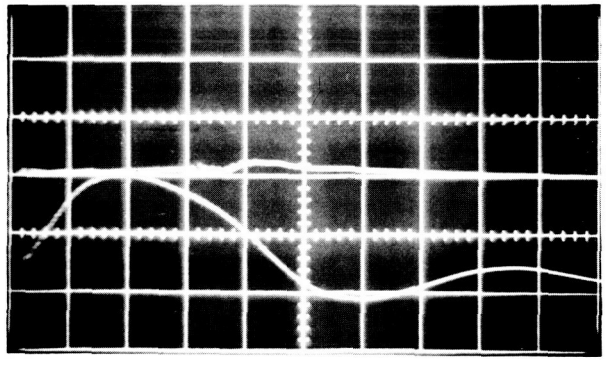

(f) Z = 29.5 cm

Figure 30. B_θ Probe Signals for Different Axial Positions - Mod. A-4 Gun, 2 KV Capacitor Voltage.

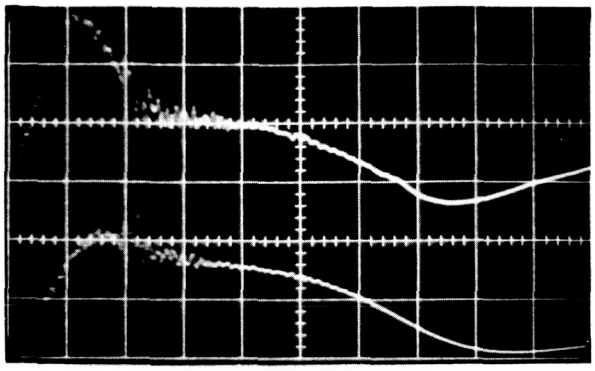

(a) Z = 1 cm

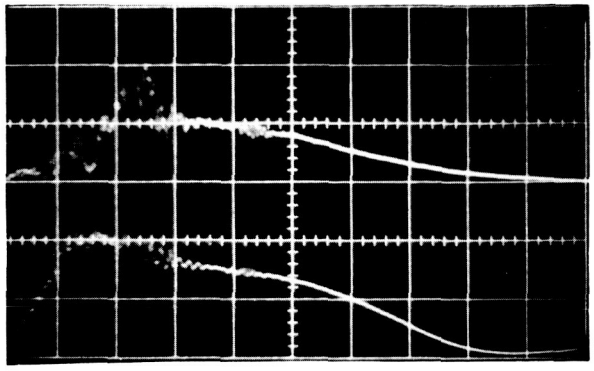

(d) Z = 17.8 cm

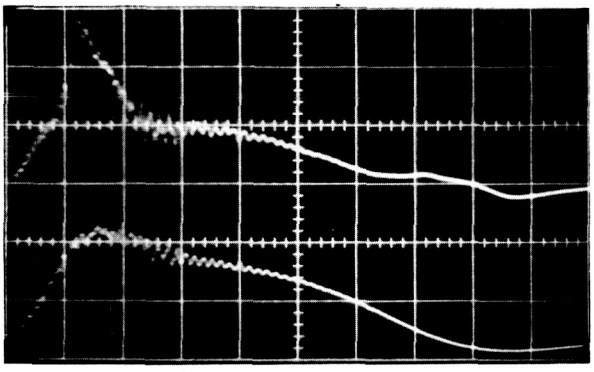

(b) Z = 6.6 cm

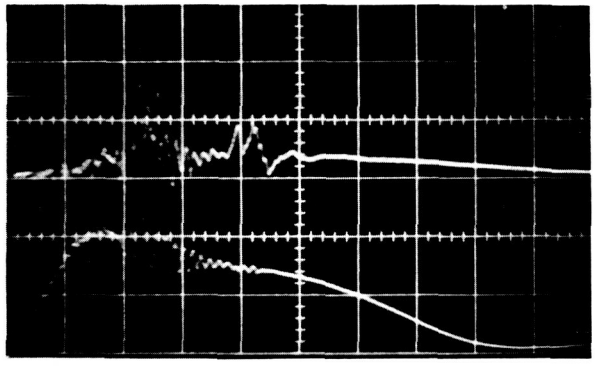

(e) Z = 23.4 cm

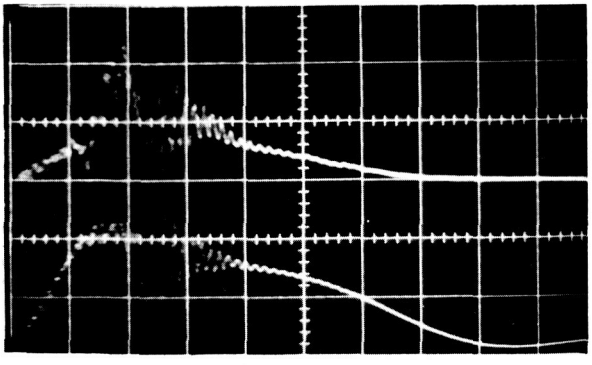

(c) Z = 12.2 cm

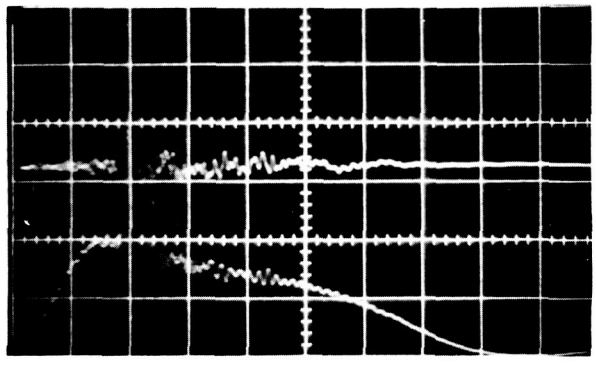

(f) Z = 43 cm(Calorimeter Location)

Figure 31. B_θ Probe Signals for Different Axial Positions - Mod. A-4 Gun, 3 KV Capacitor Voltage.

appearing between 2 and 3 microseconds after discharge on both the Rogowski loop and B_θ probe signals is interpreted as capacitive charging of the B_θ probe carriage, which is insulated from ground, since the hash disappears when the probe carriage is removed. That very small currents are involved is implied by the following: 2) the gross shape of the total current signal is not altered, and b) the hash has a damped oscillatory characteristic of about a 5 mc frequency, implying a low capacitance in the circuit. The B_θ probe signals are replotted as $B_{\theta\,max}$ vs axial position in Figs. 32 and 33. Again, the curves are intended primarily to connect the experimental points. Position of the current sheet as a function of time is plotted in Fig. 34.

As to the information contained in Figs. 30 to 34, several points are apparent:

a) In neither the 2 KV nor the 3 KV case is the simple current sheet model realized in practice; the current is not sufficiently localized in a thin sheet.

b) The period of the discharge is significantly extended in going from 2 to 3 KV operation.

c) The B_θ signal is essentially zero at all times when the probe is at the axial position normally occupied by the calorimeter.

d) The velocity of the current sheet is nearly constant in time.

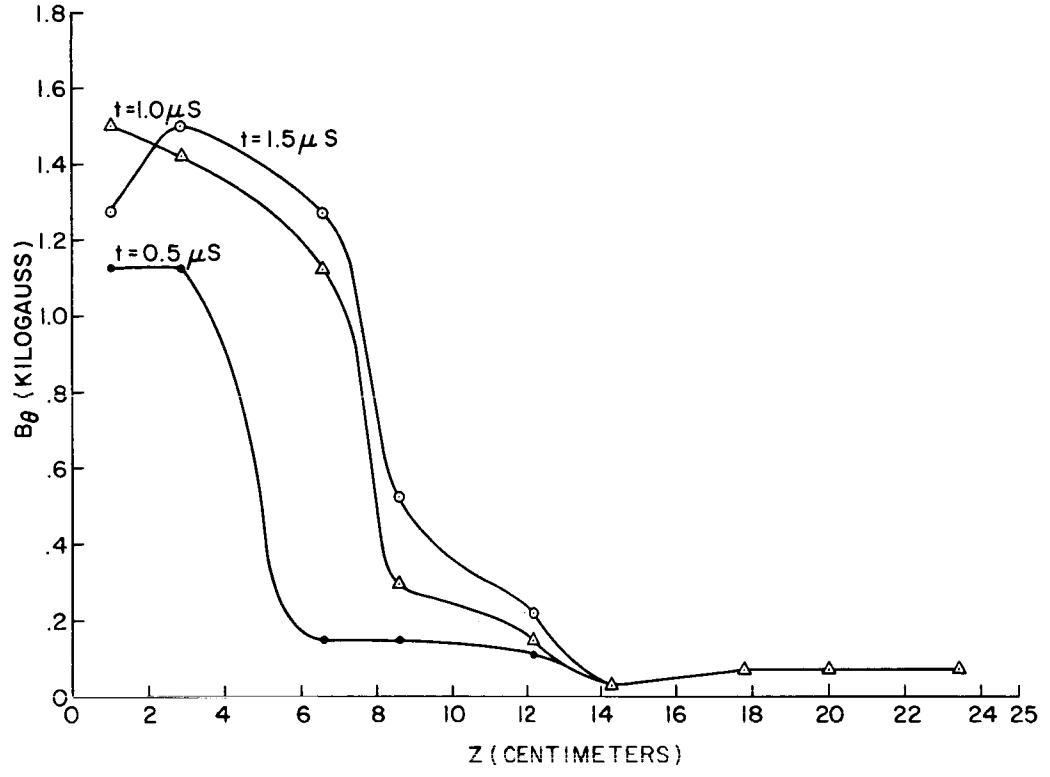

Figure 32a. B_θ vs Axial Position, Mod. A-4 Gun @ 2 KV.

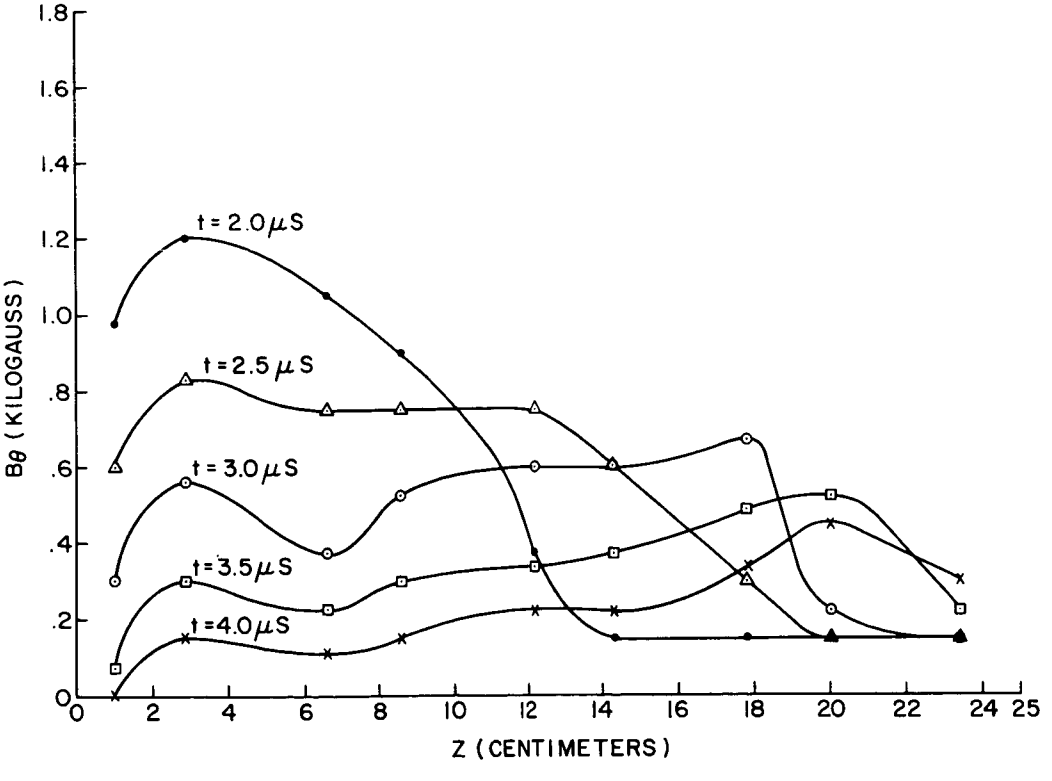

Figure 32b. B_θ vs Axial Position, Mod. A-4 Gun @ 2 KV.

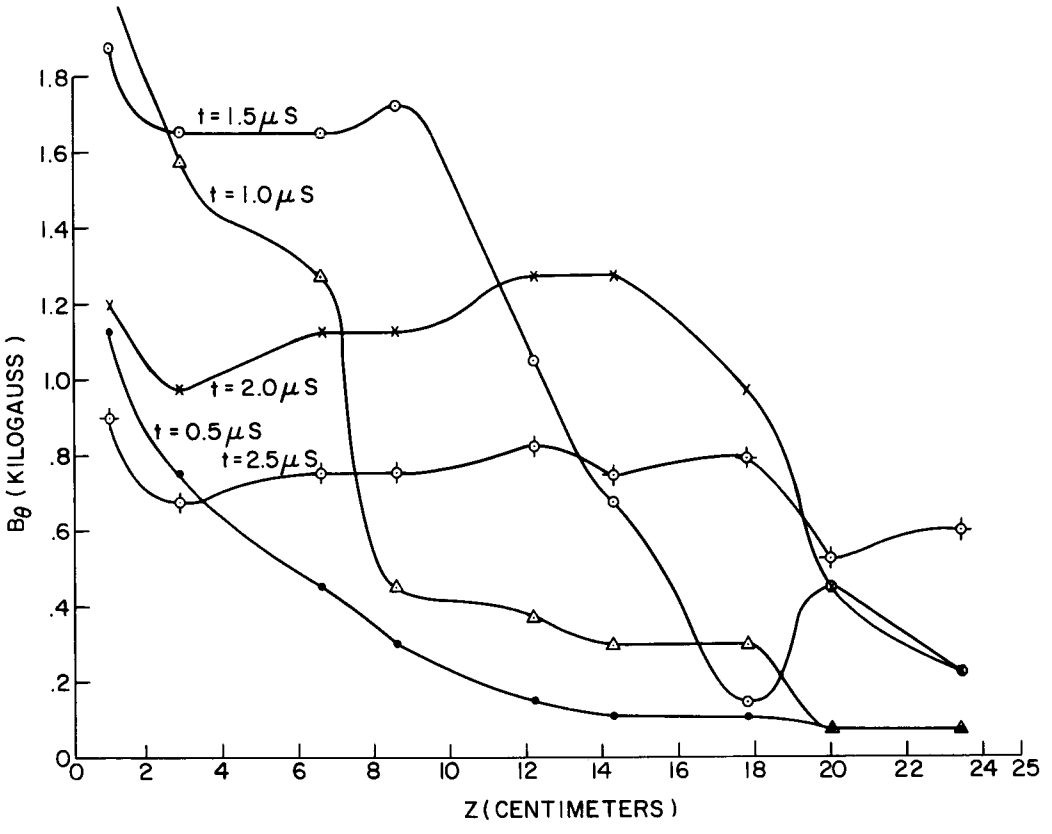

Figure 33a. B_θ vs Axial Position, Mod. A-4 Gun @ 3 KV.

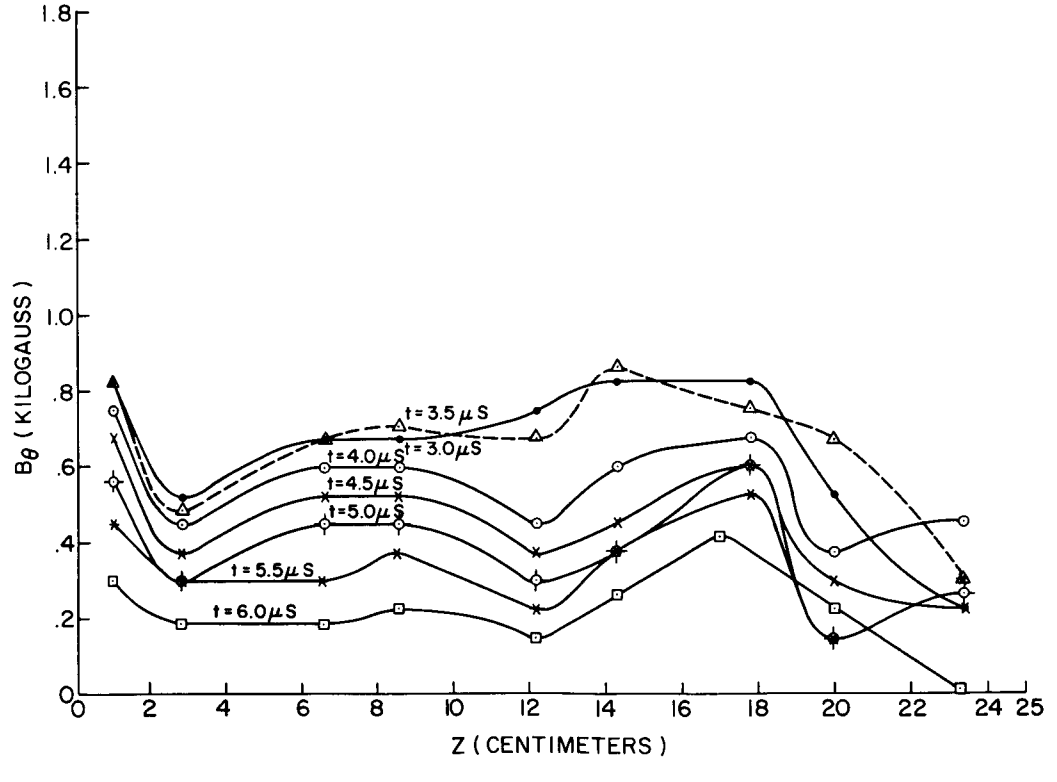

Figure 33b. B_θ vs Axial Position, Mod. A-4 Gun @ 3 KV.

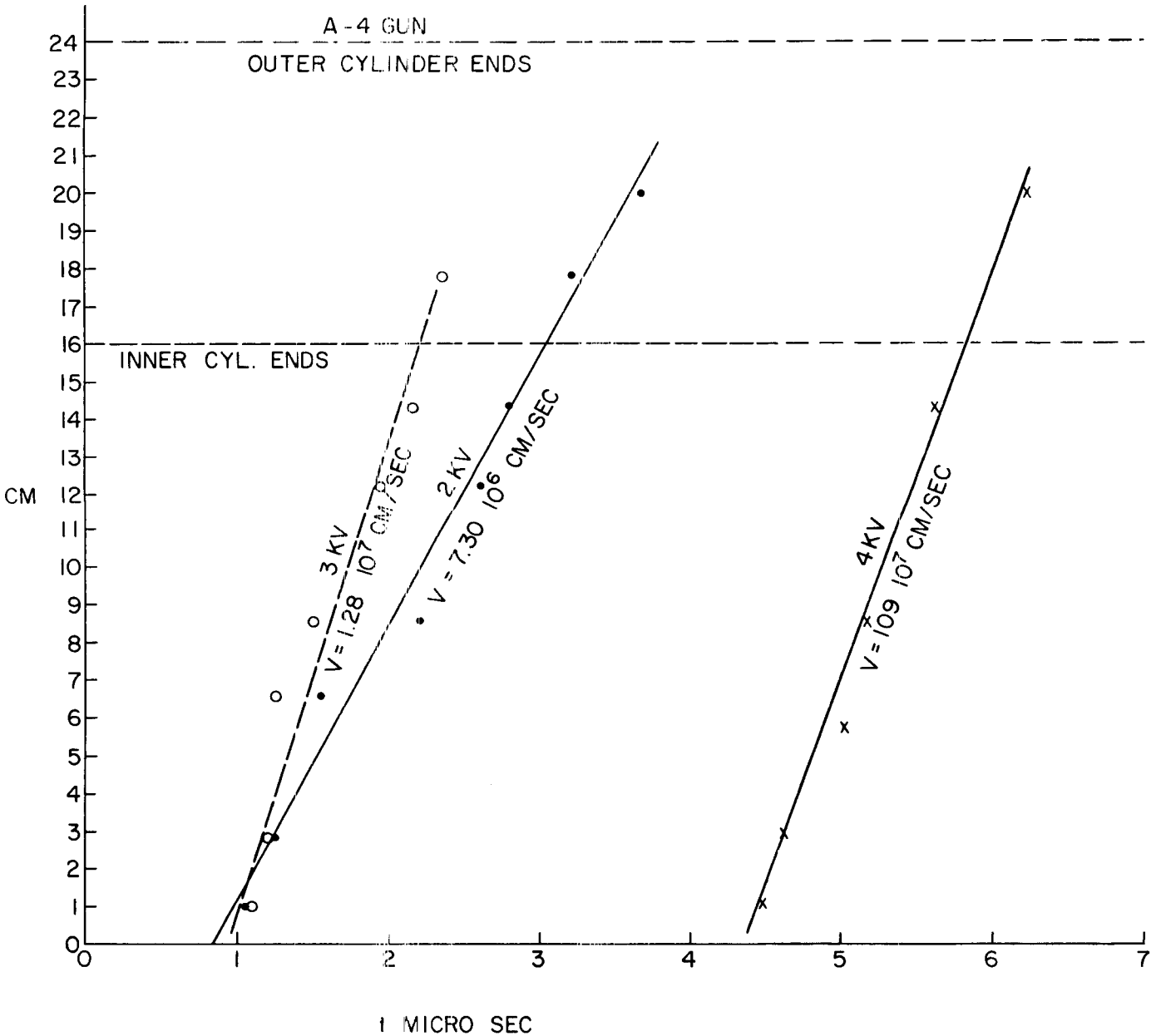

Figure 34. Current Sheet Position vs Time Mod. A-4 Gun.

10.8 Current Waveform Measurements on the Mod. A-4 Accelerator

Current waveforms obtained with a Rogowski loop at the terminals of the Mod. A-4 accelerator are shown with the series of B_θ probe signals in Fig. 30 and 31. In the course of these measurements and in scattered previous observations, an effect was observed which may manifest itself in a variety of pulsed gas triggered accelerators. With any interval between shots exceeding about 1 minute, a current signal considerably different in amplitude and period from that obtained with shorter intervals was obtained. Figure 35 shows two current waveforms for both the "long" and the "short" firing intervals. The lower amplitude, longer period signal is associated with the "short" interval, and normal mode of operation for our experiments. It is quite reproducible in all characteristics. The other signal shown occurred with the first firing of every run and disappeared after no more than three succeeding firings. For this reason these firings were discarded prior to making any of the performance measurements in this report.

The higher peak current and shorter period characteristic of the spurious waveform was at first attributed to the initial relaxation of the valve seat. This possibility was subsequently eliminated by the simple expedient of firing the valve 2-3 times prior to triggering the gun discharge. This preconditioning of the valve had no noticeable effect on the initial discharge waveform. Only actual firing of the gun anywhere from 1-3 times brought the asymptotic low current, long period waveform. Thus, the role of adsorbed gas and/or vacuum system oil on the electrodes or insulator is

suggested as a more likely factor influencing the nature of the discharge. The initial location of the discharge does not appear profoundly different in the two discharge modes observed since the rate of current rise appears unchanged in both cases.

It is important to note that it is indeed possible that for guns operated on a single shot basis, (i.e. with intervals of a minute or longer between shots), the assymptotic waveform may never be realized, and hence the data obtained may provide misleading indications of engine performance on a repetitive basis.

10.9 The Use of Propellants Other Than Nitrogen

Helium and argon, in addition to nitrogen have been used in the operation of the accelerator with little change in overall operating efficiency. In order to study the effect of a considerably heavier propellant on gun performance, xenon was introduced into the previously evacuated gun valving system. Calorimeter measurements indicated overall efficiency of from 50% - 52% at an optimum voltage of 3 KV, as compared with the 54% obtained for nitrogen under otherwise similar conditions. The discharge current waveform was of approximately 10% shorter duration with about the same peak current as observed with nitrogen. The study was cut short in the interest of more immediately pressing measurements.

10.10 Two-Stage Modification of the Accelerator

The center electrode and flange of the accelerator were rebuilt to accommodate the six first stage trigger electrodes without changing the basic configuration of the original electrode. With the trigger electrode in

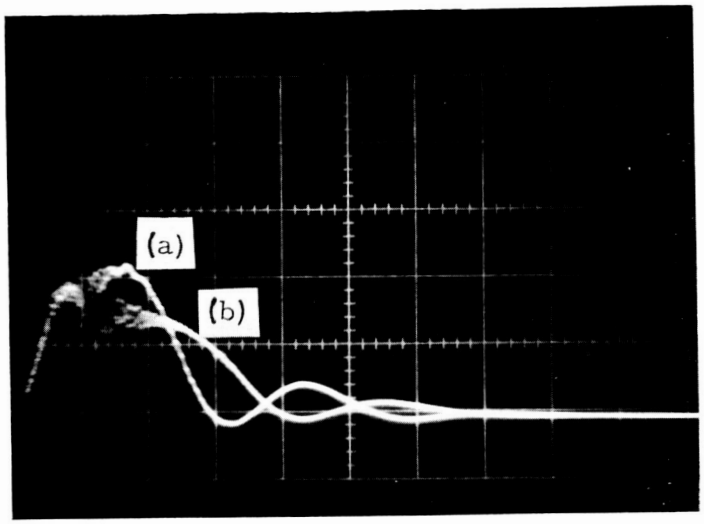

t = 2 usec/div.
i = 22.4 Kamps/div.

(a) Initial Firing
(b) Subsequent Firings

Figure 35. Current Waveforms for Different Firing Intervals Mod. A-4 Gun.

place but not firing, an overall efficiency of 55% was measured. This result is encouraging in the light of the severe drop in efficiency experienced with the previous Mod. A-2 gun, modified for the trigger electrodes.

Actual firing of the trigger electrodes was not carried out because circuit difficulties developed which could not be remedied before it became necessary to remove the entire engine assembly for mounting on a thrust balance.

10.11 Preparation of Accelerator for Thrust Measurement

Preliminary repetitive operations of the accelerator at rates up to 4 shots per second were carried out in the course of calorimetric measurement of exhaust stream energy. These operations supplied indication of component modifications necessary for long term operation of the engine. The most obvious modifications involved the drive coil for the fast acting valve. The electrical energy necessary for operation of the valve ranged from 10 to 15 joules per shot. Most of this energy is dissipated in the coil, and the resulting heating of the coil at the 4 sec^{-1} firing rate enough to deleteriously affect the operation of the valve. In order to accommodate the hundreds of watts of coil dissipation contemplated at the 10 sec^{-1} and higher pulsing rates, a new drive coil was constructed of 1/8" diameter thin wall copper tubing. Coolant (Convoil diffusion pump oil) was circulated through the coil by a high capacity pump operating in conjunction with a chilled water-oil heat exchanger. In this manner the coil temperature was maintained at a tolerable level.

Calorimeter measurements of exhaust stream energy were performed with the new coil to determine any effects on efficiency due to possible changes in the injected gas density profile. The efficiencies over the entire voltage range were unchanged with the new valve coil.

No other changes were made in adapting the accelerator for repetitive operation although provisions for electrode cooling were built into the auxiliary components to the system.

10.12 Thrust Measurements

a. Description of Thrust Balance

In preparation for the direct measurement of engine thrust, the capacitor bank and accelerator were removed from their position external to the .91 meter diameter vacuum tank and mounted in a 1.14 meter diameter, .38 meter long stainless steel housing, so that only the accelerator barrel was exposed. The package was then placed on the thrust balance which was mounted to a support frame attached to the vacuum pumping plate for the 1.83 meter diameter chamber which enclosed the entire assembly. A description of the thrust balance, its operating principles, and more detailed discussion of auxiliary components was supplied in Reference 1. The thrust balance components including flexures and measuring system were identical to those used previously. Only the original capacitor rack superstructure was removed to permit installation of the new engine housing on the balance. Photos of the thrust balance and engine housing are shown in Figs. 36 and 37.

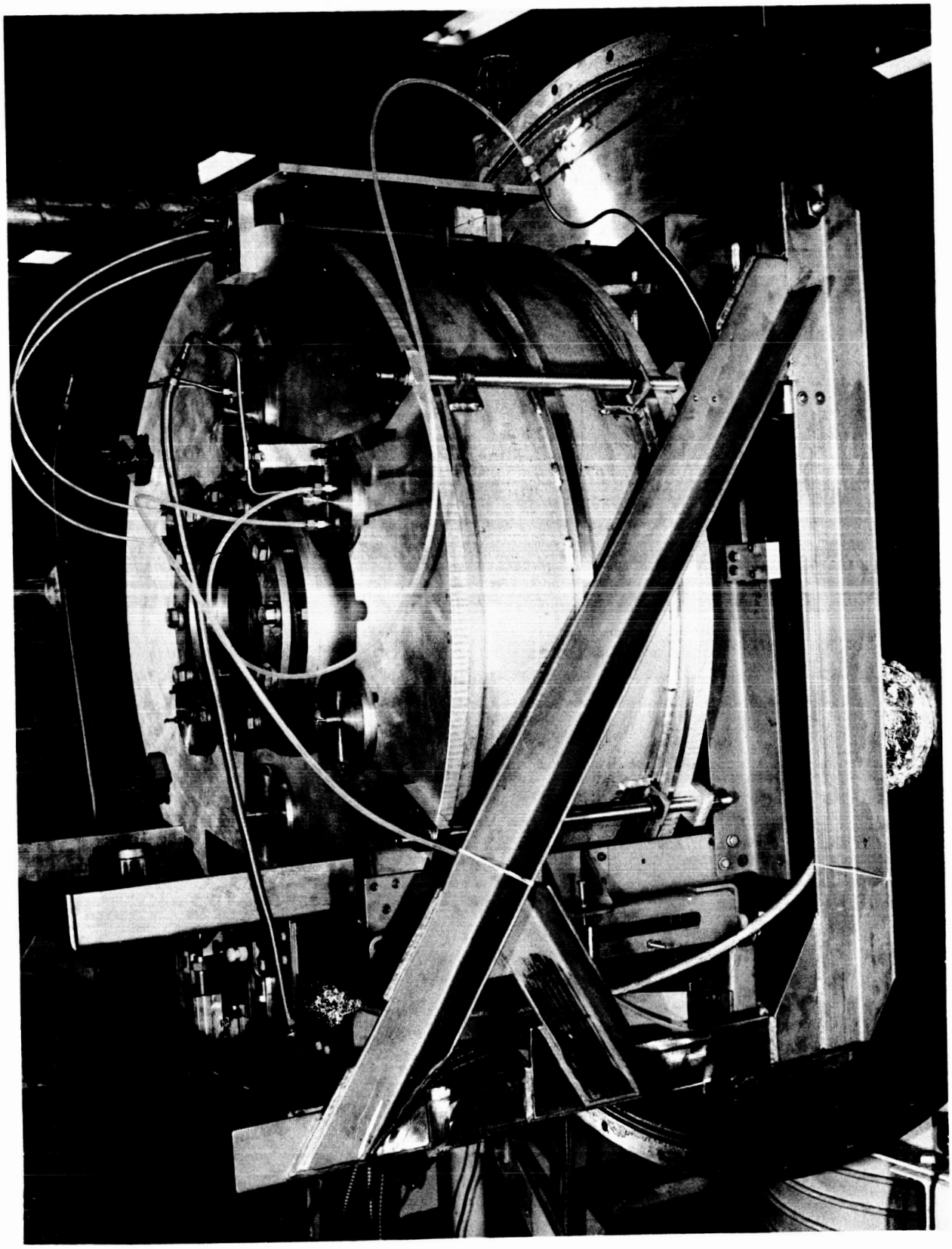

Figure 36. Thrust Balance and Engine Housing.

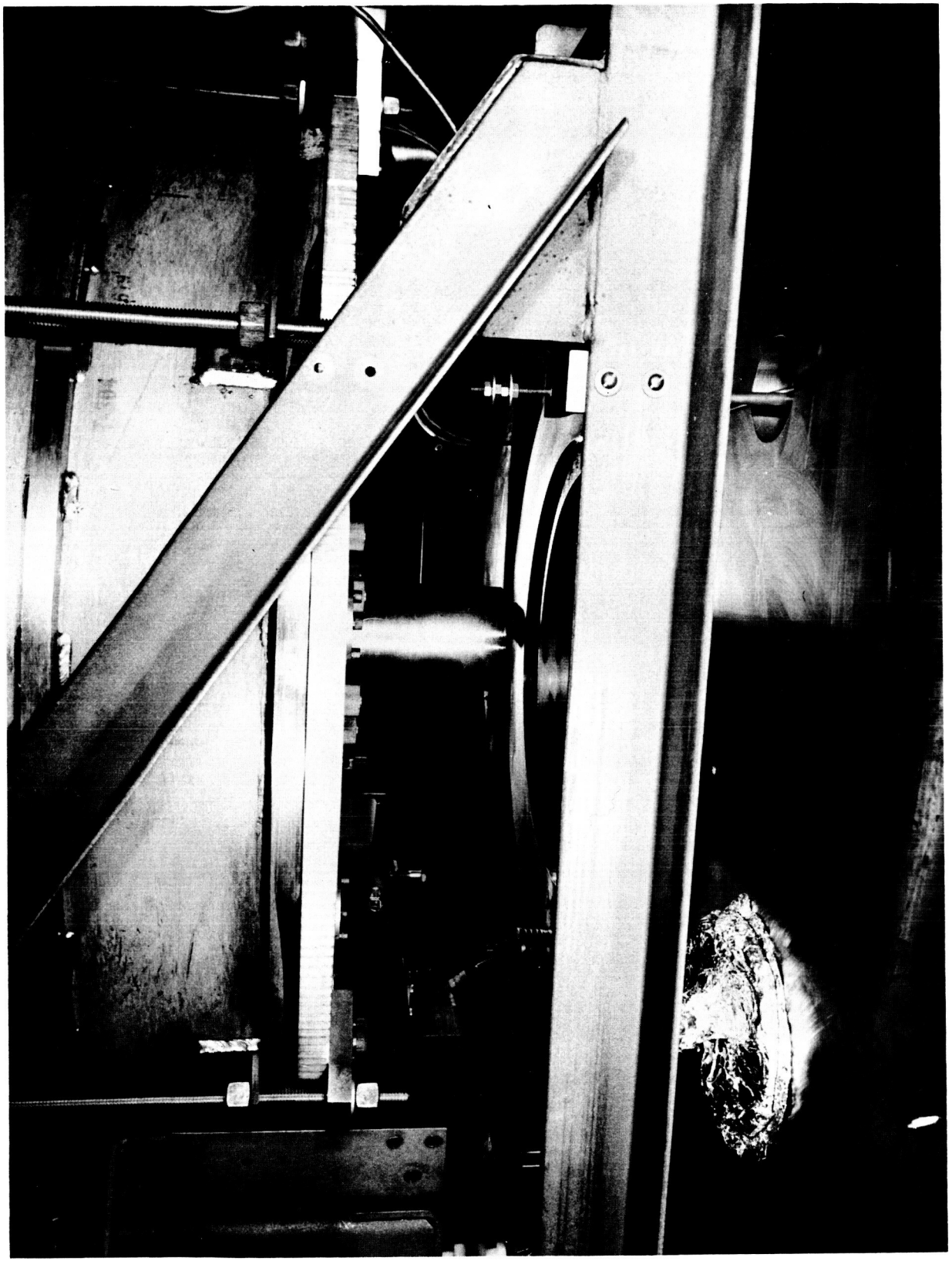

Figure 37. Engine Housing with Accelerator Barrel Protruding.

The use of a pressurized container for the capacitors and gun flanges eliminated virtually all of the problems which plagued operation when thrust had been measured previously. Capacitors, switching elements, external insulators, and a good portion of the wiring now operate at atmospheric pressure, where previously they were in the vacuum environment. As a result, breakdown across insulators, spurious secondary discharges between capacitors, capacitor rupture and leakage, etc., are no longer experienced.

b. Measurements

The Mod. A-4 engine was operated at pulse rates ranging from 2 to 10 shots per second in the voltage range from 2 to 6 KV. The maximum operating power level for the 45 ufd bank therefore was 8KW. The maximum thrust measured at this power level was 38 millinewtons. A plot of thrust vs power at different voltages, different propellant flow rates, and a constant firing rate of 10 cps is given in Fig. 38. It should be noted that the thrust was essentially independent of the input mass flow rate over the range studied. The implication is that similar thrusts could have been obtained with even lower flow rates than those used here. The gun could not be operated in the gas triggered mode at lower flow rates, however. With varying repetition rate at fixed voltage, as might be expected, thrust was directly proportional to repetition rate. The thrust due soley to the amount of propellant required to fire the gun at 3 KV was as high as 3.67 millinewtons at a pulse repetition rate of 10 cps. Assuming sonic velocity of the propellant, the flow rate calculated from this thrust is 1.08×10^{-5} Kg/sec. For twice sonic velocity,

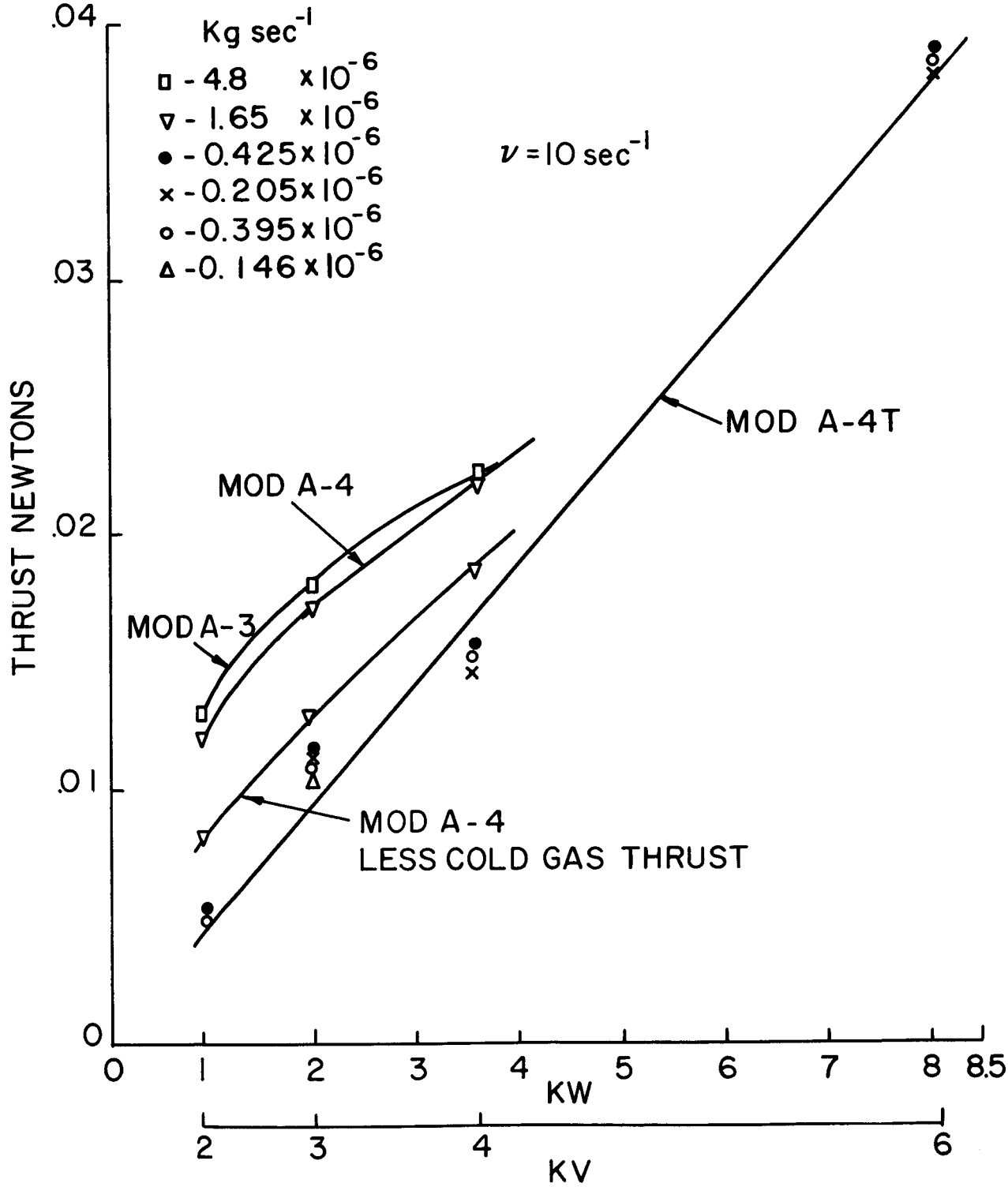

Figure 38. Trust vs Power - Mod. A-3, Mod. A-4 and Mod. A-4T Guns.

the result is more in agreement with the direct measurement of mass flow (see Section 10.13).

10.13 Propellant Flow Measurement

The mass of propellant injected into the accelerator was measured both by volumetric and average flow rate techniques. The volumetric determination was made by firing the valve, into a known volume (12.75) and measuring the increase in pressure of this volume after samples of 100 or more shots fired in rapid succession. A graph showing propellant mass injected per shot over a range of valve drive coil voltages is shown in Fig. 39.

The flow rate measurement was made using a calibrated tapered capillary and ball flowmeter inserted in the valve plenum propellant feed line. At a repetition rate of 10 cps, the stainless steel and glass flowmeter balls remained sufficiently steady to provide accurate readings. Below this rate, the excursions of the balls about the average flow reading due to the pulsating gas flow became too large for good readings, so that flows were obtained from the calibration curve of mass per shot vs valve voltage (Fig. 39).

Comparison of the above methods of determining mass flow, carried out by measuring the flow rate into the known volume indicated less than 10% difference in results.

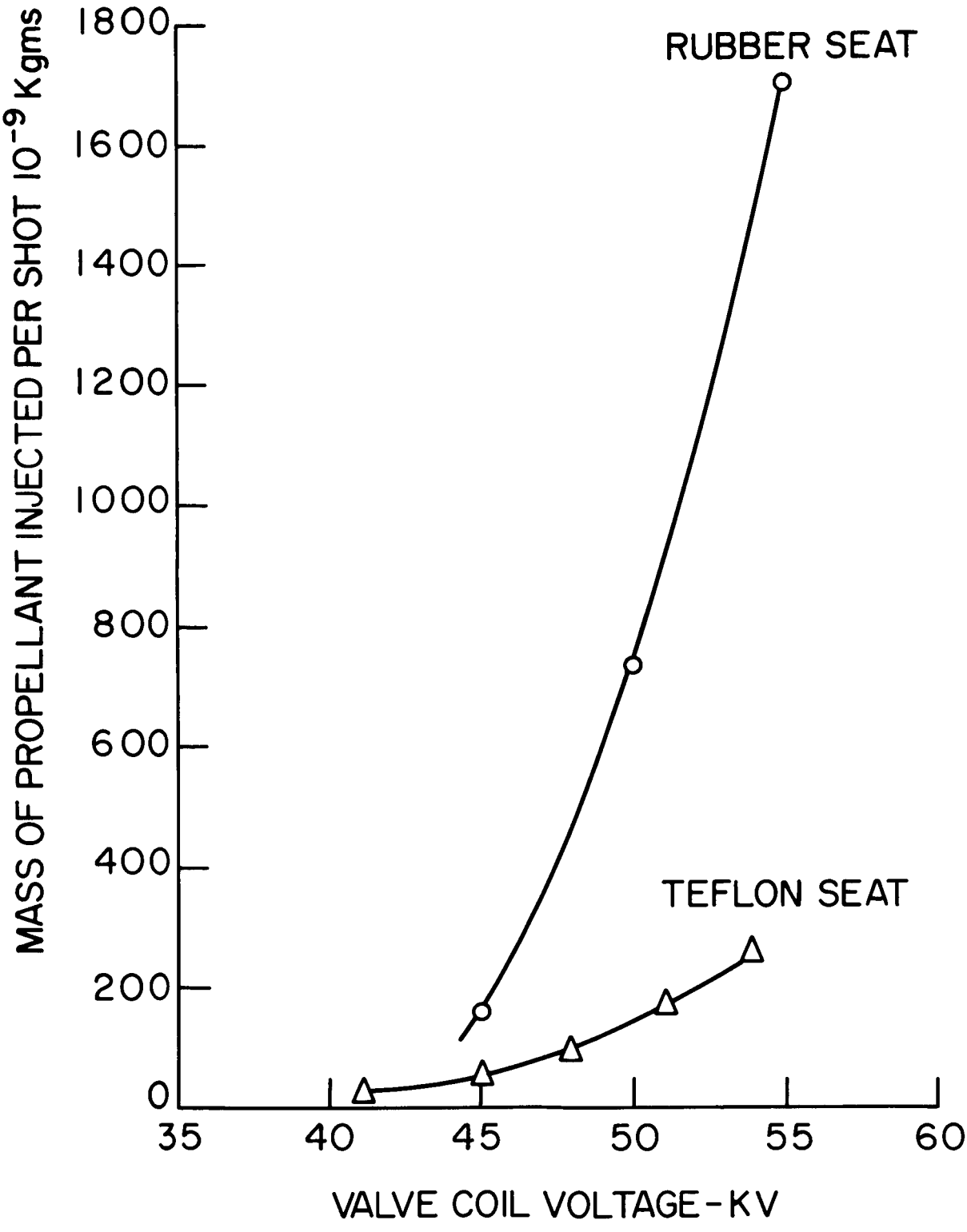

Figure 39. Propellant Mass Injected vs Valve Drive Coil Voltage.

10.14 Overall Efficiency of the Accelerator

The overall efficiency of the engine can be determined from the measurement of thrust, propellant mass flow and input power:

$$\eta = \frac{T^2}{2 \dot{m} P}$$

Overall efficiencies, as obtained above, have been plotted vs voltage in Fig. 43. It should be noted here that $\dot{m}$ as presented here, has taken into account only the cold gas flow into the accelerator. Electrode and insulator erosion have been neglected. Although the engine was not weighed before and after each series of thrust runs, visual inspection of the accelerator after about 10^5 shots suggests that the contribution of eroded mass was negligible, at least at 4 KV and below. (Relatively few shots were taken at 6 KV). With a cold gas flow rate of 4.8×10^{-6} Kg/sec., approximately 48 gms of propellant were used throughout the thrust runs with the Mod. A-4 accelerator. If erosion had contributed as much as 10% to the accelerated mass, the loss of about 4.8 gms of electrode and insulator material would have been observed. This was not the case.

As implied in the discussion of the thrust measurements (Section 10.12), the propellant injection scheme appeared to supply more mass than was utilized in the discharge. This was evidenced by the independence of thrust from flow rate, down to the limit where gas triggering of the discharge could no longer be accomplished. Comparison of the data for the Mod. A-4 and Mod. A-3 accelerators, as presented in Fig. 38 also appears to verify this contention. The Mod. A-4 accelerator requires less than 1/3 the amount of injected propellant than does the Mod. A-3 accelerator. This might be

expected since a larger fraction of the injected gas is likely to be ejected from the larger diameter nozzles of the Mod. A-4 accelerator at the time of breakdown. In other words, in order to obtain a similar breakdown density with the A-3 configuration, it was necessary to inject more through the valve, since a smaller fraction of the gas was ejected from the A-3 nozzles by the time of electrical breakdown.

It was strongly suspected that the excessive propellant loading was caused by bounce in the valve due to the rubber "O" ring seat, as had been experienced previously[2]. An attempt to minimize this loss was made by rebuilding the Mod. A-4 valve with a Teflon seat and greater spring loaded compression, to reduce the extent of valve disc travel. Since the basic accelerator configuration was unchanged, the designation has been changed to Mod. A-4T ("T" for teflon).

11. MOD. A-4T ACCELERATOR

11.1 Specifications

*Propellant feed:	Axial injection 5 cm from the front face of the insulator; pulsed nitrogen into 10^{-5} - 10^{-6} mm background. Teflon valve seat substituted for rubber seat.
Port size:	Six holes, each 4.50 mm diameter.
Operating mode:	Single stage; gas triggered discharge.
Outer Electrode:	12.5 cm diameter, 20 cm long.
Inner Electrode:	5 cm diameter to a distance 3.5 cm from the front face of the insulator, followed by a 27° transition to 2.54 cm diameter, a straight section 1 cm long, and a second 27° transition to 1.27 cm diameter; end of the electrode 8 cm from the end of the outer electrode.
Capacitor Bank:	Mark II

11.2 General Description

The accelerator was operated at voltages up to 8 KV, and repetition rates to 10 cps. This configuration was the final one studied during the present contract period.

11.3 Calorimetric Measurements of Exhaust Stream Energy

In order to determine whether possible changes in the gas density profile had influenced the total energy in the exhaust stream, the calorimetric technique was reinstituted and the calorimeter first described in section 10.3.2 was placed at its original location 20 cm from the accelerator muzzle. The peak efficiency (55%) and the voltage at which this peak occurred (3 KV) were unchanged, but the dropoff of efficiency with voltage was more

*Change from Mod. A-4 Accelerator.

gradual than had been observed previously. A plot of efficiency vs voltage for the A-4T accelerator is given in Fig. 40.

11.4 Thrust Measurements

Thrust measurements were carried out with accelerator operation at repetition rates up to 10 sec^{-1} and power levels up to 8 KW. Temporary limitations in the current capacity of the power supply and in the house supply lines did not permit operation at higher repetition rates than 10 sec^{-1} at 6 KV or higher voltages than 6 KV at 10 sec^{-1}.

A plot of thrust vs power at constant repetition rate for the different voltages examined is given in Fig. 38.

11.5 Propellant Flow Measurement

The minimum mass of propellant required to fire the Mod. A-4T accelerator was lower by more than a factor of ten than that required for the Mod. A-4 unit. Depending on the second stage capacitor voltage, the amount of injected mass required ranged from 15×10^{-9} to 45×10^{-9} Kg per shot.

The time between actuation of the valve and onset of the discharge was measured by monitoring the voltage of the valve drive coil capacitor and that of the second stage capacitor bank with Tektronix high voltage probes. A representative plot of interval to breakdown vs accelerator voltage for a typical valve capacitor voltage is shown in Fig. 41. The minimum time shown represents not only the time for mechanical motion of the valve to achieve sufficient opening for gas flow, but also the time for flow of sufficient amount of propellant to increase the density in the interelectrode space to

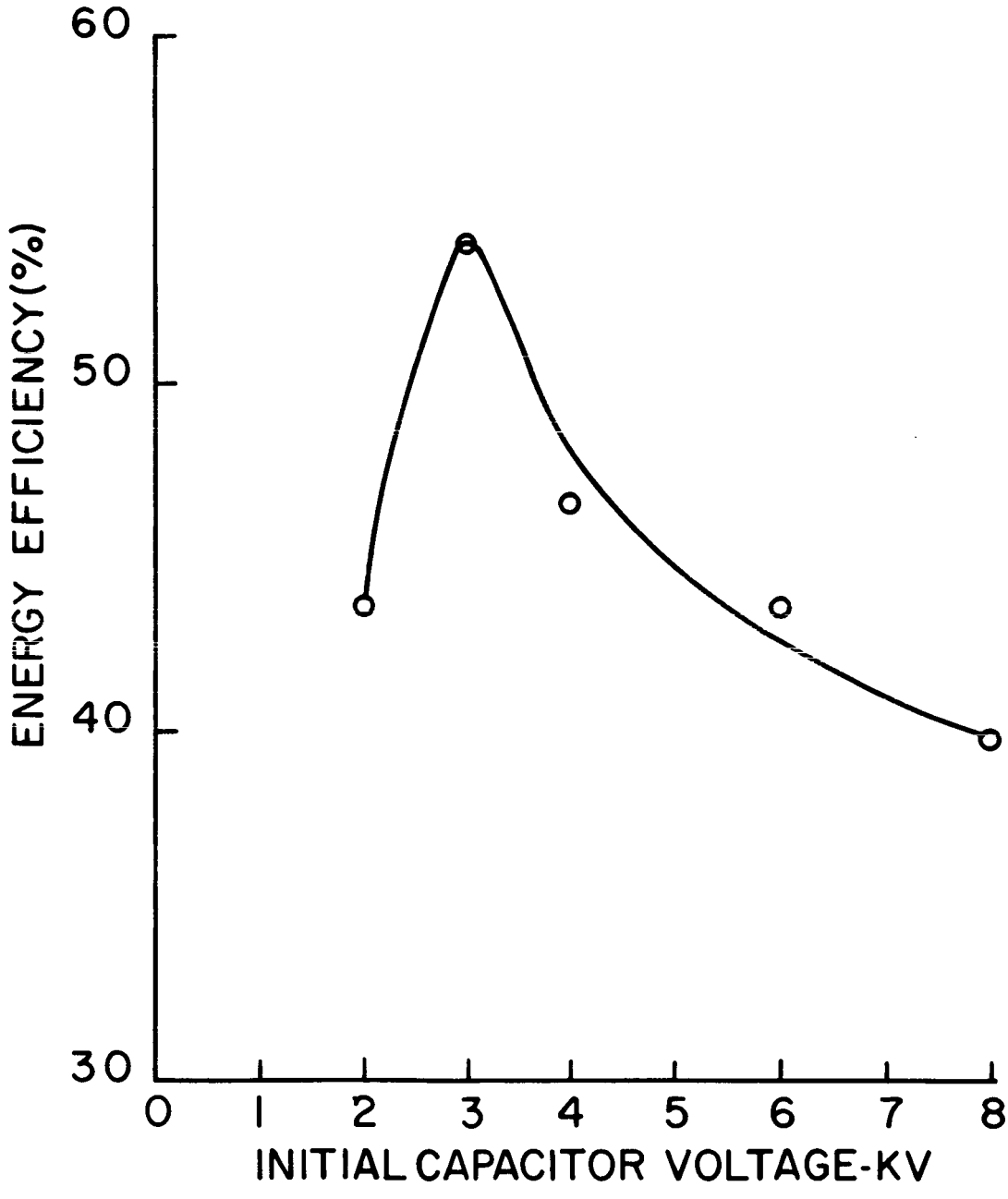

Figure 40. Energy Efficiency vs Initial Capacitor Voltage - Mod. A-4T Gun.

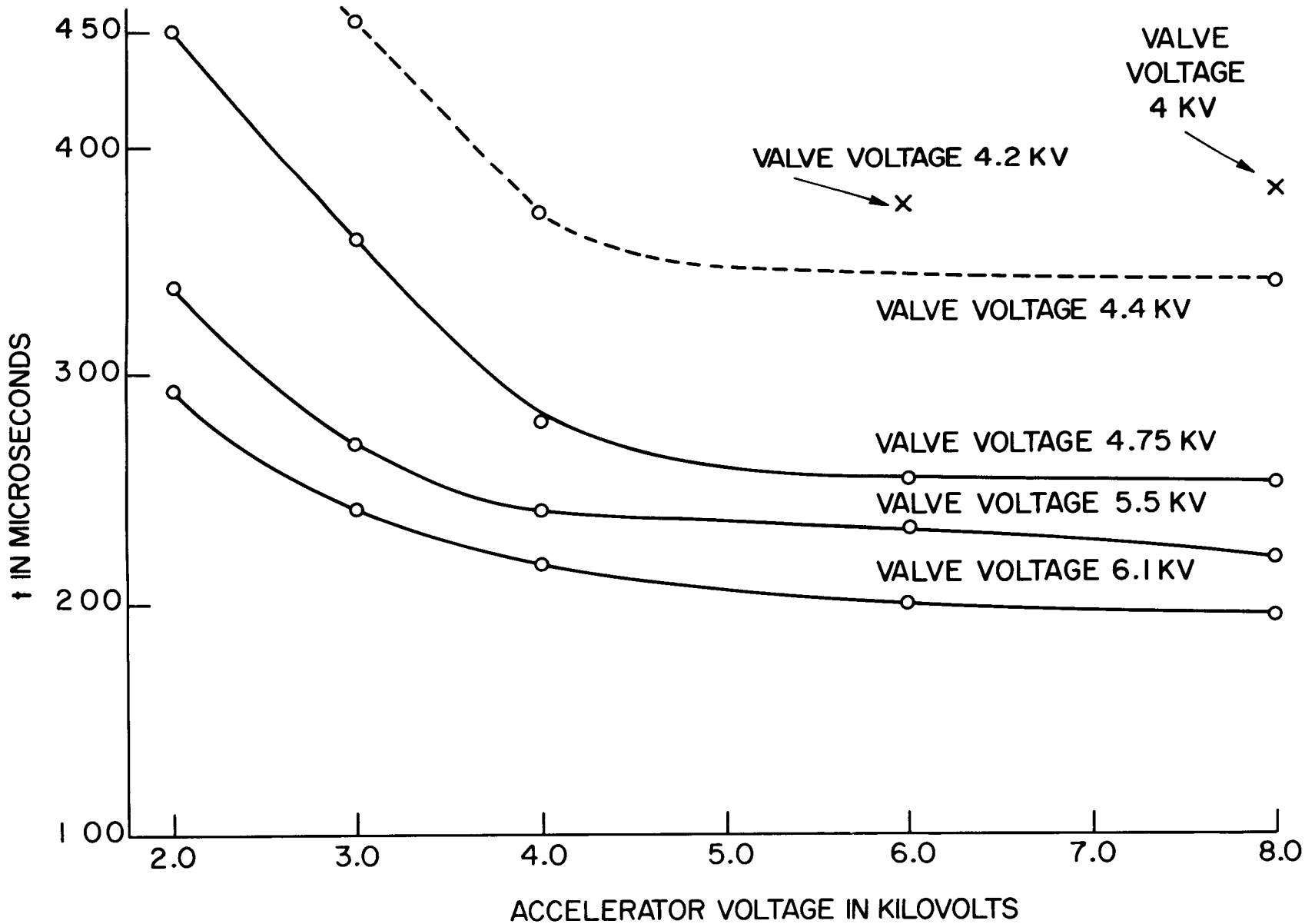

Figure 41. Interval to Breakdown vs Voltage for Different Valve Drive Coil Voltages, Mod. A-4T Gun.

that necessary for breakdown. The fact that from 2 to 8 KV, the breakdown interval decreased from 450 to 250 microseconds (for a valve voltage of 4.75 KV) indicates that there is at least 200 microseconds of propellant flow time prior to discharge at 2 KV, for example. With gas expansion at a rate somewhere between sonic and twice sonic velocity, this time would represent a travel of 6 - 12 cm in the accelerator barrel. This latter figure would represent complete traversal of the barrel from the injection ports.

11.6 Measurements of Luminous Front Velocities

A pair of collimated photomultipliers was used to determine average luminous front velocities at distances of .37 and 3.0 meters downstream from the muzzle of the accelerator. The reference point for these measurements, which corresponded to discharge breakdown time, was the luminosity first emitted from the muzzle of the accelerator. The time of flight of the luminous front from the muzzle to an obstacle placed .37 meters downstream and to another obstacle placed 3.0 meters downstream, was recorded on an oscilloscope in which the sweep was triggered by a signal from the photomultiplier aimed perpendicular to the muzzle. At voltages from 2 KV to 4 KV, luminous front velocities ranged from 5.8×10^4 m/sec to 14.2×10^4 m/sec, respectively, at the .37 meter position. At the 3 meter position the average velocities measured ranged from 7.5×10^4 m/sec to 37.5×10^4 m/sec for 2 to 4 KV capacitor voltage. The results are plotted in Fig. 42. The fact that the velocities at the point furthest downstream from the muzzle are significantly

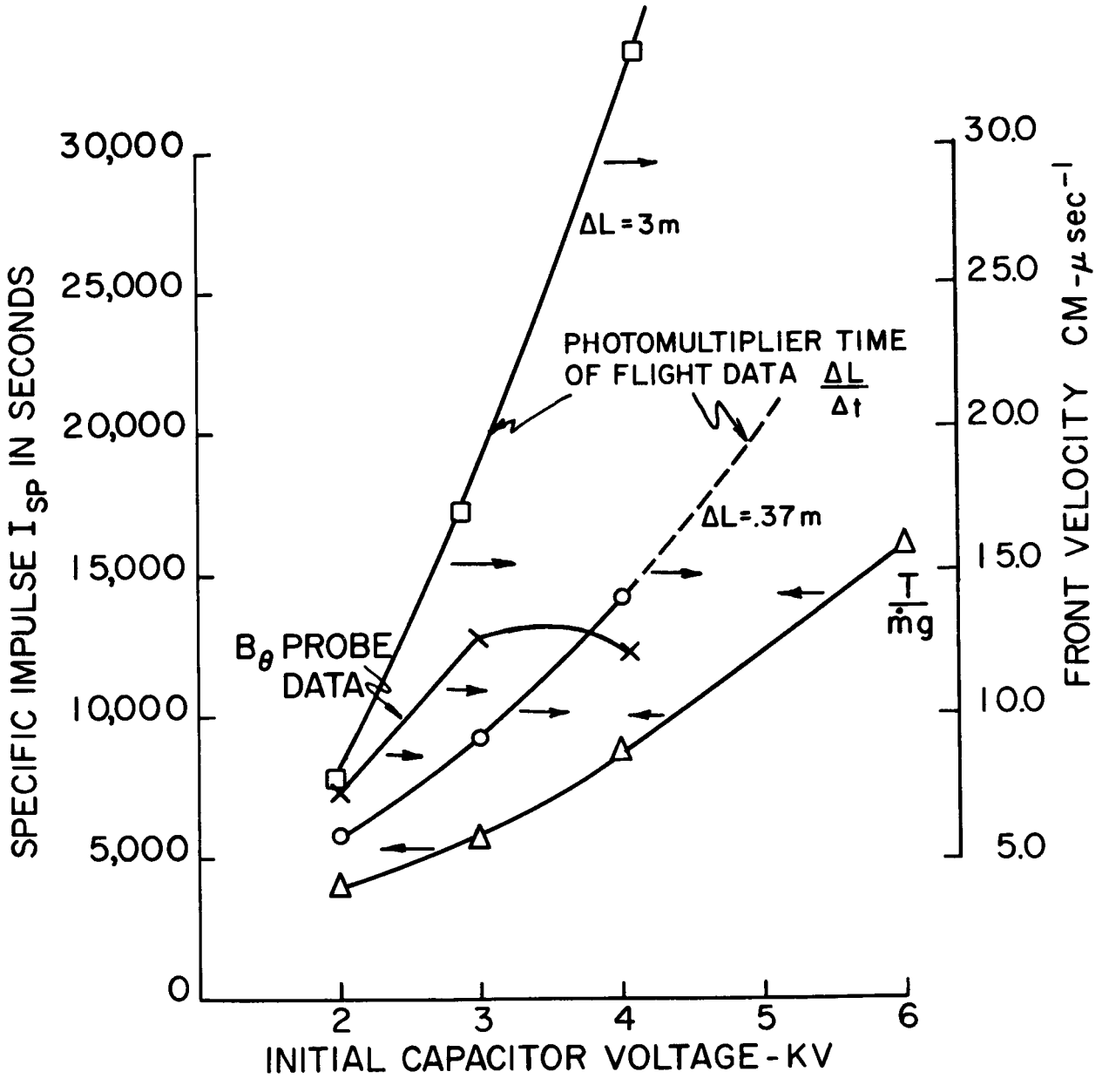

Figure 42. Specific Impulse vs Voltage - Mod. A-4T Gun.

higher than those in closer proximity to the accelerator is understandable when one considers the fact that the population of the fastest moving directed particles relative to the slower ones is enhanced as the distance from the muzzle is increased, provided that all of the particles have comparable transverse energies. The relative intensities of the photomultiplier signals at the two positions also implied that far fewer particles were involved at the 3.0 m position than at the 0.37 m point. In view of the apparent delay in current sheet motion relative to the discharge breakdown time (Fig. 34), the propriety of using the latter time as zero reference for velocity measurements is open to question. It should be noted that any later zero reference time would result in increases in the luminous velocities, particularly for those data obtained at $\Delta L = 0.37$ m.

The velocities obtained by optical methods were compared with those obtained from B_θ probe measurements of current sheet velocities. The sheet velocities are also plotted in Fig. 42. While these velocities are 25-30% higher than the luminous front velocities, at 2 and 3 KV, there is an unexplained marked departure at 4 KV, where lower sheet velocities are indicated.

11.7 Overall Efficiency of the Mod. A-4T Accelerator

Overall efficiencies as defined by $T^2 / 2 \dot{m} P$ have been plotted vs voltage in Fig. 43. The profound increase in overall efficiency from that obtained with the Mod. A-4 accelerator appears to be due primarily to the decreased amount of propellant admitted by the valve while injecting that amount necessary to initiate breakdown. It is indeed possible that for the valve and injector nozzle configurations used, these amounts are still not optimum, and that the mechanical valve either injects more propellant than can be

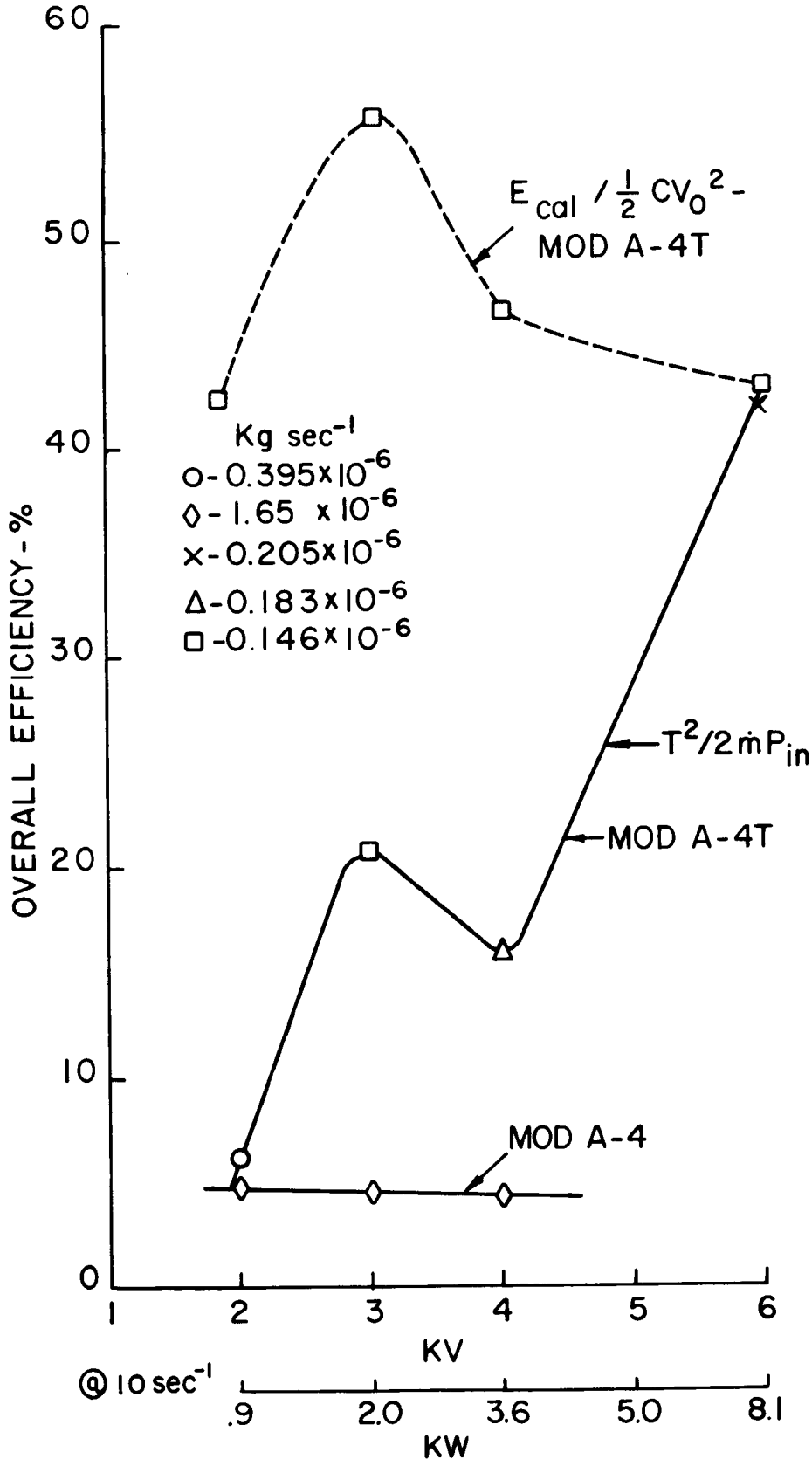

Figure 43. Overall Efficiency vs Initial Capacitor Voltage - Mod. A-4 and Mod. A-4T Guns.

efficiently accelerated or allows propellant to flow after the current sheet has departed from the region of gas entry, or both.

The sharp increase in overall efficiency at 6 KV, is observed in spite of the fact that the mass of propellant required for breakdown increased from that required at 4 KV. Possible reasons for this increase are the unaccounted for contribution of erosion to the mass flow and/or increased mass utilization efficiency at 6 KV. The first possibility cannot be completely ruled out in the present absence of quantitative determinations of erosion, however, significant erosion appeared to be ruled out on the basis of visual inspection of the electrodes and insulators after 10^5 shots on the Mod. A-4T gun, at least 4 KV and below. (See also the detailed argument of Section 10.14). Another unresolved question is what contribution desorbed gas from the electrodes might give towards the total mass flow.

The increase of the overall efficiency

$$\eta_{overall} = \left(\frac{\dot{m}_{out}}{\dot{m}_{in}}\right) \quad \eta_{E_i} \quad \left(\frac{\bar{v}^2}{\overline{v^2}}\right) \quad \begin{pmatrix}\text{spreading}\\ \text{factor}\end{pmatrix} \quad \begin{pmatrix}\text{frozen}\\ \text{flow}\\ \text{factor}\end{pmatrix}$$

in the face of decreasing exhaust stream energy efficiency (η_{cal}) in going from 4 to 6 KV (Fig. 34) is consistent with either of these possibilities since in either case, the ratio $\frac{\dot{m}_{out}}{\dot{m}_{in}}$ increases with voltage.

The energy efficiencies shown in Figure 34 may well be generally too low because a) the calorimeter is known not to collect the entire exhaust stream and b) the collecting efficiency may be less than unity.

11.8 Discussion

Although a peak exhaust stream energy efficiency exists at 3 KV for this configuration, the fact that relatively high efficiencies are measured at higher voltages, and that the overall efficiency, from thrust measurement, is in excess of 40% at 6 KV suggests that more consideration should be given to the higher voltages, with possible erosion quantitatively taken into account.

The Mod. A-4T gun represents the most successful attempt to date in minimizing the amount of propellant required to operate the gun. Since no decrease in thrust was found even for this minimum amount of propellant, further improvements along this line appear possible. Such improvements might well be accomplished through further changes in the size and shape of the injector nozzles or auxiliary triggers.

Results have already shown that auxiliary triggering from a first stage provides the means for discharge breakdown at densities below those which would otherwise cause breakdown. The first stage, as stated previously, offers an opportunity to control both the timing and the position of discharge initiation.

12. CONCLUSIONS AND SUMMARY

12.1 Summary of Accomplishments

The end results of the work carried out during the contract period have been the following:

1. The observation of an exhaust stream energy efficiency as high as 63%.

2. The achievement of an overall engine efficiency, $T^2/2\dot{m}P$, of 42% where $\dot{m}$ is based on the input mass flow only.

3. The reduction of external circuit losses to 13% of the total initially stored in the capacitor.

4. The repetitive operation of the most efficient engine configuration at power levels up to 8 KW and repetitition rate of 10 cps.

5. The successful repetitive operation of a fast-acting valve injecting sufficiently small samples of gas so that good mass utilization is indicated.

6. The establishment of trends in accelerator operation which show promise, if fully exploited, of bringing still further improvement in overall engine performance.

7. The further refinement of measuring techniques required for determining the operating characteristics of the engine.

12.2 Summary of Efficiency Trends

The data presented in the preceding sections have been summarized in Figures 44-46 to show trends in the energy efficiency as various system parameters are varied. In surveying Figures 44-46, it is quite apparent that over the range of parameters studied, the major influence on the energy efficiency was the gun geometries and mode of gas loading. Caution should be exercized in the compiled data to predict trends beyond the range of system parameters studied since the parameters are not independent variables.

The variation of energy efficiency with external capacitance and inductance is summarized in Figure 44, for each of the three basic variations in propellant loading modes. The only condition under which variation of either of these parameters had any significant effect was for the Model R accelerator, for which there was a marked change in efficiency with changing capacitance. Otherwise, inductance was varied over a factor ten and capacitance over a factor three without any major alteration in performance.

In Figure 45, an attempt is made to indicate the separate effects of changing gun geometry and propellant loading modes, although it should be kept in mind that both parameters are changed when the electrode radii ratio is altered. Clear separation of the two effects is possible when comparing the Model R with the Mod R-1 and the Mod A-3 with the Mod A-4 guns, for given radii ratios. It is clear that both variations cause major gun performance changes.

Finally, in Figure 46 it is shown that gun length also plays a

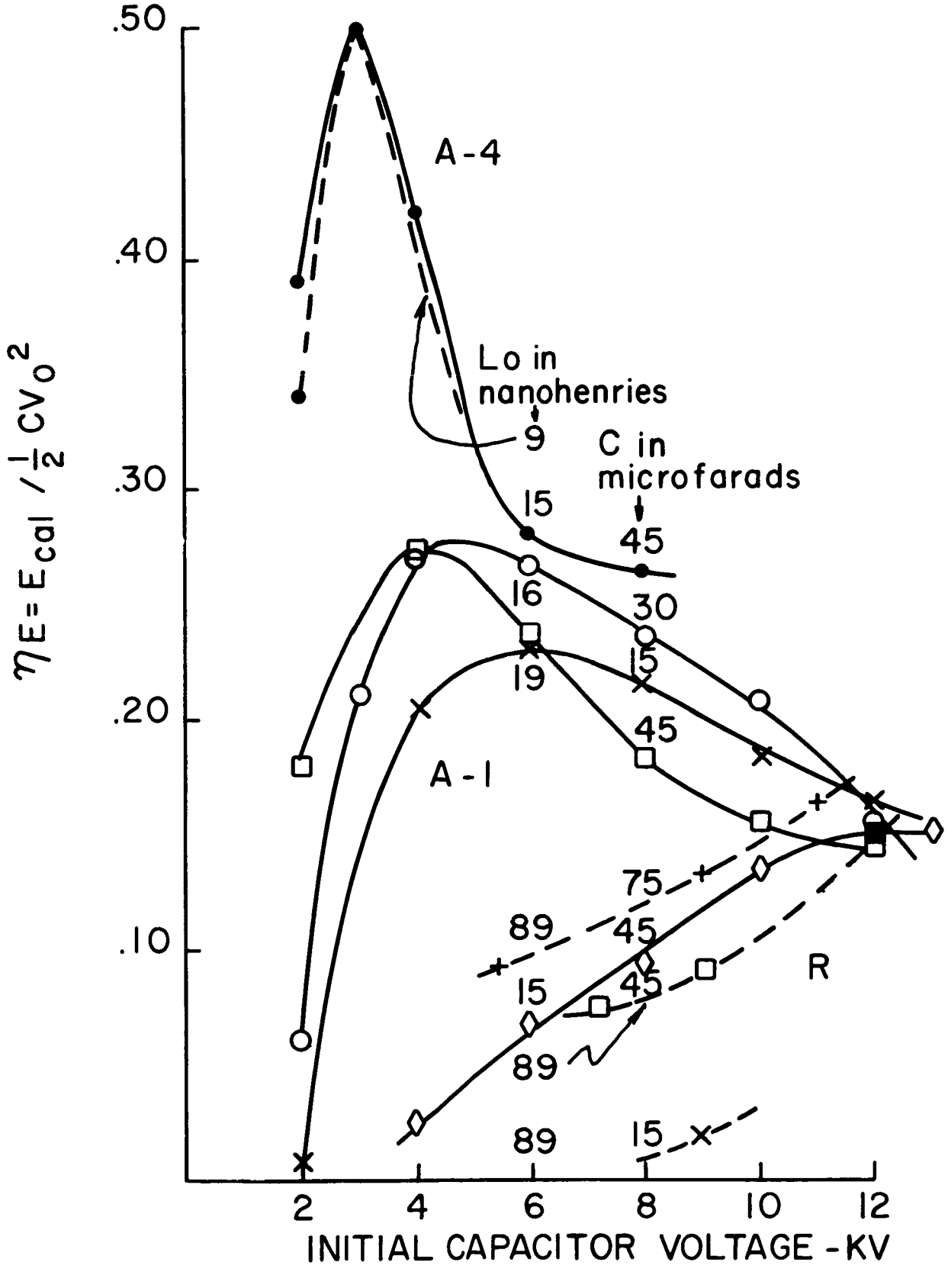

Figure 44. Variation of ηE with C, Lo for Three Different Gun Geometries and Propellant Loading Modes.

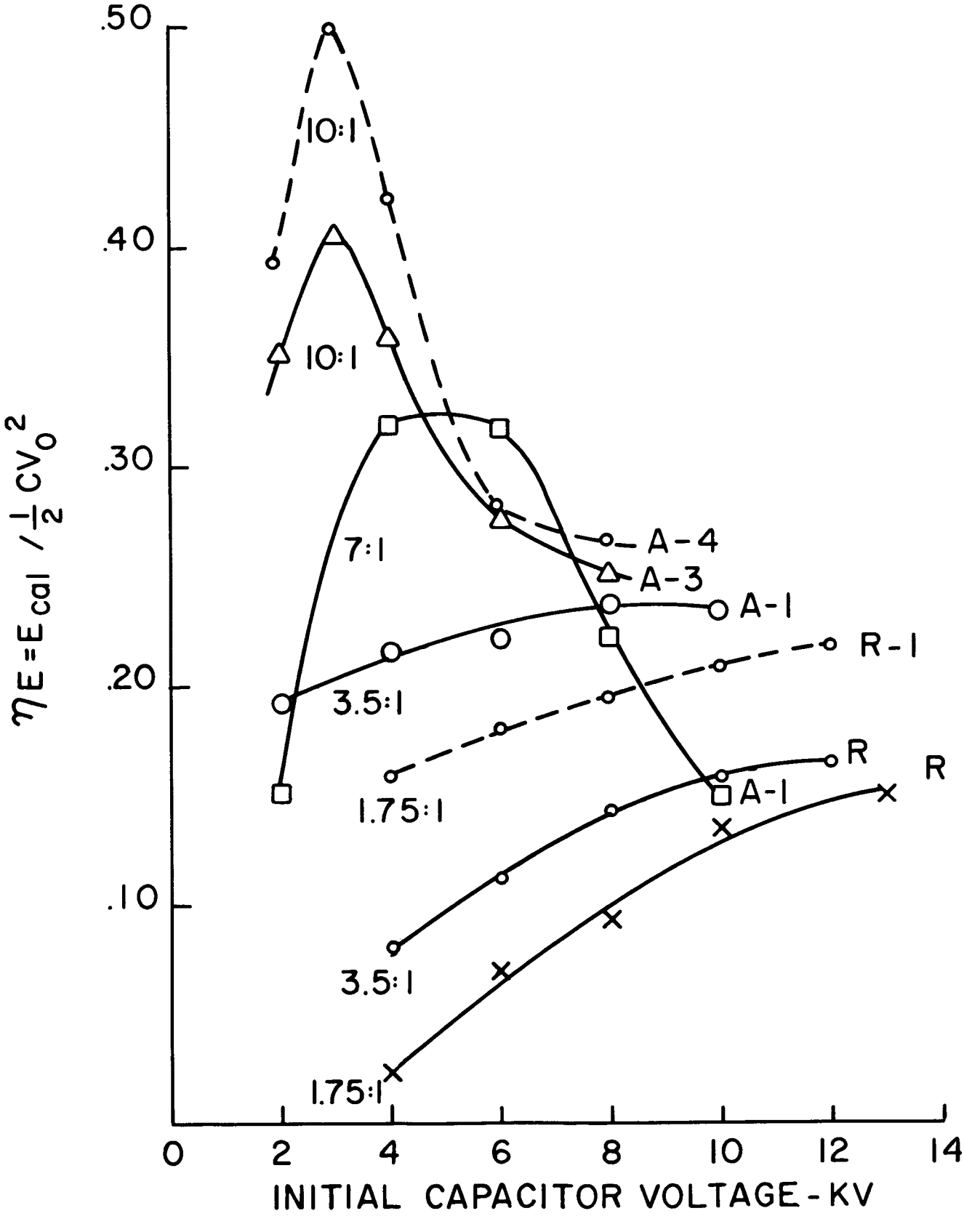

Figure 45. Variation of ηE with Radius Ratio and Gas Loading Mode.

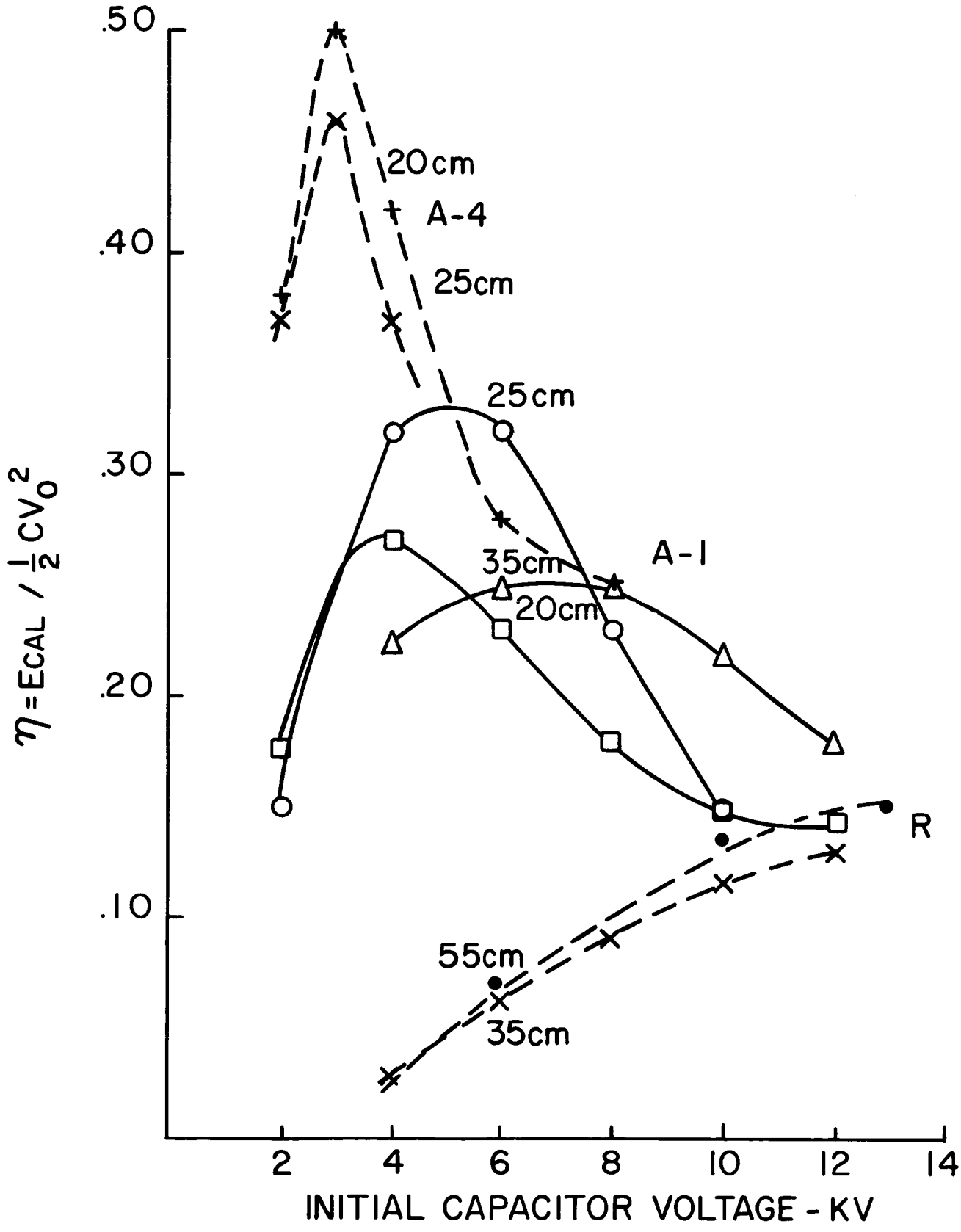

Figure 46. Variation of ηE with Gun Length for Three Different Gun Geometries and Gas Loading Modes.

minor role, within reasonable limits, in determining the energy efficiency of the engine system. This is particularly striking in the case of the Model R accelerator, since it might have been concluded from Figure 44 that gun length and capacitance were badly mismatched for these runs.

If a tentative conclusion were to be drawn from these observations, it would be that future significant alterations in gun performance are more likely to come about as a result of gun geometry changes and gas loading techniques rather than by variation of the characteristics of the energy storage system.

12.3 Areas for Immediate Improvement

The optimization of engine system efficiency has continued to be the overriding goal of this program and, as has already been stated, the knowledge gained from the results described above has provided many useful indications of the directions to be taken toward reaching this goal.

The areas having the greatest potential for further improvement of the gun efficiency include the following: 1) Additional modifications in the geometry of the injector nozzles, e.g by increasing the nozzle diameter to continue the indicated trend thus far established. 2) Reinstitution of the trigger electrodes. 3) Further increase in the electrode diameter ratio. 4) Use of a diverging outer electrode. 5) Modification of the diameter transition in the inner electrode to give a more sudden diameter change and a relatively larger initial diameter. 6) Optimization of gun length for each new condition.

It is felt at this point that while many obvious parametric changes remain to be tried and evaluated, the time has now come for a more concerted effort towards understanding the details of the plasma acceleration process in the most efficient configuration at hand.

Additional information is necessary regarding charged particle and neutral density and velocity distributions prior to, during, and after the accelerator discharge. The B_θ probe and other electrical measurements described above should be expanded to yield more information regarding the distribution of currents and fields in the accelerator. Correlation of the results of these measurements with those of the macroscopic processes of engine operation, such as thrust, exhaust stream energy, electrical

transients and electrode and capacitor losses may yield the development of an analytical model, from which the accelerator response to various parametric changes can be more reliably predicted.

With respect to the measurement of gross operating characteristics, it is important that these be carried out with engine operation at higher repetition rates and with runs of extended duration so that a quantitative determination of erosion rates will be possible. The effects of electrode and insulator temperature and surface conditions on engine thrust and efficiency should be determined, and as many other accelerator characteristics as is possible should be monitored under these conditions. A by-product of this effort would be an indication of the lifetime of vital components including electrodes, insulators, fast-acting valves, and capacitors.

At the end of the previous contract period, the loss in efficiency due to the energy dissipated in the capacitor bank and energy transfer system was singled out as the area requiring most immediate attention. At that time as much as 67% of the energy initially stored in the capacitor was dissipated outside the active portion of the gun. This loss has been reduced to approximately 13% in the A-4T gun, and additional improvement appears possible. The high equivalent series resistance (low Q) of the present capacitor bank can be reduced by at least a factor of 10 (and possibly a factor of 50) through the use of improved capacitors now being made available. Advances in capacitor technology involving the use of

paper, film, and inorganic dielectrics in conjunction with less lossy impregnants, and improvements in foil and lead configurations are responsible for such potential gains in performance. Additional improvements important for space flight application include reduced capacitor weight per joule, increased capability for operation at elevated temperatures, and a capability for operation in the vacuum environment.

Early in the contract period, it appeared that the laminated sheet foil-pressed mica capacitor design developed by Tobe Deutschmann Laboratories, Inc. embodied all of these advantages. In the course of planning the application of these units, it became apparent that an array which was most compatible with our vacuum chamber and thrust balance capabilities could be also designed to act as a variable length transmission line energy source. Such a line might offer not only an increase in transfer efficiency, but would greatly simplify the analysis of energy distribution in the discharge circuit. An unexpected catastrophe in the manufacturing process caused these capacitors to be unavailable during this contract period.

Another capacitor design, not investigated previously, is the film dielectric type, which may off higher Q and higher energy storage density than the oil impregnated paper units used to date. An accelerator and capacitor bank using nine, 3 KV, 5 ufd. aluminum foil-mylar film units connected in parallel is shown in Fig. 47. The total weight of the bank is approximately 9 Kg; its inductance is comparable to that of the Mark II

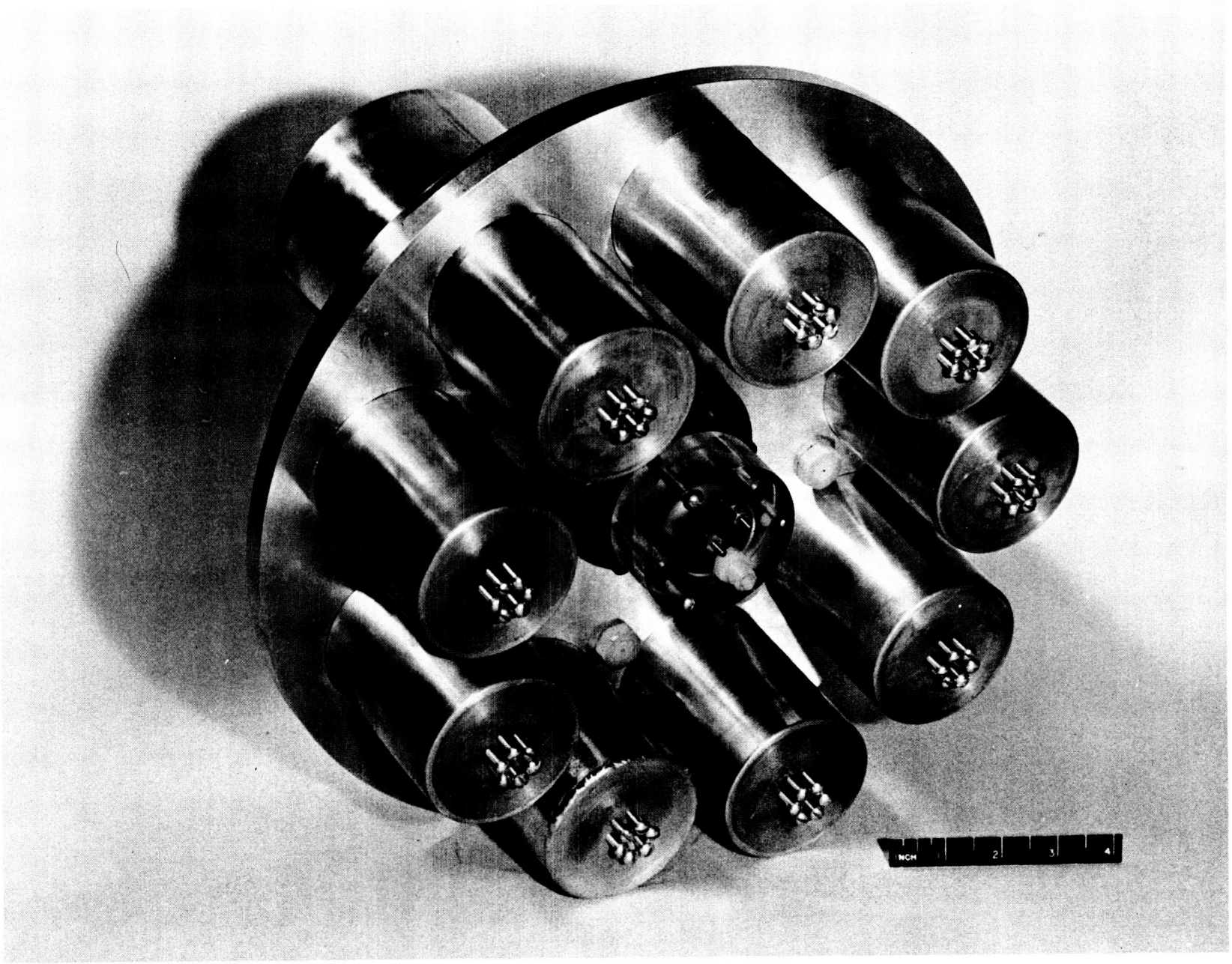

Figure 47a. Small, Lightweight Capacitor Bank with Mod. A-4T Gun.

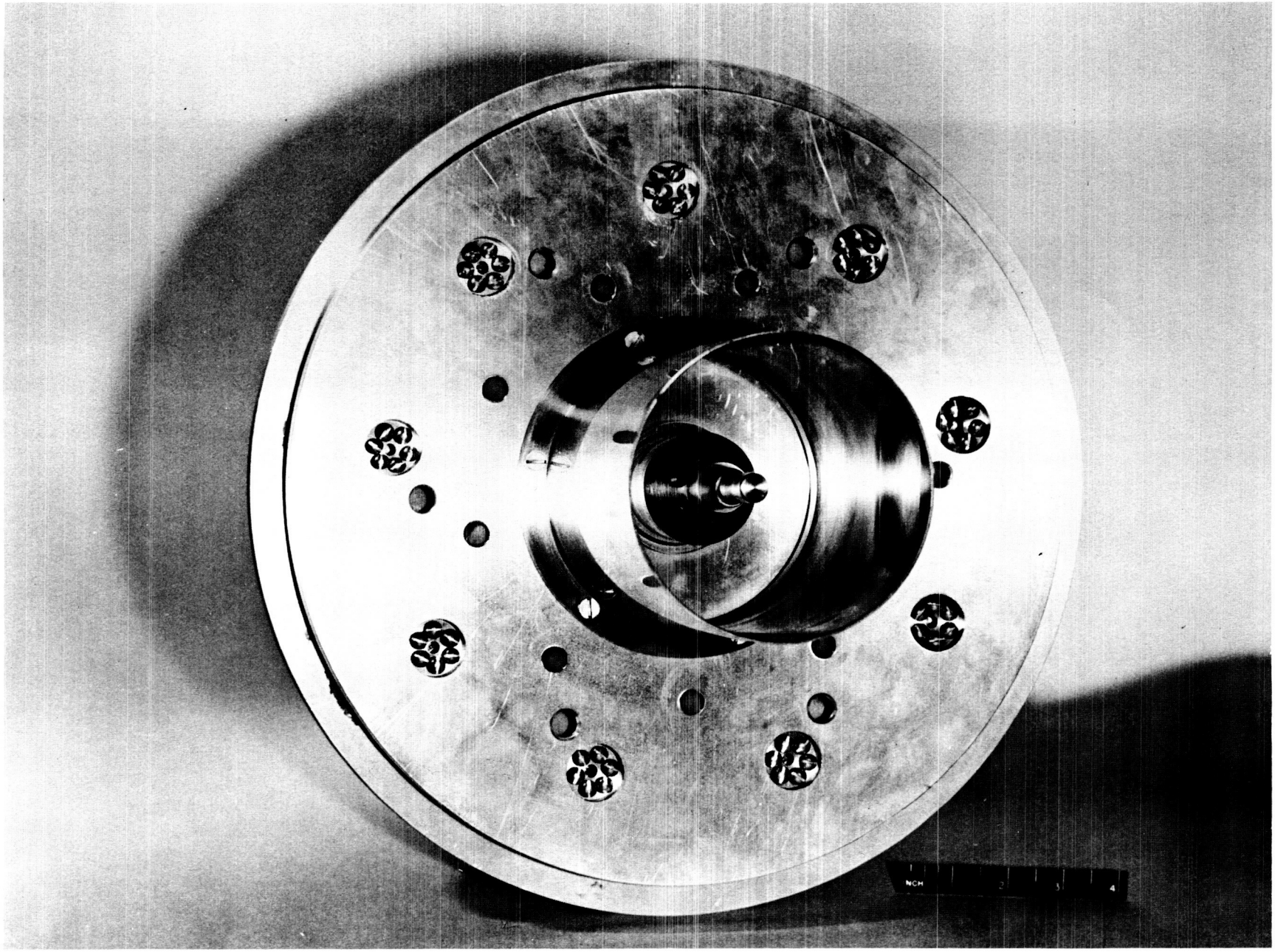

Figure 47b. Small, Lightweight Capacitor Bank with Mod. A-4T Gun.

capacitor bank presently in use, while its Q is about five times higher than that of the present bank.

More conventional capacitors using oil impregnated paper and oil impregnated "Samica" dielectrics with Q's in the range from 50 to 200 at 100 KC, will also be available for testing in the next contract period.

13. CONCLUDING REMARKS

The consistent improvement in engine system efficiency which has been achieved during this contract period has been encouraging indeed. Still more encouraging is the fact that there is ample opportunity for further improvement since neither convincing analysis nor experiment indicate that an upper limit of engine performance has been approached. Some of the means for the further refinement of engine operation have been discussed above. These are but a few of the problem areas which must be identified, investigated, and brought to final solutions before what is presently a laboratory device can be developed to a true engine prototype. The results of the past year and the promise for the future have considerably increased the desirability of such additional studies.

14. GENERAL ACKNOWLEDGMENTS

The authors wish to cite the continuing support of Joseph Farber and F. W. Mezger in encouraging and facilitating the progress of these studies. Valuable experimental and analytical support was given by Mr. Gerard Brimmer and Mr. Stephen Collins, respectively.

REFERENCES

1. B. Gorowitz, P. Gloersen, and J. H. Rowe, "Performance Study of a Repetitively Pulsed Two-Stage Plasma Propulsion Engine", Final Report, Contract No. NAS3-2502, November 20, 1963.

2. B. Gorowitz, P. Gloersen, and K. Moses, "Magnetically Driven Fast Acting Valve for Gas Injection into High Vacua", The Review of Scientific Instruments, Vol. 31, No. 2, pp. 146-148, February, 1960.

3. P. Gloersen, B. Gorowitz, and W. Palm, "Experimental Performance of a Pulsed Gas Entry Coaxial Plasma Accelerator," Paper No. 1535-60 at the ARS 15th. Annual Meeting, Washington, D. C., December 1960.

4. L. C. Burkhardt and R. H. Lovberg, "The Current Sheet in a Coaxial Plasma Gun," Phys. Fluids 5, 341 (1962).